SPIN WAVE SPECTRUM AND RELATED PROBLEMS FOR FERROMAGNETIC 3 d-GROUP TRANSITION METALS AND ALLOYS

HIDEJI YAMADA

Department of Applied Physics

(Received 18th May, 1968)

ABSTRACT

Calculations on temperature variations of the magnetizations for nickel and iron metals are performed by the Stoner theory. Exchange energy is expanded as a power series of the magnetization M and values of its coefficients are estimated from the comparisons between calculated and experimental results of the temperature variations of M for nickel and iron metals. In a phenomenological way, a new expression for the magnetic energy due to fluctuations of the magnetization density is found for an isotropic continuous ferromagnetic medium. By using the Holstein-Primakoff transformation, it is shown that many terms in this expression, except the term discussed by Herring and Kittel, correspond to spin wave-spin wave interactions. From the microscopic point of view, the dispersion relations of spin waves in ferromagnetic metals with multiple bands are obtained by the method of normal modes within the random phase approximation and a certain approximation for the Coulomb interaction. It is found that spin wave spectra consist of some branches; one acoustical intra-band branch, one acoustical inter-band branch and some optical intra- and inter-band branches. The inter-band transitions have an important effect on the acoustical intra-band branch at larger momenta of spin waves. Within the (extended) random phase approximation, the equation of motion for normal modes in an electron gas is solved by the iteration method and the dispersion relations of a plasmon in the paramagnetic and ferromagnetic electron gases are obtained. It is shown that there is no difference between constant terms in the dispersion relation with respect to the momentum of a plasmon in the paramagnetic and ferromagnetic states, but coefficients of the terms proportional to the square of the momentum of a plasmon are different in the two states. High field susceptibilities for ferromagnetic iron metal and its alloys are estimated at 0°K, by making use of the density of states curve determined by the rigid band model. A satisfactory agreement between the calculated and observed results on the concentration dependences of high field susceptibilities at 0°K is obtained for iron-cobalt and iron-nickel alloys. The dependences on temperature and magnetic field of the high field susceptibility are calculated by the model of non-interacting free spin waves. The observed temperature dependence of the high field susceptibility is satisfactorily explained by the calculated result.

Chapter I

Introduction and Summary

Ferromagnetism of 3 d-group transition metals and their alloys is usually investigated on the basis of the itinerant electron model, where not only 4 s-

electrons but also 3 d-electrons are itinerant electrons and run over the crystal. The earlier theoretical works on the ferromagnetism in this model are carried out by Bloch[1], Slater[2], Stoner[3] and Mott[4] and showed a great success in qualitative explanations of experimental results such as non-integer Bohr magneton numbers per atom for the spontaneous magnetization, the temperature variation of the electronic specific heat and so on for 3 d-group transition metals and their alloys. In their works it is shown that various magnetic properties are related to two fundamental quantities, that is, the "density of states" and a "molecular field coefficient".

By assuming the rigid band model, the density of states curve can be deduced from the observed data of the low temperature specific heat, and the value of the molecular field coefficient can also be deduced from the analyses of the susceptibilities using the density of states curve. From this point of view, Shimizu *et al.*[5] have obtained the density of states curves and the values of the molecular field coefficient for 3 d-, 4 d- and 5 d-group transition elements in a series of their works. They have also shown that the correlation between the temperature variations of the electronic specific heat and the susceptibility is explained by the shape of the density of states curve. Moreover, they have obtained a satisfactory agreement between the calculated and observed temperature variations of the electronic specific heat and estimated the values of the orbital susceptibility from the analyses of the temperature variation of the susceptibilities for the transition metals and their alloys in the paramagnetic states.

Using the density of states curves given by Shimizu *et al.*[6][7] we calculate the temperature variations of the magnetizations for nickel and iron metals in the Stoner model[3] and will estimate the magnetization dependences of the molecular field coefficients, which are important to compare the calculated results with the observed ones, in chapter II. The outline of the magnetic properties for 3 d-group ferromagnetic metals and their alloys can be explained in the Stoner model[3], but the detailed magnetic properties, for instance, the temperature variation of the magnetization at low temperature cannot be explained satisfactorily in the Stoner model.

It is experimentally found that the spontaneous magnetization decreases with increasing temperature T as $T^{3/2}$ in lower temperatures[8]. Theoretically, Bloch[9] has first shown that there exists a collective motion of spins in a ferromagnet, so-called "spin wave", and the excitation of spin waves decreases the magnetization as $T^{3/2}$ in the Heisenberg model. Herring and Kittel[10] have phenomenologically obtained spin waves and shown that spin waves can also exist in the ferromagnetic metals. They have derived the spin wave motion from the leading term in the energy due to the fluctuation of the magnetization. In chapter III, we find the higher-order terms in the energy due to the fluctuation of the magnetization for an isotropic and continuous ferromagnetic medium from the consideration of the symmetry. By using the Holstein-Primakoff transformation, it is shown that the terms in our expression of the energy except the first term, which was discussed by Herring and Kittel[10], correspond to spin wave-spin wave interactions. An expression for the exchange field up to the term corresponding to the fourth power of spin wave momentums in the energy of spin waves is found.

Recently, by using the method of the many body problems, spin waves in

the ferromagnetic metals have been discussed by many investigators[11)12)]. However, in the most of works, the spin wave is treated in the single band model. In the multiple band model, two attempts have been so far made by Mattis[13)] and Thompson[12)]. In both calculations, excitations of an electron from one sub-band with up spin to another sub-band with down spin are neglected, so that the effects of the inter-band transitions on the spin waves are not taken into account correctly. In chapter IV, taking into account these inter-band transitions, we find the dispersion relations of spin waves in ferromagnetic metals with multiple bands by the method of normal modes within the random phase approximation and a certain approximation for the Coulomb interaction. It is found that spin wave spectra consist of one acoustical intra-band branch, some optical intra-band branches and other branches due to inter-band transitions which are called "*inter-band spin waves*". The inter-band spin waves have an important effect on the dispersion relation of the acoustical intra-band branch of spin waves at larger momentum. The coefficient of the square of momentum in the dispersion relation of the acoutical intra-band branch of spin waves is found to be the sum of D_R and D_H which are derived from the intra-atomic Coulomb and inter-atomic exchange interactions, respectively. For nickel, the value of D_R is estimated as about 0.1 eVÅ^2 by using the model of two overlapping bands and it is concluded that $D_R \lesssim D_H$. Using the effective mass approximation for the bands of electrons, we get the whole spectra of excitations of an electron with a reversed spin up to the cut-off momentum of spin wave in the single band and two band models and it is shown that the cut-off momentum of spin wave in the single band model is fairly affected by the inter-atomic exchange integral.

It is well-known that there is another collective motion due to the density fluctuation of electrons in metals, which is called a plasma oscillation or a plasmon[14)]. We discuss a plasmon in a ferromagnetic electron gas in chapter V. Within the frame of the extended random phase approximation, the equation of motion for normal modes of the density oscillation in an electron gas is solved by the iteration method and we get the dispersion relation of a plasmon for the paramagnetic and ferromagnetic electron gases, including terms of the exchange correction. It is shown that there is no difference between the constant terms in the dispersion relation with respect to the momentum of a plasmon in the paramagnetic and ferromagnetic states, but coefficients of the terms proportional to the square of the momentum in the dispersion relation are different in the paramagnetic and ferromagnetic states. This difference is roughly estimated for the real ferromagnetic metals, iron, cobalt and nickel and a possibility of the observations of this difference is discussed in chapter V.

The excitation energy of a plasmon is the order of 10 eV in the real ferromagnetic metals[14)] and the plasmon has no effect on the magnetic properties at ordinary temperatures. On the other hand, the excitation energies of spin waves are lower than the energies of the individual excitations of an electron with a reversed spin, that is, Stoner excitations. Therefore, spin waves play an important role to determine the magnetic properties of a ferromagnet at lower temperatures. For instance, the temperature variations of the magnetization[8)] and the high field susceptibility[15)] at low temperature can be explained by spin waves. In chapter VI, high field susceptibilities for ferromagnetic iron metal and its alloys with cobalt, nickel, chromium and vanadium are estimated at 0°K, by

using the same density of states curve as that used in chapter II. A satisfactory agreement between the calculated and observed results[15] on the concentration dependences of the susceptibility at 0°K is obtained for iron-cobalt and iron-nickel alloys. The dependences of susceptibility on temperature and magnetic field are calculated by the model of non-interacting free spin waves, of which energies are determined by the experiments of the inelastic neutron scattering. And it is shown that the observed temperature dependences of the susceptibility[15] are explained by the calculated results.

Chapter II. Temperature Variations of the Magnetization in the Stoner Model

§ 1. Introduction

Many years ago, Stoner[3] showed that ferromagnetism is expected for electrons in a simple normal band, where the density of states is proportional to the square root of the energy, if the assumed molecular field, which is proportional to the magnetization, is sufficiently large. The model of a normal band is too simple to apply to electrons in a real transition metal, where the density of states curve shows a very complicated change with energy, although this model and some extensions[16] have been used with considerable success to explain the various magnetic properties for transition metals and alloys. Shimizu[17][18] has extended the Stoner model to the case of a general density of states curve and magnetic (exchange) energy, by discussing the difference between the free energies in the ferromagnetic and paramagnetic states.

The density of states can be deduced from the observed data on the low temperature specific heat and on the spontaneous magnetization for metals and alloys by assuming the rigid band model. From this point of view, Shimizu *et al.*[6][7] have obtained the density of states curves for nickel and iron metals, respectively. By making use of these density of states curves, we calculate the temperature variations of magnetizations for nickel and iron metals in the Stoner model[3]. The effective exchange energy is expanded as a power series of the magnetization and the values of its coefficients are estimated from the comparison between the calculated and experimental results on the temperature variation of the magnetizations for nickel and iron metals, in § 2 and § 3, respectively. In § 4, we discuss the criticism of the Stoner model, by comparing the calculated result of the temperature variation of the magnetization at low temperature in the Stoner model with the experimental one.

§ 2. Calculation and Comparison with Experiment for Nickel Metal[19]

The calculation of the magnetization for nickel metal is performed by making use of the density of states curve which was determined by Shimizu *et al.*[6] from the low temperature specific heat data for nickel and copper metals and nickel-iron and nickel-copper alloys assuming the rigid band model, as shown in Fig. 1, where ζ_0, ζ_+ and ζ_- denote the Fermi level in the paramagnetic state and the Fermi levels of plus and minus spin bands in the ferromagnetic state at 0°K, respectively, for nickel metal.

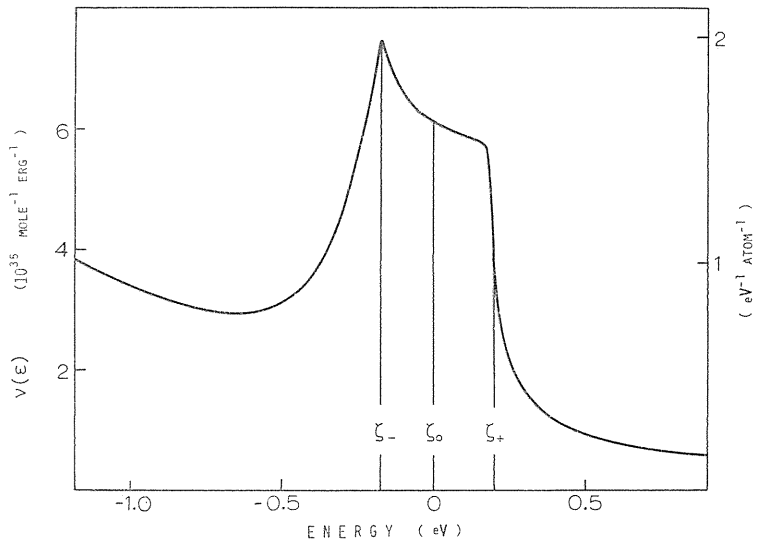

FIG. 1. Density of states curve for nickel metal[6]. Fermi levels of plus spin band, ζ_+, and minus spin band, ζ_-, in ferremagnetic state and ζ_0 in paramagnetic state at 0°K are shown.

For a ferromagnetic state with the magnetization M in the band model, there are following relations at 0°K:

$$\int_{\zeta_-(0)}^{\zeta_0} \nu(\varepsilon)\, d\varepsilon = \int_{\zeta_0}^{\zeta_+(0)} \nu(\varepsilon)\, d\varepsilon = n, \tag{2.1}$$

$$M = 2\, n\mu_B, \tag{2.2}$$

and

$$\zeta_+(0) - \zeta_-(0) = 2\, \mu_B \alpha M, \tag{2.3}$$

where $\zeta_+(0)$, $\zeta_-(0)$ and ζ_0 are the Fermi levels of plus and minus spin bands at 0°K in the ferromagnetic state and that in the paramagnetic state, respectively, and $\nu(\varepsilon)$ and αM are the density of states and a molecular field, respectively. At a temperature T,

$$\int_{-\infty}^{\infty} \nu(\varepsilon) f\left(\frac{\varepsilon - \zeta_\pm(T)}{kT}\right) d\varepsilon = N \pm n, \tag{2.4}$$

and

$$\Delta\zeta = \zeta_+(T) - \zeta_-(T) = 2\, \mu_B \alpha M, \tag{2.5}$$

where f is the Fermi distribution function and

$$N = \int_{-\infty}^{\zeta_0} \nu(\varepsilon)\, d\varepsilon. \tag{2.6}$$

Using the equations (2.1) to (2.6) and taking M as a parameter, we numerically calculate the temperature variations of ζ_+, ζ_-, and α from (2.5). Calculated

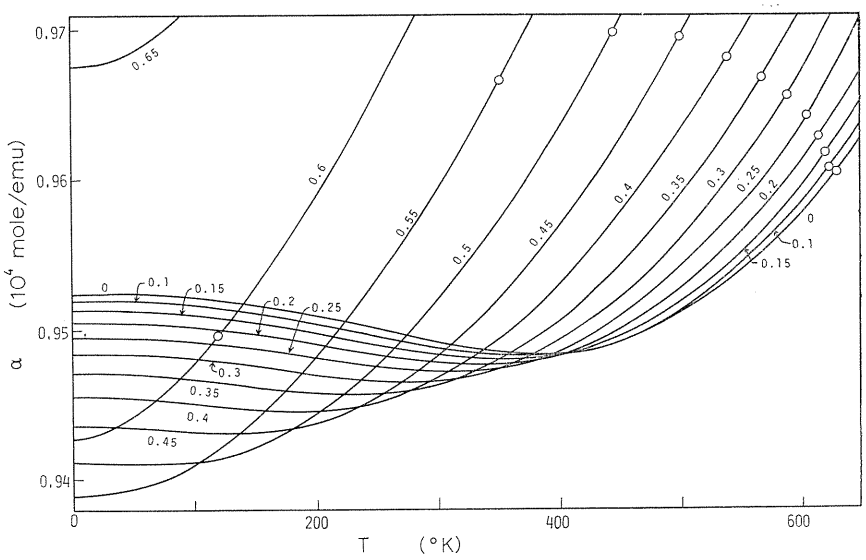

FIG. 2. Temperature variation of the molecular field coefficient, α, where M is taken as a parameter. The curves are specified by the values of M in μ_B/atom. The curve specified by $M=0$ is the reciprocal of the calculated value of the spin paramagnetic susceptibility without the molecular field, χ_0. Open circles are the experimental values of α estimated from the experimental M vs T curve for nickel metal[20].

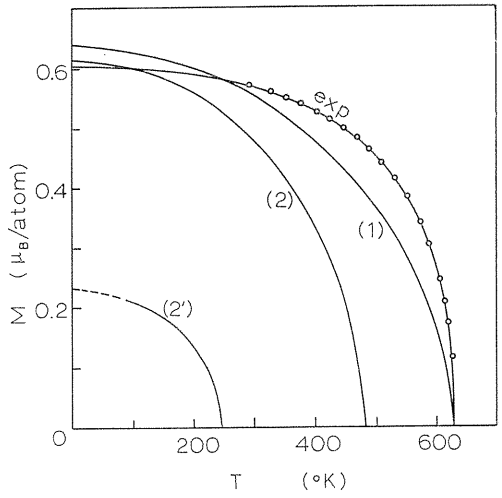

FIG. 3. Temperature variation of the magnetization of nickel metal. Curve (1) is the calculated result with $\alpha=0.96\times10^4$ mole/emu. Curves (2) and (2') are the calculated result with $\alpha=0.95\times10^4$ mole/emu. In the latter case two values of M are obtained at each temperature and curves (2) and (2') correspond to the stable and unstable solutions, respectively. The curve specified by exp is the experimental one[20].

results are shown in Fig. 2 for some values of M. The curve specified by $M=0$ is the reciprocal of the calculated value of the spin paramagnetic susceptibility without the molecular field, χ_0, for nickel metal.

We obtain $\alpha=0.96\times10^4$ mole/emu from the condition that $\chi_0^{-1}-\alpha=0$ at the Curie temperature, 630°K, and if we assume this value of α at all temperatures,

the magnetization behaves like curve (1) in Fig. 3. In this case, the magnetization shows larger values at lower temperatures ($M=0.64\ \mu_B$/atom at 0°K) and smaller values at higher temperatures than the observed ones[20]. If α takes a constant value, 0.95×10^4 mole/emu, which gives $M=0.61\ \mu_B$/atom at 0°K, the magnetization behaves like curve (2) in Fig. 3. In this case, the corresponding Curie temperature, 480°K, is too low.

Although a part of the reason for this discrepancy will be attributable to the crudeness of the density of states curve, we have tried to get a better agreement between the calculated result and the experiment, taking account of the magnetization dependence of α. As easily seen from Fig. 2, the value of the magnetization depends sensitively on the value of α at a constant temperature, while the value of α does not so sensitively depend on the value of M. Therefore, the calculated values of M can be made agree with the experiment by taking account of the magnetization dependence of α. Previously, Hunt had calculated the temperature variation of M using the parabolic density of states curve and taking into account the term proportional to M^4 as well as the term proportional to M^2 in the exchange energy[21]. Here, if the effective exchange energy is expanded as a power series in M and taken up to the term of M^6, that is,

$$E_{ex}=-(1/2)\alpha'M^2-(1/4M_0^2)\beta M^4-(1/6M_0^4)\gamma M^6, \tag{2.7}$$

where M_0 is the value of M at 0°K, the molecular field, H_m, is

$$H_m=\{\alpha'+\beta(M/M_0)^2+\gamma(M/M_0)^4\}M, \tag{2.8}$$

where β/α' corresponds to A in Hunt's paper[21]. Therefore, we get

$$\Delta\zeta=2\mu_BM\{\alpha'+\beta(M/M_0)^2+\gamma(M/M_0)^4\}=2\mu_B\alpha M, \tag{2.9}$$

where

$$\alpha=\alpha'+\beta(M/M_0)^2+\gamma(M/M_0)^4. \tag{2.10}$$

We take the value of α' being equal to the value of α determined from the relation, $\chi_0^{-1}-\alpha=0$, at the Curie temperature, so that we get $\alpha'=0.96\times10^4$ mole/emu. The experimental values of α are estimated from the α vs T curves shown in Fig. 2 and the experimental M vs T curve. These experimental values of α are shown by open circles in Fig. 2, and are plotted as a function of M in Fig. 4. The values of α calculated from (2. 10) with $\alpha'=0.96\times10^4$, $\beta=218$ and $\gamma=0$, -40 and -95 mole/emu are shown by curves (1), (2) and (3) in Fig. 4, respectively. From the comparison between these curves and the experimental curve, we estimate the value of the coefficients as $\alpha'=0.96\times10^4$, $\beta=218$ and $\gamma=-40\sim-95$ mole/emu. The disagreement with the experiment at large values of M may be attributed to the effect of the spin wave, because we consider here the single particle excitations only and do not take account of the spin wave excitations which are dominant at low temperature. From the values of α', β and γ estimated above, we get $\beta/\alpha'=0.023$ and $\gamma/\alpha'=-0.004\sim-0.01$. On the other hand, Hunt[21] estimated $A=\beta/\alpha'=0.1$ for nickel metal which is four times larger than our value (In his analysis, the term of M^6 in E_{ex} was neglected.).

From the values of α', β and γ found above, the exchange splitting at 0°K, $\Delta\zeta_0=\zeta_+(0)-\zeta_-(0)=2\mu_BM_0(\alpha'+\beta+\gamma)$, is estimated as $\Delta\zeta_0=0.380$ eV. This value is

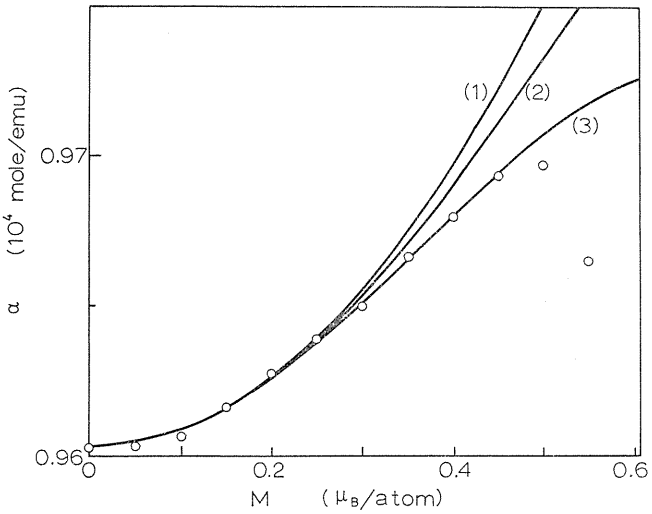

FIG. 4. Values of the molecular field coefficient, α, plotted as a function of the magnetization, M. Curves (1), (2) and (3) are calculated from (2.10) with $\alpha'=0.96\times10^4$, $\beta=218$ and $\gamma=0$, -40 and -95 mole/emu, respectively. Open circles are the experimental values corresponding to the open circles in Fig. 2 which are obtained from the experimental M vs T curve[20].

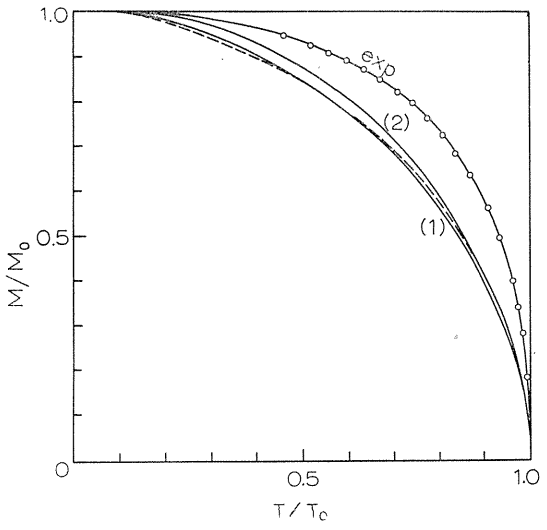

FIG. 5. Temperature variation of the reduced magnetization. Curves (1) and (2) are the calculated result with $\alpha=0.96\times10^4$ mole/emu and $\alpha=0.95\times10^4$ mole/emu, respectively, and a broken curve is Stoner's result for the parabolic band with $k\theta'/\varepsilon_0=0.794$ and $\zeta_0=1$ in Stoner's notation[3]. Wohlfarth's result for the rectangular band with $k\theta'/\varepsilon_0=1.04$[16] almost precisely coincides with the curve (1). The curve specified by exp is the experimental one[20].

larger than the corresponding value, 0.364 eV, obtained directly from the separation between the Fermi levels at 0°K of plus spin and minus spin[17]. The origin of this discrepancy may be due to a fairly large tailing in the upper part of the 3d band shown in Fig. 1.

For the sake of comparison between our result and Stoner's and Wohlfarth's ones[3][16], the reduced M vs T curves are shown in Fig. 5. Although the density

of states curve used in our calculation is fairly different from the parabolic band used in Stoner's calculation and the rectangular band used in Wohlfarth's one, the obtained M vs T curves resemble with each other.

§ 3. Calculation and Comparison with Experiment for Iron Metal[22]

Temperature variation of the magnetization for iron metal is calculated by the same method given in the previous section. The density of states curve for iron metal was deduced by Shimizu and Katsuki[7] from the experimental data of the low temperature specific heat and spontaneous magnetization for iron metal and iron-cobalt and chromium-iron alloys with bcc structure by assuming the rigid band model and taking into account the effect of g-factor on the magnetization, as shown in Fig. 6, where ζ_0, ζ_+ and ζ_- are the Fermi level in the paramagnetic state and the Fermi levels of the plus and minus spin bands in the ferromagnetic state, respectively, for iron metal at 0°K.

Using (2. 1) ~ (2. 6) and taking M as a parameter, we numerically calculate the temperature variations of ζ_+ and ζ_- and those of α from (2. 5). Calculated results of $\alpha = \Delta\zeta/(2\mu_B M)$ as a function of temperature are shown in Fig. 7 for some values of M. The curve specified by $M=0$ in Fig. 7 corresponds to the temperature variation of the reciprocal of the calculated spin paramagnetic susceptibility without the molecular field, χ_0, for iron metal. Open circles in Fig. 7 are the experimental values of α which are obtained by fitting the calculated M vs T curve with the experimental result for iron metal[23].

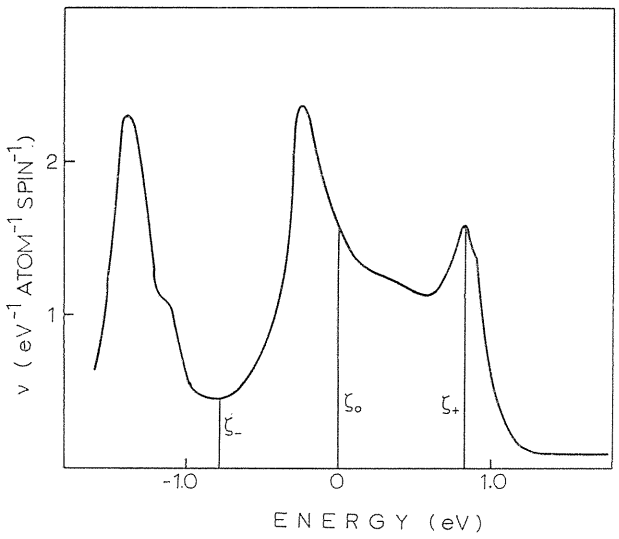

FIG. 6. Density of states curve for iron metal, obtained from low temperature specific heat data and saturation magnetization data for iron metal and iron-cobalt and chromium-iron alloys[7]. Fermi levels of up and down spin bands of iron, ζ_+ and ζ_-, in the ferromagnetic state and ζ_0 in the paramagnetic state at 0°K are shown.

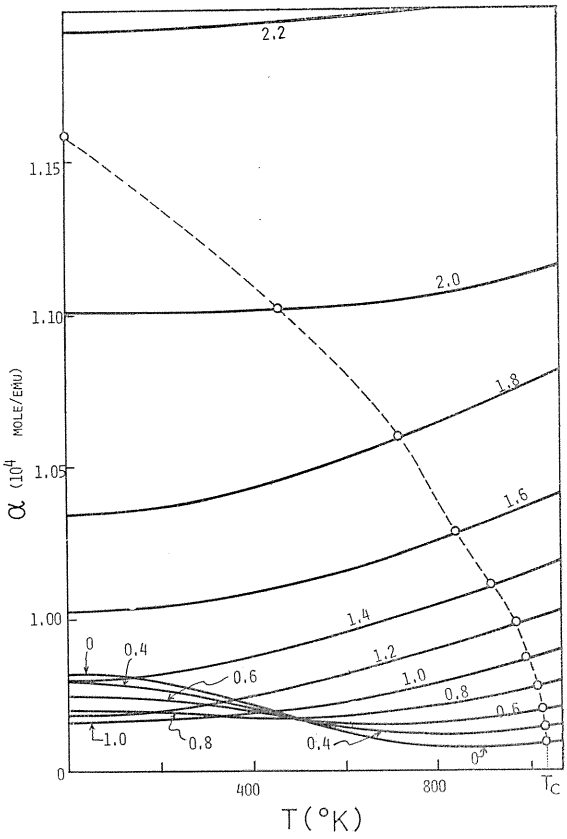

FIG. 7. Temperature variation of the molecular field coefficient, α, where curves are specified by values of M in μ_B/atom. The curve specified by $M=0$ is the reciprocal of the calculated values of spin paramagnetic susceptibility without molecular field, χ_0. Open circles are the experimental values of α estimated from the experimental M vs T curve for iron[23].

We can estimate the value of α as 0.96×10^4 mole/emu from the condition, $\chi_0^{-1}-\alpha=0$, at $T_c=1040$°K. On the other hand, we can estimate the value of α at 0°K as 1.16×10^4 mole/emu from the exchange splitting $\Delta\zeta$ in (2.3) ($\Delta\zeta=1.59$ eV) shown in the density of states curve in Fig. 6, and from the experimental value of the Bohr magneton number, 2.125 μ_B/atom, which is deduced from the observed value of the saturation magnetization at 0°K, 2.2 μ_B/atom, by taking into account the effect of g-factor. There is a considerable difference between the values of α at 0°K and T_c. As discussed in the last section, we expand the exchange energy as a power series of M, and take up to the term of M^6 as (2.7).

We take the value of α' in (2.10) being equal to the value of α determined from the relation, $\chi_0^{-1}-\alpha=0$, at T_c, then $\alpha'=0.96\times10^4$ mole/emu. The experimental values of α, which are obtained from the comparison between the α vs T curves shown in Fig. 7 and the experimental M vs T curves[23], and shown by

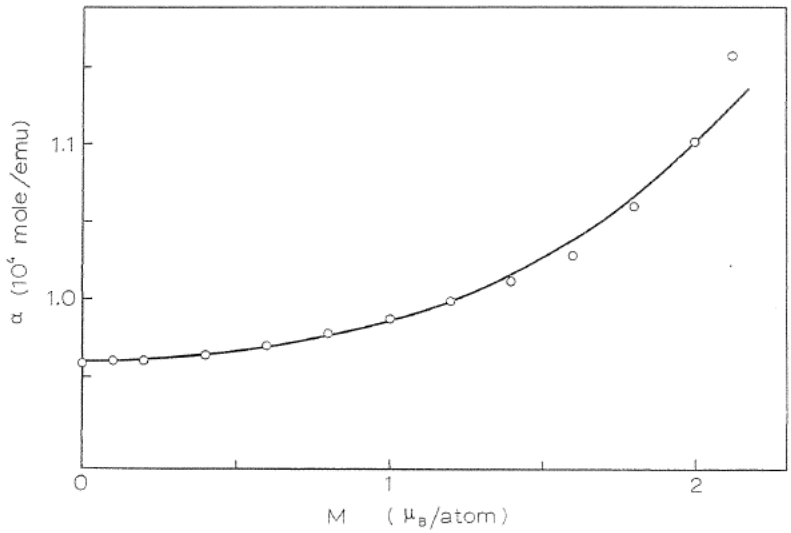

FIG. 8. Values of the molecular field coefficient, α, plotted as a function of M. The curve is calculated from (2. 10) in the text with $\alpha'=0.96\times10^4$, $\beta=0.10\times10^4$ and $\gamma=0.06\times10^4$ mole/emu. Open circles are the experimental values corresponding to the open circles in Fig. 7.

the open circles in Fig. 7, are plotted as a function of M by open circles in Fig. 8. We can estimate the values of the coefficients β and γ in (2. 10) so as to give the experimental values of α which are determined from the experimental M vs T curve, using $\alpha'=0.96\times10^4$ mole/emu fixed above, and we find $\beta=0.10\times10^4$ mole/emu and $\gamma=0.06\times10^4$ mole/emu. The values of α given by (2. 10) with these numerical values of α', β and γ are shown by a solid curve in Fig. 8. From these estimated values of α', β and γ, we get $\beta/\alpha'=0.104$ and $\gamma/\alpha'=0.063$ for iron metal. On the other hand, we have estimated $\alpha'=0.96\times10^4$, $\beta=218$ and $\gamma=-40\sim-95$ mole/emu for nickel metal in the last section. It is noted that the values of β and γ in (2. 10) are larger for iron metal than those absolute values for nickel metal.

We estimate the temperature variation of the molecular field coefficient above T_c, by comparing the calculated and experimental results of the temperature variation of the magnetic susceptibility above T_c for bcc iron. The relation between the calculated and measured paramagnetic susceptibilities, χ_0 and χ, is given by $\chi^{-1}=\chi_0^{-1}-\alpha'$ above T_c, where we neglect the contribution to the χ from the constant magnetic susceptibility, namely, a sum of core diamagnetic and orbital paramagnetic susceptibilities[5], which will not depend on the temperature. From this relation, using the calculated result of χ_0^{-1} shown in Fig. 7 and the observed data of χ[24], we can estimate the temperature dependence of the molecular field coefficient α' above T_c for iron metal as shown by solid curves in Fig. 9 ($\alpha=\alpha'$ above T_c because $M=0$.). Since the iron metal shows fcc structure in the temperature range shown by the broken line above T_c, we can get no information about α for bcc iron in this temperature range.

If the contribution of the constant susceptibility to the measured susceptibility

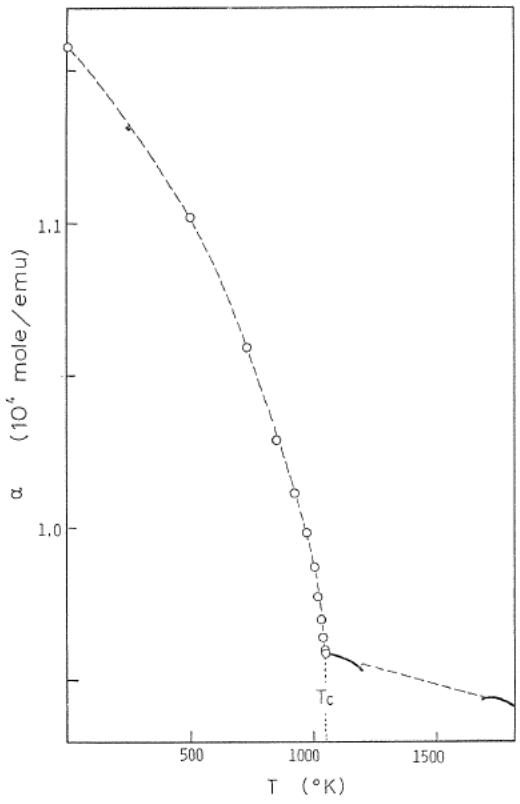

FIG. 9. Temperature dependence of the molecular field coefficient, estimated from the calculated and observed[24] values of spin susceptibility above T_c for bcc iron. Open circles below T_c are the same as shown in Fig. 7.

is taken into account, the values of α' at higher temperatures in δ phase of iron, shown in Fig. 9, will be reduced a little. This effect, however, seems to be not so important, because the measured value of susceptibility at 1805°K is still large and 1.70×10^{-3} emu/mole[24] as compared with the estimated value of the constant susceptibility, $\sim1.4\times10^{-4}$ emu/mole, for chromium metal[5].

For the sake of comparison between the temperature dependences of α above and below T_c, the values of α shown in Fig. 7, which are determined from the calculations and experiments, are denoted by open circles in Fig. 9. As seen from Fig. 9, it may be concluded that the temperature dependences of α are different from each other above and below T_c. This fact will be explained in the following way. It is considered that the molecular field coefficient α depends in general both on the magnitude of the magnetization and temperature, so that below T_c, the value of α may be expanded as a power series of M^2 for small M as (2. 10), and the coefficients will be dependent on temperature. We have estimated the values of α', β and γ, neglecting their temperature dependences. On the other hand, above T_c, the values of α decrease with increasing temperature as shown by solid curves in Fig. 9 and this behavior of α will be an intrinsic temperature dependence of α or α' in (2. 10) as $M=0$.

The origin of the molecular field coefficient is considered to be an average value of the exchange integrals over singly occupied electrons[2)25)26)], which is proportional to an average value of the terms, $|\boldsymbol{k}-\boldsymbol{k}'|^{-2}$, in the case of an electron gas, where $\boldsymbol{k}$ and $\boldsymbol{k}'$ are momenta of electrons. At higher temperatures, the terms with large difference between $\boldsymbol{k}$ and $\boldsymbol{k}'$ will appear by thermal excitations, so that the average value of the terms $|\boldsymbol{k}-\boldsymbol{k}'|^{-2}$, that is, α will decrease with increasing temperature for an electron gas. For the real transition metals, the circumstances are more complex because we must consider several sub-bands and the correlation energy among Bloch electrons. We consider, however, that the discussion similar to that given above for α in an electron gas may be applicable to the qualitative understanding for the decrease of α above T_c for bcc iron metal.

§ 4. Utility and Criticism of the Stoner Model

In the preceding two sections, the temperature variations of the magnetizations for nickel and iron metals have been calculated in the Stoner model[3] and it has been concluded that the magnetization dependence of α is important to fit the calculated result on the observed one. The values of β/α' and γ/α' for nickel and iron metals are shown in Table 1.

TABLE 1. The Estimated values of α', β/α' and γ/α' for nickel and iron metals

	α' (emu/mole)	β/α'	γ/α'	
Ni	0.96×10^4	0.023	$-0.004\sim-0.01$	present
		0.1		Hunt[21]
Fe	0.96×10^4	0.104	0.063	present

Previously Wohlfarth[25] has shown that within the Hartree-Fock approximation the dependence on M of the exchange energy is of the form $\Sigma_n A_n M^n$, taking into account not only intra-atomic Coulomb integral but also inter-atomic Coulomb, exchange and other two-center integrals based on the wave functions in the tight-binding approximation. Until now we do not satisfactorily get even the value of α from the first principle, although a few attempts are made by Kanamori[27] and Hubbard[28], taking into account correlations between electrons in metals. These problems are left in future.

It is experimentally found[29] that specific heats for ferromagnetic metals and alloys at low temperature are proportional to T. This experimental fact can be explained in the Stoner model, as the electronic specific heat is written as

$$C_E = \frac{\pi^2 k^2 T}{3}(\nu_+ + \nu_-), \tag{2.11}$$

at low temperature, where ν_+ and ν_- are the values of the density of states at the Fermi levels of the plus and minus spin bands, respectively. On the other hand, it is considered that the change of the specific heat at the Curie temperature for ferromagnetic metals cannot be explained in the Stoner model[30]. Recently, however, it is shown by Shimizu and Terao[31] that this change of specific heat can be well explained in the improved Stoner model[18]. They have shown the difference between the specific heats in the ferromagnetic and paramagnetic states is composed of that part due to the ordinary magnetic ordering and the one due to the intrinsic variation of α with temperature. The former is obtained from the simple Stoner model, but the latter is a new term and plays an important role at $T \lesssim T_c$. Shimizu and Terao[31] have obtained an excellent agreement between the calculated and observed results of the electronic specific heat for iron and nickel metals below T_c, by making use of the density of states curve shown in Fig. 1 and Fig. 6 and the intrinsic variations of α with temperature which are deduced from the comparison between the calculated and expeirmental results of the susceptibility above T_c (*cf.* Fig. 9 for iron metal).

It is noted that not only for paramagnetic metals and alloys but also for ferromagnetic ones, the temperature variation of the electronic specific heat can be explained in the band model, by making use of the density of states curve which is determined from the experimental data of the low temperature specific heat by assuming the rigid band model.

As seen in this chapter, the outline of the magnetic and caloric properties for ferromagnetic metals and alloys can be explained in the Stoner model. However, the detailed magnetic properties, for instance, the temperature variation of the magnetization at low temperature[8] and the temperature variations of the susceptibility and specific heat just above T_c[32], cannot be explained in the Stoner model. The precise calculation of thermodynamical properties just above T_c has been carried out in the Ising model and the Heisenberg model and it is found that the short-range ordering of spins seems to play an important role[33]. Until now, these properties, however, have not been studied in the itinerant electron model.

In the Stoner model[3], the temperature variation of the magnetization at low temperature is expanded in the power series of kT as

$$\frac{M_0 - M}{\mu_B} = \frac{(\pi kT)^2}{3} \frac{\nu'_-/\nu_- - \nu'_+/\nu_+}{\nu_+^{-1} + \nu_-^{-1} - 4\mu_B^2\alpha}, \tag{2.12}$$

up to the power of T^2, where ν'_+ and ν'_- are first derivatives of the density of states with respect to the energy at the Fermi levels of the plus and minus spin bands, respectively, and M_0 denotes the value of the magnetization at 0°K. The numerical values of the coefficient of T^2 in the right-hand side of (2.12) for nickel and iron metals are roughly estimated from the densities of states shown in Fig. 1 and Fig. 6 as 0.2×10^{-5} deg^{-2} atom^{-1} and 0.1×10^{-7} deg^{-2} atom^{-1}, respectively. It is, however, experimentally found that the magnetization decreases with increasing temperature as $T^{3/2}$ not as T^2 at low temperatures[8]. This discrepancy between the calculated and experimental results on the temperature variation of M depends on the fact that the fluctuations of the magnetization, that is, spin waves are neglected in the Stoner model, which is discussed in the next two chapters.

Chapter III. Phenomenological Theory of Spin Waves

§ 1. Introduction

In the Heisenberg model, Bloch[9] has first shown that spin waves exist in a ferromagnet and make the magnetization to decrease with increasing temperature as $T^{3/2}$. Herring and Kittel[10] have shown in a phenomenological way that spin waves can exist in ferromagnetic metals and alloys as follows; the energy due to the fluctuation of the magnetization can be expressed as

$$\frac{A}{M_S^2} \sum_{\nu,\alpha} \int \left(\frac{\partial M_\nu}{\partial x_\alpha} \right)^2 d\tau, \tag{3.1}$$

for an isotropic ferromagnetic medium, where M_ν, M_S and x_α are the ν-component of the magnetization, the magnitude of the magnetization and one of the coordi-

nates, respectively. Herring and Kittel[10] showed that the Hamiltonian for free spin waves is derived from (3.1) as

$$\mathcal{H} = \sum_q \hbar\omega_q n_q, \tag{3.2}$$

where n_q is the number operator of spin waves with momentum q and

$$\hbar\omega_q = Dq^2, \tag{3.3}$$

for the long wave length limit of a spin wave, and $D=4\,\mu_B A/M_s$. The coefficient A in (3.1) is the so-called "exchange stiffness constant".

From (3.3) and by using the Bose distribution function for spin waves, it is easily shown that both the magnetization and the specific heat at lower temperatures vary with temperature as $T^{3/2}$. At first sight, the fact that the specific heat at lower temperatures varies with temperature as $T^{3/2}$ seems to be incompatible with the experimental results, although the dependence on T of the magnetization can be explained in this theory. But this is not true, because (3.1) denotes only the energy due to the fluctuation of the magnetization. For ferromagnetic metals, there is another energy which depends on the average magnetization and is taken into account in the Stoner model, as shown by Shimizu[17][18]. Therefore, at lower temperatures the dependence on T of the specific heat given by (2.11) in the Stoner model is a dominant term, but the dependence on T of the magnetization (2.12) is not so.

In this chapter, we treat only the energy due to the fluctuation of the magnetization. The Hamiltonian for the free spin wave is derived from (3.1), while the spin wave interactions are not contained in (3.1), as suggested by Keffer and Loudon[34]. This is due to the fact that the expression (3.1) is valid only for the long wave length limit of a spin wave. Thus we must find an expression for higher-order terms than the terms in (3.1), in order to discuss the spin wave interactions.

Recently, Marshall[35] has phenomenologically discussed the spin wave interactions and obtained a dispersion relation for spin waves,

$$\hbar\omega_k = ak^2 + \sum_{k'} bk^2k'^2 n_{k'}, \tag{3.4}$$

by a simple physical consideration, where n_k is the occupation number of spin wave with momentum k'. The second term in (3.4) shows the spin wave-spin wave interactions. In the Heisenberg model[34][36], the spin wave interactions are obtained in the same form as the second term in (3.4). On the other hand, a form similar to (3.4) was derived in the itinerant electron model[37].

Herring has semi-phenomenologically obtained the value of A in (3.1), by studying the response of a uniformly magnetized material to a perturbing field[38]. In § 4, we try to determine the parameters given in § 2, in the perturbation method.

§ 2. Spin Wave Interactions by a Continuous Medium Model[39]

(A) Effective Energy

The energy density due to the fluctuation of the magnetization density $\boldsymbol{M}(\boldsymbol{r})$

may be expressed by a power series of the derivatives of $\boldsymbol{M}$ with respect to the space coordinates. For an isotropic ferromagnetic medium, the expression for the energy density should be invariant for the inversion of the direction of the magnetization and for that of the coordinate axes. The expression for the energy density can be classified in the following way.

I) Terms with two M_ν's and two derivatives:

$$\left(\frac{\partial M_\nu}{\partial x_\alpha}\right)^2, \quad M_\nu \frac{\partial^2 M_\nu}{\partial x_\alpha^2}.$$

II) Terms with four M_ν's and two derivatives:

$$M_\nu M_\mu \frac{\partial M_\nu}{\partial x_\alpha}\frac{\partial M_\mu}{\partial x_\alpha}, \quad M_\nu^2\left(\frac{\partial M_\mu}{\partial x_\alpha}\right)^2, \quad M_\nu^2 M_\mu \frac{\partial^2 M_\mu}{\partial x_\alpha^2}.$$

III) Terms with two M_ν's and four derivatives:

$$M_\nu \frac{\partial^4 M_\nu}{\partial x_\alpha \partial x_\beta \partial x_\gamma \partial x_\delta}, \quad \frac{\partial M_\nu}{\partial x_\alpha}\frac{\partial^3 M_\nu}{\partial x_\beta \partial x_\gamma \partial x_\delta},$$
$$\frac{\partial^2 M_\nu}{\partial x_\alpha \partial x_\beta}\frac{\partial^2 M_\nu}{\partial x_\gamma \partial x_\delta},$$

IV) Terms with four M_ν's and four derivatives:

$$\frac{\partial M_\nu}{\partial x_\alpha}\frac{\partial M_\nu}{\partial x_\beta}\frac{\partial M_\mu}{\partial x_\gamma}\frac{\partial M_\mu}{\partial x_\delta},$$
$$M_\nu \frac{\partial M_\nu}{\partial x_\alpha}\frac{\partial M_\mu}{\partial x_\beta}\frac{\partial^2 M_\mu}{\partial x_\gamma \partial x_\delta}, \quad M_\nu \frac{\partial^2 M_\nu}{\partial x_\alpha \partial x_\beta}\frac{\partial M_\mu}{\partial x_\gamma}\frac{\partial M_\mu}{\partial x_\delta},$$
$$M_\nu^2 \frac{\partial^2 M_\mu}{\partial x_\alpha \partial x_\beta}\frac{\partial^2 M_\mu}{\partial x_\gamma \partial x_\delta}, \quad M_\nu M_\mu \frac{\partial^2 M_\nu}{\partial x_\alpha \partial x_\beta}\frac{\partial^2 M_\mu}{\partial x_\gamma \partial x_\delta},$$
$$M_\nu^2 \frac{\partial M_\mu}{\partial x_\alpha}\frac{\partial^3 M_\mu}{\partial x_\beta \partial x_\gamma \partial x_\delta}, \quad M_\nu M_\mu \frac{\partial M_\nu}{\partial x_\alpha}\frac{\partial^3 M_\mu}{\partial x_\beta \partial x_\gamma \partial x_\delta},$$
$$M_\nu^2 M_\mu \frac{\partial^4 M_\mu}{\partial x_\alpha \partial x_\beta \partial x_\gamma \partial x_\delta},$$

where $\alpha=\beta$, $\gamma=\delta$ or $\alpha=\gamma$, $\beta=\delta$ or $\alpha=\delta$, $\beta=\gamma$ in III) and IV). We discuss only the terms which belong to these four classes in the expression for the energy density. As discussing in (B), we need not find the terms which have more M_ν's and more derivatives than the terms shown above, in order to discuss the leading terms in the spin wave interactions.

As an energy of the isotropic ferromagnetic medium is given by an integration of the energy density over the whole volume, all terms in the above expression I)–IV) for the energy density can be reduced to a few terms. As we assume an isotropic medium, the energy density must be invariant with respect to a rotation of the coordinate axes by an arbitrary angle. A term in one class of I)–IV) is never mixed with a term in another class by a rotation of the coordinate axes, because the expression in the new coordinate system after a rotation must be the same derivative form of the magnetization as that in the old coordinate system; for instance, $\partial M_\nu/\partial x_\alpha$ is transformed to a linear combination of $\partial M_n/\partial \xi_i$

by a rotation of the coordinate axes, where ξ_i is a new axis after the rotation and is connected with old axes, x, by Euler's angles and M_n is the n-component of M in the new coordinate system. Therefore, we can treat the terms I)-IV) separately.

Case I) The second term is reduced to the first one by a partial integration. The expression for the energy in this case can be written as

$$E^{(1)} = \frac{A}{M_S^2} \sum_{\alpha,\nu} \int \left(\frac{\partial M_\nu}{\partial x_\alpha} \right)^2 d\tau, \tag{3.5}$$

where M_S is the average magnetization. This expression is the same as (3.1) obtained by Herring and Kittel[10].

Case II) Since the first and second terms are not mixed with the third one by a rotation of the coordinate axes, we treat the first and second terms at first. The energy density for these terms is written generally as,

$$\sum_{\alpha,\nu,\mu,\rho,\sigma} b^{\nu\mu\rho\sigma} M_\nu M_\mu \frac{\partial M_\rho}{\partial x_\alpha} \frac{\partial M_\sigma}{\partial x_\alpha}. \tag{3.6}$$

From the condition for the invariance of this expression (3.6) by a rotation of the coordinate axes, we can obtain the following relations,

$$b^{\nu\nu\mu\mu} = b^{\nu\mu\nu\mu} = b^{\nu\mu\mu\nu} = (1/3) b^{\nu\nu\nu\nu},$$

for all ν and μ ($\nu \neq \mu$), and other $b^{\nu\mu\rho\sigma}$'s are zero. Substituting these into (3.6), we can obtain the same expression as (3.5) by using the relation, $\sum_\nu M_\nu^2 = M_S^2$. (As mentioned in § 1, there is another kind of energy which depends on the average magnetization, from which the value of M_S is determined. Using that value of M_S, we calculate only the energy due to the fluctuation of the direction of M_S, but we do not consider the energy due to the change of the value of $|M_S|$.)

By the same consideration as shown above, the third term in II) is also reduced to (3.5).

Case III) As the energy of the medium is given by an integration of the energy density over the whole volume, the first and second terms in III) can be reduced to the third term by partial integrations. By the consideration similar to that in the case II), we can obtain a new expression for the energy in the case III) as,

$$E^{(2)} = \frac{B}{M_S^2} \sum_{\nu,\alpha,\beta} \int \left(\frac{\partial^2 M_\nu}{\partial x_\alpha \partial x_\beta} \right)^2 d\tau. \tag{3.7}$$

Case IV) We can obtain another expression for the energy connected with the terms in IV) as follows:

$$E^{(3)} = \frac{C}{M_S^4} \sum_{\nu,\mu,\alpha,\beta} \int \left(\frac{\partial M_\nu}{\partial x_\alpha} \right)^2 \left(\frac{\partial M_\mu}{\partial x_\beta} \right)^2 d\tau + \frac{D}{M_S^4} \sum_{\nu,\mu,\alpha,\beta} \int \left(\frac{\partial M_\nu}{\partial x_\alpha} \right) \left(\frac{\partial M_\nu}{\partial x_\beta} \right) \left(\frac{\partial M_\mu}{\partial x_\alpha} \right) \left(\frac{\partial M_\mu}{\partial x_\beta} \right) d\tau. \tag{3.8}$$

The expression for the total energy due to the fluctuation of M can be written by the sum of (3.5), (3.7) and (3.8).

(B) Transformation to Spin Wave Operators

We transform $M(r)$ to the field variables defined by Holstein and Primakoff, $a(r)$ and $a^+(r)$, which are assumed to satisfy the following commutation relation[40],

$$[a(r),\ a^+(r')] = \delta(r-r'). \tag{3.9}$$

We have

$$\left.\begin{aligned} M^+(r) &= (2g\beta M_s)^{1/2}\left\{1-\frac{g\beta}{2M_s}a^+(r)a(r)\right\}^{1/2}a(r), \\ M^-(r) &= (2g\beta M_s)^{1/2}a^+(r)\left\{1-\frac{g\beta}{2M_s}a^+(r)a(r)\right\}^{1/2}, \\ M^z(r) &= M_s - g\beta a^+(r)a(r), \end{aligned}\right\} \tag{3.10}$$

where $M^\pm = M_x \pm iM_y$, g and β are the gyromagnetic ratio and Bohr magneton, respectively.

Creation and annihilation operators of spin waves, $a_k^+ a_k^-$, are obtained by the Fourier transformation of $a^+(r)$ and $a(r)$ as follows:

$$\left.\begin{aligned} a(r) &= \frac{1}{\sqrt{V}}\sum_k \exp(ikr)a_k^-, \\ a^+(r) &= \frac{1}{\sqrt{V}}\sum_k \exp(-ikr)a_k^+, \end{aligned}\right\} \tag{3.11}$$

for volume V, and the commutation relation is given by

$$[a_k^-,\ a_{k'}^+] = \delta_{k,\,k'}. \tag{3.12}$$

Assuming that M_s is large enough, we can expand the square roots in (3.10), and by using (3.11), $M^\pm$ and M^z are expressed by the spin wave operators in the following way.

$$\begin{aligned} M^\pm = \left(\frac{2g\beta M_s}{V}\right)^{1/2}\Bigg[&\sum_k \exp(\pm ikr)a_k^\mp \\ &- \frac{g\beta}{4M_sV}\sum_{1,2,3}\exp\{i(-k_1\pm k_2+k_3)r\}a_1^+a_2^\mp a_3^-\Bigg], \\ M^z = M_s - \frac{g\beta}{V}&\sum_{1,2}\exp\{-i(k_1-k_2)r\}a_1^+a_2^-, \end{aligned} \tag{3.13}$$

where 1, 2, 3 denote k_1, k_2, k_3. We assume that k has a cutoff momentum k_c such as $(V/6\pi^3)k_c^3 = N$, where N is the total number of particles with spin.

By substituting those expressions (3.13) into (3.5), (3.7) and (3.8), the Hamiltonian can be written by the field variables of spin waves. For the first part of the energy (3.5), we can obtain diagonal part, taking up to the order of M_s^{-2}, as follows,

$$\frac{2g\beta A}{M_s}\left\{1+\frac{g\beta N}{2VM_s}\right\}\sum_k k^2 n_k, \tag{3.14}$$

without a constant energy, where $n_k = a_k^+ a_k^-$. On the other hand, the off-diagonal part is obtained as,

$$\frac{g^2\beta^2 A}{2VM_s^2}\sum_{1,2,3,4}{}' \{2(k_2-k_4)^2 - k_1^2 - k_4^2\} a_1^+ a_2^+ a_3^- a_4^- \delta(k_1+k_2-k_3-k_4), \tag{3.15}$$

where Σ' denotes the summation except the terms of $k_1=k_3$, $k_2=k_4$ and $k_1=k_4$, $k_2=k_3$. Therefore, the contribution to the energy from this off-diagonal part is higher-order than M_s^{-3}.

For the second and third parts of the energy, (3.7) and (3.8), we can obtain the diagonal part up to the order of M_s^{-2}.

$$\frac{2g\beta B}{M_s}\left(1+\frac{g\beta N}{2VM_s}\right)\sum_k k^4 n_k + \frac{2g^2\beta^2 B}{VM_s^2}\sum_{1,2}\{k_1^2k_2^2 + 2(k_1\cdot k_2)^2\} n_1 n_2, \tag{3.16}$$

and

$$\frac{2g^2\beta^2}{5\pi^2 M_s^2}\left(\frac{6\pi^2 N}{V}\right)^{5/3}\left(\frac{4}{3}C+D\right)\sum_k k^2 n_k + \frac{2g^2\beta^2}{VM_s^2}\sum_{1,2}\{(2C+3D)(k_1\cdot k_2)^2 + (2C+D)k_1^2k_2^2\} n_1 n_2, \tag{3.17}$$

respectively. The off-diagonal parts of (3.7) and (3.8) contribute to the energy at the order of M_s^{-3}.

From (3.14), (3.16) and (3.17), the total energy up to the order of M_s^{-2} is given by

$$E = \frac{2g\beta A'}{M_s}\sum_k k^2 n_k + \frac{2g\beta B'}{M_s}\sum_k k^4 n_k + \frac{2g^2\beta^2}{VM_s^2}\sum_{1,2}\{(2B+2C+3D)(k_1\cdot k_2)^2 + (B+2C+D)k_1^2k_2^2\} n_1 n_2, \tag{3.18}$$

where A' and B' are written as,

$$A' = A\left\{1+\frac{g\beta N}{2VM_s}\right\} + \frac{g\beta}{5\pi^2 M_s}\left(\frac{6\pi^2 N}{V}\right)^{5/3}\left(\frac{4}{3}C+D\right).$$

$$B' = B\left(1+\frac{g\beta N}{2VM_s}\right).$$

In the case where C and D are zero (as in the case of the Heisenberg model), our treatment is a good approximation, when $(g\beta N/2VM_s) \ll 1$ (This condition is equivalent to the condition, $2S \gg 1$, in the Heisenberg model, because N is the number of atoms and $g\beta/M_s = V/NS$ in this model, where S is the magnitude of the spin per one atom). The terms proportional to $n_1 n_2$ in (3.18) represent the spin wave interactions and have the same form as (3.4), which was found by Marshall[35], when we write

$$\sum_{1,2}(k_1 \cdot k_2)^2 n_1 n_2 = \frac{1}{3}\sum_{1,2} k_1^2 k_2^2 n_1 n_2,$$

because n_k does not depend on the direction of k by the assumption of the isotropic spin waves. These interaction terms can be approximately reduced to the coefficient in the energy for one-body, A, as

$$\sum_{1,2} k_1^2 k_2^2 n_1 n_2 \simeq 2\sum_k \langle k'^2 n_{k'} \rangle k^2 n_k = 12\pi V\left(\frac{M_s k_B T}{8\pi g\beta A}\right)^{5/2}\zeta(5/2)\sum_k k^2 n_k,$$

where $\langle\ \rangle$ denotes the mean value for the thermal equilibrium states and k_B and $\zeta(n)$ are the Boltzmann constant and ζ-function, respectively. The dispersion relation for spin wave is given by

$$\hbar\omega_k = \frac{2g\beta}{M_s}A^* k^2 + \frac{2g\beta}{M_s}B' k^4, \tag{3.19}$$

where

$$A^* = A' + \frac{12\pi g\beta}{M_s}\left(\frac{M_s k_B T}{8\pi g\beta A}\right)^{5/2}\left(\frac{5}{3}B + \frac{8}{3}C + 2D\right)\zeta(5/2).$$

This shows that the effective exchange stiffness constant, A^*, varies with the temperature as $T^{5/2}$, which was observed by neutron diffraction experiments even for 3 d-transition metals and alloys[41].

Now we discuss the validity of the approximation where we have taken account only of the terms in cases I)–IV) in the expression for the energy density in (A) of this section. As we can see from (3.13), one spin wave momentum, k, is derived from the first derivative of M with respect to x in the energy. On the other hand, it can be seen that one M gives at least one spin wave operator, a_k^+ or a_k^-, in the leading term of the energy as follows. The leading term of $M^\pm$ is $a_k^\mp$, but in the case of M^z, one M^z gives two spin wave operators, when a term consists only of derivative forms of M_ν. When a term has one M_ν not as a derivative, another M_ν must be included as a derivative unless this term will be reduced to a simpler form by using $\sum_\nu M_\nu^2 = M_s^2$, *e.g.* one M^z gives M_s and another M^z gives two spin wave operators in the leading term, if $\nu = z$. Thus we can consider that the leading term in the energy has the same number of spin wave operators as the number of M included in the energy due to the fluctuation of the magnetization. Therefore, the three terms, $k^2 n_k$, $k^4 n_k$ and $k^2 k'^2 n_K n_k$ are the leading terms obtained only from the cases I)–IV), and other cases lead to higher-order terms in the expression for the energy than the terms given in (3.18) at low temperature, for instance, $k^6 n_k$, $k^4 k'^2 n_K n_k$ *etc.*

(C) Classical Treatment of Spin Waves with the New Expression for the Energy

We have obtained the expressions (3.5), (3.7) and (3.8) for the energy due to the fluctuation of the magnetization. It has been found that the leading term derived from (3.8) corresponds to the interactions between spin waves as shown in the previous section, so that we can approximately include the contribution of the interaction part in (3.8) to the energy if we make use of A^* and B' instead of A and B in (3.5) and (3.7), as shown in the following Hamiltonian,

$$\mathscr{H} = \frac{A^*}{M_s^2}\sum_{\nu,\alpha}\int\left(\frac{\partial M_\nu}{\partial x_\alpha}\right)^2 d\tau + \frac{B'}{M_s^2}\sum_{\nu,\alpha,\beta}\int\left(\frac{\partial^2 M_\nu}{\partial x_\alpha \partial x_\beta}\right)^2 d\tau.$$

The equations of motion for the magnetization density at point r are given by

$$-i\hbar\dot{M}_\alpha(r) = [\mathscr{H}, M_\alpha(r)].$$

Using the commutation relations such as,

$$[M_x(r), M_y(r')] = ig\beta M_z(r)\delta(r-r'),$$

which are obtained from (3.9) and (3.10), we can get a equation of motion as

$$\dot{\boldsymbol{M}} = \gamma \boldsymbol{M}\times \boldsymbol{H}_{ex}, \tag{3.20}$$

where

$$\boldsymbol{H}_{ex} = \frac{2A^*}{M_s^2}\nabla^2\boldsymbol{M} - \frac{2B'}{M_s^2}\nabla^4\boldsymbol{M}, \tag{3.21}$$

$$\nabla^2 = \sum_\alpha \frac{\partial^2}{\partial x_\alpha^2}, \quad \nabla^4 = \sum_{\alpha,\beta}\frac{\partial^4}{\partial x_\alpha^2 \partial x_\beta^2},$$

and γ is $g\beta/\hbar$ and $\boldsymbol{H}_{ex}$ denotes the exchange field. The first term in $\boldsymbol{H}_{ex}$ was already derived by Landau and Lifshitz[42], and Herring and Kittel[10]. The second term is the correction to the first term and corresponds to the fourth power of spin wave momentum in the energy of the spin waves. It will be seen that this expression (3.21) is very useful for the classical analyses of the spin wave with finite wave length.

§ 3. Observed Values of the Exchange Stiffness Constant

In experiments the values of D $(=4\mu_B A/M_s)$ are observed by the following three methods for ferromagnetic metals and alloys.

(I) Inelastic neutron scattering

In this method, Sinclair and Brockhouse[43] first observed the dispersion relation of spin waves for fcc cobalt. Recently this method has been advanced and many measurements of the spin waves for various ferromagnetic metals and alloys have been reported by the diffraction method, the small angle inelastic scattering method and the triple axis spectrometry. Shirane *et al.*[44][45] have reported the dispersion relation of spin waves which deviates considerably from the quadratic law (3.3) for iron and fcc cobalt metals. This fact shows that the value of B' in (3.19) is large for these metals.

At present, there is an interesting question where the dispersion relation of spin waves for fcc cobalt has an anomaly or not. Frikkee and Riste[46], Furrer *et al.*[47] and Frikkee[48] have found an anomaly in the dispersion relation of spin waves for fcc cobalt. They have connected this anomaly with the Kohn anomaly or with the interaction between spin waves and phonons. However, the connection with Kohn anomaly cannot be expected from the calculation within the random phase approximation, as mentioned by Mattis[49]. On the other hand,

Riste *et al.*[50] and Pickart *et al.*[51] have not observed such an anomaly in the dispersion curve for fcc cobalt.

(II) Spin wave resonance

The experiments of the spin wave resonance have been carried out for thin ferromagnetic films. In the model which was proporsed by Kittel[52], the surface spins on the film are pinned out by the surface anisotropy, under this boundary condition for spins the equation of motion (3. 20) with the first term of (3. 21) gives a series of resonance frequencies, and the value of D can be deduced from the separations between these resonance frequencies.

Weber and Tannenwald[53] have measured the temperature variation of the absorbed line separations and reported the $T^{5/2}$ dependence of D below 80°K for permalloy film. On the other hand, Phillips and Rosenberg[54] have observed the $T^{3/2}$ dependence of D for nickel film. Recently Phillips[55] has observed the temperature variation of D for iron film and shown that the data can be analysed into the terms of T^2 and $T^{5/2}$, though the data show the dependence closed to $T^{3/2}$. The $T^{5/2}$ dependence of D is led from the spin wave-spin wave interactions as shown in this chapter, A^* in (3. 19).

(III) Temperature variation of magnetization at low temperature

As mentioned previously in this chapter, the magnetization decreases with increasing temperature as $T^{3/2}$ (Bloch's law). The coefficient of $T^{3/2}$ is proportional to $D^{-3/2}$. Thompson *et al.*[56] have shown that for unsaturated ferromagnetic metals the coefficient of $T^{3/2}$ in the temperature variation of the magnetization is composed of the two terms which are derived from the free spin waves and from the coupling between spin waves and individual electrons via the molecular field. However the basis of this theory is not confirmed.

The observed values of D by the three methods mentioned above are shown

TABLE 2. Observed values of D by inelastic neutron scattering (NS), spin wave resonance (SR) and the temperature variation of the magnetization at low temperature (M). The unit is eV Å^2

	NS	SR	M
Fe	0.32 (41) 0.28 (57) 0.27 (44) 0.28 (45)	0.34 (55) 0.27 (58)	0.31 (59) 0.23 (60) 0.28 (61)
Co (fcc)	0.37 (43) 0.17 (46, 47)* 0.28 (48)* 0.38 (51) 0.37 (45)	0.35 (62)	0.33 (63)
(hcp)	0.49 (64)		0.40 (60)
Ni	0.40 (41) 0.36 (50) 0.37 (51)	0.41 (62) 0.44 (58)	0.33 (65) 0.46 (8) 0.34 (60, 66) 0.37 (61)

Numbers in the bracket denote the number of references.
* An anomaly was found in the dispersion curve of the spin wave.

in Table 2 for iron, cobalt and nickel metals. The fact that a good agreement is obtained among those values shows the validity of the phenomenological theory given in this chapter.

§ 4. Evaluation of Exchange Stiffness Constants A and B

In this section, we determine the coefficients A in (3.5) and B in (3.7) for ferromagnetic metals by the perturbation method as Herring evaluated the value of A[38].

When a perturbing field

$$\left.\begin{aligned} H_x &= h\cos(q\cdot r),\\ H_y &= h\sin(q\cdot r),\end{aligned}\right\} \tag{3.22}$$

is put on a uniformly magnetized material, the magnetization will fluctuate as

$$\left.\begin{aligned} M_x &= m\cos(q\cdot r),\\ M_y &= m\sin(q\cdot r),\end{aligned}\right\} \tag{3.23}$$

where m is the amplitude determined later. The increase of the energy due to the fluctuation of the magnetization (3.23) is obtained as

$$\left\{\frac{A}{M_s^2}m^2q^2+\frac{B}{M_s^2}m^2q^4+\frac{C+D}{M_s^4}m^4q^4\right\}V, \tag{3.24}$$

from (3.5), (3.7) and (3.8), where V denotes the total volume. On the other hand, the gain in the energy due to the magnetic field (3.22) is written as

$$-\int(M\cdot H)\,d\tau=-mhV. \tag{3.25}$$

The amplitude of the fluctuation of the magnetization m is determined so as to minimize ΔE, the sum of the energies (3.24) and (3.25), and we get

$$m=\frac{hM_s^2}{2(Aq^2+Bq^4)}-\frac{(C+D)q^4h^3M_s^4}{4(Aq^2+Bq^4)^4}. \tag{3.26}$$

Using (3.24), (3.25) and (3.26), we obtain

$$\Delta E=-\frac{h^2M_s^2V}{4(Aq^2+Bq^4)}+\frac{h^4(C+D)M_s^4q^4V}{16(Aq^2+Bq^4)^4}. \tag{3.27}$$

From (3.27) it is found that the values of A and B can be evaluated from the coefficient of h^2 in ΔE, but C and D are evaluated from the coefficient of h^4.

In the Heisenberg model the Hamiltonian is the sum of scalar products of two spin vectors on the different lattice sites. Therefore, the term of h^4 in (3.27) does not appear in the Heisenberg model (*cf.* (3.8)). On the other hand, in the band model the change of the energy ΔE by the perturbing field (3.22) in a ferromagnetic metal can be expanded in an even power series of h by the usual perturbation method, so that the terms of C and D are characteristic of the band model (In the s-d model[67], the indirect interaction between two spins is obtained

by the second-order perturbation theory and fourth-order perturbation theory gives an interaction between four spins, so that the terms C and D exist also in the s-d model.). Unfortunately, the fourth-order perturbation calculation is very complicated and tedious for electrons in metals and we calculate only the term of the second-order perturbation, that is, the term proportional to h^2 in ΔE and find the values of A and B.

The Hamiltonian of electrons in the perturbing field (3.22) is written as

$$\mathscr{H}=\sum_i\left[-\frac{\hbar^2\nabla_i^2}{2m}+\sum V(r_i-R_n)-\frac{\mu_B h}{2}\{\exp(iq\cdot r_i)\sigma_-+\exp(-iq\cdot r_i)\sigma_+\}\right]$$
$$+\frac{1}{2}\sum_{i\neq j}v(|r_i-r_j|), \tag{3.28}$$

where $V(r_i-R_n)$ is the potential of the i-th electron due to the ion at R_n, σ denotes the Pauli spin matrix and $\sigma_\pm=\sigma_x\pm i\sigma_y$ and $v(|r_i-r_j|)$ is the Coulomb interaction between the i-th and j-th electrons. We assume the wave function of electrons to be expressed by a single Slater determinant.

For the sake of simplicity, we take the unperturbed ground state to be a saturated ferromagnetic one and assume the unperturbed wave function of an electron with momentum k and spin σ to be a product of the orbital wave function ϕ_k and the spin one ξ_σ. The perturbed wave function of an electron can be expanded in a power series of h as

$$\psi_{k\sigma}=\phi_k\xi_\sigma+\sum_{l,\sigma'}\{hU(k\sigma,\ l\sigma')+h^2V(k\sigma,\ l\sigma')\}\phi_l\xi_{\sigma'}, \tag{3.29}$$

where the quantities U and V are determined later so as to minimize the total energy. The orthonormal condition of $\phi_{k\sigma}$ is written as

$$\left.\begin{aligned}&U(k\sigma,\ l\sigma')+U^*(l\sigma',\ k\sigma)=0,\\&V(k\sigma,\ l\sigma')+V^*(l\sigma',\ k\sigma)+\sum_{p,\sigma''}U^*(l\sigma',\ p\sigma'')U(k\sigma,\ p\sigma'')=0.\end{aligned}\right\} \tag{3.30}$$

Using the single Slater determinant which is constructed from (3.29), we calculate the expectation value of the Hamiltonian (3.28) up to the order of h^2. The wave function ϕ_k is expressed by the Wannier functions as

$$\phi_k(r)=\frac{1}{\sqrt{N}}\sum_n\exp(ik\cdot R_n)w(r-R_n), \tag{3.31}$$

where N is the number of atoms. To calculate expectation value of the third term in the square bracket of (3.28), the quantity

$$\int\phi^*_{k+q}\exp(iq\cdot r)\phi_k d\tau$$

is rewritten by the Wannier functions. We assume that the Wannier functions are well localized, and take only the integrals on a single lattice site as

$$\frac{1}{N}\sum_{n,m}\int \exp\{-i(k+q)\cdot R_n + iq\cdot r + ik\cdot R_m\} w^*(r-R_n)w(r-R_m)d\tau$$
$$\cong \int \exp(iq\cdot r)|w(r)|^2 d\tau = P(q). \tag{3.32}$$

For the Coulomb matrix elements, we make use of the approximation

$$\int d\tau \int d\tau' \phi^*_{k_1}(r)\phi^*_{k_2}(r')v(|r-r'|)\phi_{k_4}(r)\phi_{k_3}(r')$$
$$\cong \frac{1}{N}\{I+J(k_4-k_2)\}\delta(k_1+k_2-k_3-k_4), \tag{3.33}$$

where

$$I = \int d\tau \int d\tau' |w(r)|^2 |w(r')|^2 v(|r-r'|),$$

$$J(q) = \sum_{n(\neq 0)} \exp(iq\cdot R_n)\int d\tau \int d\tau' w^*(r)w^*(r'-R_n)v(|r-r'|)w(r-R_n)w(r'),$$

$$\delta(k_1+k_2-k_3-k_4) = \begin{cases} 1, & \text{for } k_1+k_2-k_3-k_4 = 0 \text{ or } K_n, \\ 0, & \text{otherwise,} \end{cases}$$

here K_n is a reciprocal lattice vector and I and J denote the intra-atomic Coulomb integral and the Fourier component of inter-atomic exchange integrals, respectively.

Using the conditions (3.30) and approximations (3.32) and (3.33), we get the total energy in the perturbed state as

$$E(h) = E^{(0)} + E^{(2)}h^2, \tag{3.34}$$

up to the order of h^2, where

$$E^{(0)} = \sum_k \varepsilon(k) + \frac{1}{2}\sum_{k,k'}\{J(k-k') - J(0)\}, \tag{3.35}$$

$$E^{(2)} = \sum_{k,l}[\varepsilon(l) - \varepsilon(k) - \sum_{k'}\{J(l-k') - J(k-k') - n\{I+J(0)\}\}]U(l\downarrow, k\uparrow)U(k\uparrow, l\downarrow)$$
$$- \mu_B P(q)\sum_k \{U(k\uparrow, k+q\downarrow) - U(k+q\downarrow, k\uparrow)\}$$
$$+ \{I+J(q)\}\sum_{k,k'} U(k+q\downarrow, k\uparrow)U(k'\uparrow, k'+q\downarrow), \tag{3.36}$$

$$\varepsilon(k) = \int d\tau \phi^*_k \left\{-\frac{\hbar^2\nabla^2}{2m} + \sum_n V(r-R_n)\right\}\phi_k,$$

and n is the number of electrons, that is, $\mu_B n$ is the magnetization because we assume the ground state to be a saturated ferromagnetic one. In (3.35) and (3.36), the summations over k and k' are restricted in the occupied state, that is, $|k|$, $|k'| \leq k_f$, where k_f denotes the Fermi momentum of up spin band. The summation over l is not restricted because the down spin band is empty. The energy (3.35) is the unperturbed total energy and (3.36) denotes the change of the total energy due to the perturbing field.

The value of U is determined so as to minimize the energy (3.34) with respect to U and we get

$$U(k\uparrow,\ l\downarrow)=\delta(l,\ k+q)\frac{P(q)\mu_B}{\tilde{\varepsilon}(k+q)-\tilde{\varepsilon}(k)+n\{I+J(0)\}}\times\frac{1}{1-\sum_k\dfrac{I+J(q)}{\tilde{\varepsilon}(k+q)-\tilde{\varepsilon}(k)+n\{I+J(0)\}}},\tag{3.37}$$

where

$$\tilde{\varepsilon}(k)=\varepsilon(k)-\sum_{k'}J(k-k').$$

From (3.36) and (3.37), we get

$$E=E^{(0)}-\frac{1}{2}h^2\chi(q),\tag{3.38}$$

where

$$\chi(q)=P(q)^2\frac{\chi_0(q)}{1-\{I+J(q)\}\chi_0(q)/2\mu_B^2},\tag{3.39}$$

and

$$\chi_0(q)=2\mu_B^2\sum_k\frac{1}{\tilde{\varepsilon}(k+q)-\tilde{\varepsilon}(k)+n\{I+J(0)\}}.\tag{3.40}$$

here (3.39) is the similar expression to that obtained within the random phase approximation[68) 69)].

Inserting (3.38) into (3.27), we get

$$Aq^2+Bq^4=\frac{M_S^2V}{2}\chi(q)^{-1}.\tag{3.41}$$

Expanding $\chi(q)$ in a power series of q, we get A and B as,

$$Aq^2=-\frac{Vn^2}{8}(q\cdot\nabla)^2J(0)+\frac{V}{4}\sum_k\left[\frac{1}{2}(q\cdot\nabla)^2\tilde{\varepsilon}(k)-\frac{1}{\Delta}\{(q\cdot\nabla)\tilde{\varepsilon}(k)\}^2\right].\tag{3.42}$$

$$\begin{aligned}Bq^4=&\,2Aq^2\{1-P(q)\}+\frac{V}{96}\sum_k(q\cdot\nabla)^4\tilde{\varepsilon}(k)\\&-\frac{V}{16\Delta}\sum_k\{(q\cdot\nabla)^2\tilde{\varepsilon}(k)\}^2\\&-\frac{V}{12\Delta}\sum_k\{(q\cdot\nabla)\tilde{\varepsilon}(k)\}\{(q\cdot\nabla)^3\tilde{\varepsilon}(k)\}\\&+\frac{3V}{8\Delta^2}\sum_k\{(q\cdot\nabla)\tilde{\varepsilon}(k)\}^2(q\cdot\nabla)^2\tilde{\varepsilon}(k)\\&-\frac{V}{4\Delta^3}\sum_k\{(q\cdot\nabla)\tilde{\varepsilon}(k)\}^4\\&+\frac{V}{4n\Delta}\left[\sum_k\left\{\frac{1}{2}(q\cdot\nabla)^2\tilde{\varepsilon}(k)-\frac{1}{\Delta}\{(q\cdot\nabla)\tilde{\varepsilon}(k)\}^2\right\}\right]^2\\&-\frac{Vn^2}{96}(q\cdot\nabla)^4J(0).\end{aligned}\tag{3.43}$$

The result (3.42) is exactly the same with the corresponding term in the dispersion relation of a spin wave, which was obtained within the random phase approximation for a saturated ferromagnetic state[68)69)] but in the case of the higher-order term proportional to q^4 there is a difference between our result (3.43) and the corresponding term which is obtained in the spin wave theory as,

$$
\begin{aligned}
Bq^4 = {} & \frac{V}{96}\sum_k (q\cdot\nabla)^4\tilde{\varepsilon}(k) - \frac{V}{16\Delta}\sum_k\{(q\cdot\nabla)^2\tilde{\varepsilon}(k)\}^2 \\
& - \frac{V}{12\Delta}\sum_k\{(q\cdot\nabla)\tilde{\varepsilon}(k)\}\{(q\cdot\nabla)^3\tilde{\varepsilon}(k)\} \\
& + \frac{3V}{8\Delta^2}\sum_k\{(q\cdot\nabla)\tilde{\varepsilon}(k)\}^2(q\cdot\nabla)^2\tilde{\varepsilon}(k) \\
& - \frac{V}{4\Delta^3}\sum_k\{(q\cdot\nabla)\tilde{\varepsilon}(k)\}^4 \\
& - \frac{3V}{8n\Delta^2}\left[\sum_k(q\cdot\nabla)^2\tilde{\varepsilon}(k)\right]\cdot\left[\sum_k\{(q\cdot\nabla)\tilde{\varepsilon}(k)\}^2\right] \\
& + \frac{2V}{4n\Delta^3}\left[\sum_k\{(q\cdot\nabla)\tilde{\varepsilon}(k)\}^2\right]^2 \\
& + \frac{V}{16n\Delta}\left[\sum_k(q\cdot\nabla)^2\tilde{\varepsilon}(k)\right]^2 \\
& - \frac{n^2V}{96}(q\cdot\nabla)^4J(0) \\
& + \frac{nV}{8\Delta^2}(q\cdot\nabla)^2J(0)\cdot\sum_k\{(q\cdot\nabla)\tilde{\varepsilon}(k)\}^2. \qquad (3.44)
\end{aligned}
$$

This difference is due to the fact that our results (3.42) and (3.43) are calculated from the static susceptibility $\chi(q)$ and the dispersion relation of spin waves is calculated from the dynamical susceptibility $\chi(q, \omega)$, that is, the response of the magnetization to the external field with frequency ω, within the random phase approximation[68)69)]. The dynamical effect is not treated in this section, because we have calculated the response of the magnetization to the static field (3.22), and it is a problem left in future how to treat this dynamical effect in the phenomenological theory.

Chapter IV. Microscopic Theory of Spin Waves[70)]

§ 1. Introduction

Recently, using the method of normal mode, Englert and Antonoff[68)] obtained the dispersion relation of a long wave length spin wave in metals within the random phase approximation which is used successfully in the theory of plasmon in an electron gas[71)72)]. They have shown that the coefficient of the square of momentum in the dispersion relation of spin waves consists of two parts. The first part is derived from the intra-atomic Coulomb integral based on the Wannier functions and is closely related to the electronic structures of the metals. The second part is derived from the inter-atomic exchange integral. The latter is

the same as the result which is obtained in the Heisenberg model. It is very instructive that the contributions to the dispersion relation of spin wave from the itinerant and localized characters of electrons are additive, because it is considered that the ferromagnetism of 3 d-transition metals can be explained by a compromised model of the itinerant model and the Heisenberg one.

Englert and Antonoff[68], however, have neglected the effects of the correlation among electrons and of multiple bands on the spin wave spectrum in their calculation. An appropriate treatment of the former effect will be very difficult and we will not discuss it. The purpose of this chapter is to investigate the latter effect, that is, the dispersion relation of a spin wave in ferromagnetic metals with multiple bands. Two attempts on this problem have been made by Mattis[13] and Thompson[12]. Mattis[13] has obtained the dispersion relation of a spin wave from the equation of motion for spin operators, but his treatment is restricted to the case of two degenerate bands with only the inter-band exchange interaction. On the other hand, Thompson[12] has treated more general case by the variation method and obtained two kinds of spin wave spectra, optical and acoustical branches. In both calculations, the state of electrons with a spin wave is described by a linear combination of the wave functions in the excited states which are made by reversing one spin only in the same band in the ferromagnetic ground state (*cf.* (4.8)), and off-diagonal matrix elements of the Coulomb interactions among different sub-bands are neglected, so that the effect of inter-band transitions with a reversed spin on the dispersion relation of spin waves is neglected.

Taking account of the effect of inter-band transitions on the spin wave spectra, we will investigate the spin wave spectra for ferromagnetic metals with multiple bands by the method of normal modes in this chapter. In § 2, we transform the Hamiltonian for electrons with multiple bands so as to be appropriate to the Hartree-Fock approximation for one particle energy, because we adopt the (extended) random phase approximation[71]. Using this transformed Hamiltonian, we study the equation of motion for spin flipping operators and obtain an eigenvalue equation, which gives the excitation energy of normal modes, in § 3. To examine the solution of this eigenvalue equation, we consider the limiting case where the wave vector of the normal modes is zero in § 4 and moreover, we get the dispersion relation of a spin wave with long wave length in § 5. In § 4 and § 5, it is found that spin wave spectra consist of one acoustical intra-band branch, some optical intra-band branches and other branches due to the inter-band transitions. Hereafter we call this spin wave due to the inter-band transitions as *inter-band spin wave.*

The coefficient of the square of momentum in the dispersion relation of the acoustical intra-band spin wave is given by the sum of D_R and D_H which are derived from the intra-atomic Coulomb interaction and inter-atomic exchange interaction, respectively. We roughly estimate the value of D_R, which is closely related to the electronic structures, for nickel metal, assuming two appropriate sub-bands. In § 7, it is pointed out that the inter-band transitions have important effects on the dispersion relation of the acoustical intra-band spin wave in the multiple band model.

The whole spectra of the excitations of electrons with a reversed spin are calculated in the single band and two band models and the cut-off momentum of the spin wave is discussed in the single band model in § 8 and § 9.

§ 2. Hamiltonian in the Multiple Band Model

The Hamiltonian describing electrons in a periodic lattice potential may be written as,

$$\begin{aligned}
&\mathscr{H} = \mathscr{H}_0 + \mathscr{H}', \\
&\mathscr{H}_0 = \sum_{k\nu\sigma} \in_\nu(k) c^+_{k\nu\sigma} c_{k\nu\sigma}, \\
&\mathscr{H}' = \frac{1}{2} \sum_{k_1\cdots k_4} \sum_{\nu_1\cdots\nu_4} \sum_{\sigma\sigma'} V(k_1\nu_1,\ k_2\nu_2;\ k_4\nu_4,\ k_3\nu_3) \\
&\qquad\qquad \times c^+_{k_1\nu_1\sigma} c^+_{k_2\nu_2\sigma'} c_{k_3\nu_3\sigma'} c_{k_4\nu_4\sigma},
\end{aligned} \tag{4.1}$$

where $c^+_{k\nu\sigma}$ and $c_{k\nu\sigma}$ are creation and annihilation operators of a Bloch electron with momentum k, spin σ and sub-band index ν in the first Brillouin zone, and they satisfy the usual anti-commutation relations. The matrix element $V(k_1\nu_1,\ k_2\nu_2;\ k_4\nu_4,\ k_3\nu_3)$ is given by

$$\begin{aligned}
&V(k_1\nu_1,\ k_2\nu_2;\ k_4\nu_4,\ k_3\nu_3) \\
&\quad = \iint dr_1 dr_2 \phi^*_{k_1\nu_1}(r_1) \phi^*_{k_2\nu_2}(r_2) v(|r_1 - r_2|) \phi_{k_4\nu_4}(r_1) \phi_{k_3\nu_3}(r_2),
\end{aligned} \tag{4.2}$$

where $\phi_{k\nu}(r)$ is the eigen function of the one-electron Hamiltonian, that is, the sum of kinetic energy and periodic lattice potential, and $v(|r_1 - r_2|)$ denotes the Coulomb interaction. The matrix element (4.2) subjects to the following momentum conservation,

$$k_1 + k_2 - k_3 - k_4 = 0 \quad \text{or} \quad K_n, \tag{4.3}$$

where K_n is a reciprocal lattice vector.

The sub-band indices ν_i in (4.1) are not suitable for describing one electron states, because the off-diagonal inter-band matrix elements of $\mathscr{H}'$ are not zero, as shown in the Appendix A. In order to eliminate those off-diagonal inter-band matrix elements of $\mathscr{H}'$ within the Hartree-Fock approximation, we make use of another expression for the Hamiltonian, which is derived in Appendix A, as follows,

$$\begin{aligned}
\mathscr{H} &= \sum_{k\lambda\sigma} E_{\lambda\sigma}(k) a^+_{k\lambda\sigma} a_{k\lambda\sigma} \\
&+ \frac{1}{2} \sum_{k_1\cdots k_4} \sum_{\xi_1\cdots\xi_4} \sum_{\sigma\sigma'} W(k_1\xi_1,\ k_2\xi_2;\ k_4\xi_4,\ k_3\xi_3)\, a^+_{k_1\xi_1\sigma} a^+_{k_2\xi_2\sigma'} a_{k_3\xi_3\sigma'} a_{k_4\xi_4\sigma} \\
&- \sum_{k_1k_2} \sum_{\xi_1\xi_2\xi_3} \sum_{\sigma\sigma'} W(k_1\xi_1,\ k_2\xi_2;\ k_1\xi_3,\ k_2\xi_2)\, n_{k_2\xi_2\sigma} a^+_{k_1\xi_1\sigma'} a_{k_1\xi_3\sigma'} \\
&+ \sum_{k_1k_2} \sum_{\xi_1\xi_2\xi_3} \sum_{\sigma} W(k_1\xi_1,\ k_2\xi_2;\ k_2\xi_2,\ k_1\xi_3)\, n_{k_2\xi_2\sigma} a^+_{k_1\xi_1\sigma} a_{k_1\xi_3\sigma},
\end{aligned} \tag{4.4}$$

where the Hartree-Fock energy $E_{\lambda\sigma}(k)$ and matrix element $W(k_1\xi_1,\ k_2\xi_2;\ k_4\xi_4,\ k_3\xi_3)$ are given by (A.8) and (A.6), respectively. The first term in the right-hand side of (4.4) is the Hartree-Fock Hamiltonian, the second term denotes the Coulomb interaction and the third and fourth terms are corrections to the first term. The Hamiltonian similar to (4.4) has been given by Hubbard[28] for electrons in the model of a single band which is paramagnetic.

From (A.9), we get the following condition for matrix element W, in the

same approximation as that used in obtaining (4.4),

$$\sum_{k\xi} W(k\xi,\ p\lambda\,;\ p\eta,\ k\xi)(n_{k\xi\uparrow} - n_{k\xi\downarrow}) = 0, \qquad (\lambda \neq \eta) \tag{4.5}$$

by taking up and down spins for σ in (A.9).

§ 3. Integral Equation for Normal Modes

An operator which represents a normal mode of spin flipping with momentum q is defined by

$$A_q^+ = \sum_{p\lambda\mu} f_{\lambda\mu}(q, p)\, a^+_{p+q\lambda\downarrow}\, a_{p\mu\uparrow}, \tag{4.6}$$

where we must interpret $p+q$ as $p+q-K_n$ in order to reduce $p+q$ in the first Brillouin zone when $p+q$ is outside this zone, and we take here up and down spins to be majority and minority spins, respectively. Coefficients $f_{\lambda\mu}(q, p)$ are determined by the following equation of motion,

$$\hbar\omega A_q^+ = [\mathscr{H},\ A_q^+], \tag{4.7}$$

where $\mathscr{H}$ is given by (4.4).

The spin wave state with momentum q treated by Mattis[13] and Thompson[12] is

$$\sum_{p\mu} f_{\mu\mu}(q,\ p)\, a^+_{p+q\mu\downarrow}\, a_{p\mu\uparrow}\Psi_0, \tag{4.8}$$

where Ψ_0 is a wave function of the ground state. Our aim is to find the eigenvalues of the elementary excitation with a reversed spin for the Hamiltonian (4.1) or (4.4) in the multiple band medel and to show that some of these excited states correspond to the spin wave states. Therefore, we must not define *a priori* the spin wave state as (4.8), though (4.8) is equal to (4.6) at $q=0$ as shown in § 4.

Evaluation of the commutator (4.7) is straightforward, but the result is a complicated expression involving a sum of products of either two or four creation and annihilation operators. For the products of four operators, we use the (extended) random phase approximation[71] as

$$\begin{aligned} &a^+_{k_1\xi_1\sigma_1} a^+_{k_2\xi_2\sigma_2} a_{k_3\xi_3\sigma_3} a_{k_4\xi_4\sigma_4} \\ &\quad = n_{k_1\xi_1\sigma_1}\{\delta_{1,4} a^+_{k_2\xi_2\sigma_2} a_{k_3\xi_3\sigma_3} - \delta_{1,3} a^+_{k_2\xi_2\sigma_2} a_{k_4\xi_4\sigma_4}\} \\ &\quad + n_{k_2\xi_2\sigma_2}\{\delta_{2,3} a^+_{k_1\xi_1\sigma_1} a_{k_4\xi_4\sigma_4} - \delta_{2,4} a^+_{k_1\xi_1\sigma_1} a_{k_3\xi_3\sigma_3}\}, \end{aligned} \tag{4.9}$$

where $\delta_{1,2}$ denotes a product of δ-functions, $\delta(k_1-k_2)\,\delta(\xi_1-\xi_2)\,\delta(\sigma_1-\sigma_2)$, and $n_{k\xi\sigma}$ is the expectation value of an occupation number in the ground state of the unperturbed Hamiltonian given by the first term in (4.4). Then, from (4.6), (4.7) and (4.9) we get

$$\begin{aligned} &\{E_{\lambda\downarrow}(p+q) - E_{\mu\uparrow}(p) - \hbar\omega\} f_{\lambda\mu}(q,\ p) \\ &\quad - \sum_{k\xi\eta} W(p+q\lambda,\ k\eta\,;\ k+q\xi,\ p\mu)(n_{k\eta\uparrow} - n_{k+q\xi\downarrow}) f_{\xi\eta}(q,\ k) = 0, \end{aligned} \tag{4.10}$$

by identifying the coefficients of $a^+_{p+q\lambda\downarrow} a_{p\mu\uparrow}$ in the left- and right-hand sides of

(4. 7). The excitation energies of spin waves are given by eigenvalues $\hbar\omega$ of the integral equation (4. 10).

If we start from the Hamiltonian given by (4. 1) and the normal mode (4. 6) where a^+ and a are replaced by c^+ and c we get a very complicated integral equation which is not so simple as (4. 10), and furthermore this treatment is meaningless, because the sub-band indices ν_i in (4. 1) are not suitable for describing one electron states, as mentioned in § 2.

Before discussing (4. 10), we simplify this equation by using some approximations for the matrix elements, $W(\boldsymbol{p}+\boldsymbol{q}\lambda,\ k\eta;\ \boldsymbol{k}+\boldsymbol{q}\xi,\ \boldsymbol{p}\mu)$. We first write the matrix elements in terms of the Wannier function,

$$w_\xi(\boldsymbol{r}-\boldsymbol{R}) = \frac{1}{\sqrt{N}}\sum_{\boldsymbol{k}}\exp(-i\boldsymbol{k}\boldsymbol{R})\,\varphi_{\boldsymbol{k}\xi}(\boldsymbol{r}), \tag{4.11}$$

where N is the number of lattice sites. From (A. 6), we can get

$$\begin{aligned} &W(k_1\xi_1,\ k_2\xi_2;\ k_4\xi_4,\ k_3\xi_3)\\ &\quad=\frac{1}{N^2}\sum_{R_1\cdots R_4}\exp(-ik_1R_1-ik_2R_2+ik_3R_3+ik_4R_4)\\ &\quad\times\iint dr\,dr' w^*_{\xi_1}(r-R_1)\,w^*_{\xi_2}(r'-R_2)\,v(|r-r'|)\,w_{\xi_4}(r-R_4)\,w_{\xi_3}(r'-R_3). \end{aligned} \tag{4.12}$$

The inter-atomic exchange integral ($\boldsymbol{R}_1=\boldsymbol{R}_3$, $\boldsymbol{R}_2=\boldsymbol{R}_4$ in (4. 12)) is important, although the intra-atomic Coulomb integral ($\boldsymbol{R}_1=\boldsymbol{R}_2=\boldsymbol{R}_3=\boldsymbol{R}_4$) is fairly larger than this integral, because these two integrals contribute to the dispersion relation of a spin wave in different ways as mentioned in § 1. Following the treatment of Englert and Antonoff[68], we also make use of the approximation,

$$\begin{aligned} &W(k_1\xi_1,\ k_2\xi_2;\ k_4\xi_4,\ k_3\xi_3)\\ &\quad\simeq\frac{1}{N}\{U(\xi_1,\ \xi_2;\ \xi_4,\ \xi_3)+J(k_3-k_1:\ \xi_1,\ \xi_2;\ \xi_4,\ \xi_3), \end{aligned} \tag{4.13}$$

where J denotes the inter-atomic exchange integral and U denotes the sum of the intra-atomic Coulomb integral and other multi-center integrals. Here, the momentum dependences of the multi-center integrals are neglected.

Using the approximation (4. 13) we can rewrite $E_{\lambda\sigma}(\boldsymbol{p})$ given by (A. 8) and (4. 5) as,

$$E_{\lambda\sigma}(\boldsymbol{p}) = \tilde{\varepsilon}_\lambda(\boldsymbol{p}) - \frac{1}{N}\sum_{\boldsymbol{k}\xi}\{U(\xi,\lambda;\ \lambda,\xi)+J(0:\ \xi,\lambda;\ \lambda,\xi)\}\,n_{\boldsymbol{k}\xi\sigma}, \tag{4.14}$$

and

$$\sum_\xi\{U(\xi,\lambda;\ \mu,\xi)+J(0:\ \xi,\lambda;\ \lambda,\xi)\}\,m_\xi = 0 \quad (\lambda\neq\mu), \tag{4.15}$$

respectively, where

$$\tilde{\varepsilon}_\lambda(p)=\int dr\varphi^*_{p\lambda}(r)\Big\{-\frac{\hbar^2\nabla^2}{2m}+\sum_n v(r-R_n)\Big\}\varphi_{p\lambda}(r)$$
$$+\frac{1}{N}\sum_{k\xi\sigma}\{U(\lambda,\xi;\lambda,\xi)+J(k-p:\lambda,\xi;\lambda,\xi)\}n_{k\xi\sigma}, \tag{4.16}$$

and

$$m_\xi=\frac{1}{N}\sum_k(n_{k\xi\uparrow}-n_{k\xi\downarrow}). \tag{4.17}$$

From (4. 14), we can define the exchange splitting between the λ-th sub-band with down spin and the μ-th sub-band with up spin as

$$\Delta_{\lambda\mu}=\frac{1}{N}\sum_{k\xi}[\{U(\xi,\mu;\mu,\xi)+J(0:\xi,\mu;\mu,\xi)\}n_{k\xi\uparrow}$$
$$-\{U(\xi,\lambda;\lambda,\xi)+J(0:\xi,\lambda;\lambda,\xi)\}n_{k\xi\downarrow}]. \tag{4.18}$$

Using the approximation (4. 13), we can get an integral equation for $f_{\lambda\mu}(q,p)$ from (4. 10) as follows,

$$F_{\lambda\mu}(q)-\sum_p\frac{n_{p\mu\uparrow}-n_{p+q\lambda\downarrow}}{\tilde{\varepsilon}_\lambda(p+q)-\tilde{\varepsilon}_\mu(p)+\Delta_{\lambda\mu}-\hbar\omega}\frac{1}{N}\sum_{\xi\eta}\{U(\lambda,\eta;\xi,\mu)$$
$$+J(q:\lambda,\eta;\xi,\mu)\}F_{\xi\eta}(q)=0, \tag{4.19}$$

where

$$F_{\lambda\mu}(q)=\sum_p(n_{p\mu\uparrow}-n_{p+q\lambda\downarrow})f_{\lambda\mu}(q,p). \tag{4.20}$$

It is difficult to solve (4. 19) in a general case, but, in principle, we can find the eigenvalues $\hbar\omega$ if the $r^2\times r^2$ determinant is solved, where r is the number of sub-bands.

Although we solve (4. 19) directly in § 5 for the case of two sub-bands, in order to discuss a more general case in this section, we make use of further approximations for matrix elements $U(\xi_1,\xi_2;\xi_4,\xi_3)$ and $J(q:\xi_1,\xi_2;\xi_4,\xi_3)$, and the sums of these matrix elements are written by

$$\left.\begin{aligned}
&K_0(q)=U_0+J_0(q) && \text{if}\quad \xi_1=\xi_2=\xi_3=\xi_4,\\
&K_{ex}(q)=U_{ex}+J_{ex}(q) && \text{if}\quad \xi_1=\xi_3\neq\xi_2=\xi_4,\\
&K_a(q)=U_a+J_a(q) && \text{if}\quad \xi_1=\xi_3,\ \xi_2\neq\xi_4,\\
& && \text{or}\quad \xi_2=\xi_4,\ \xi_1\neq\xi_3,\\
&K_c(q)=U_c+J_c(q) && \text{if}\quad \xi_1=\xi_4\neq\xi_2=\xi_3,\\
&\text{and} &&\\
&K_b(q)=U_b+J_b(q), && \text{otherwise},
\end{aligned}\right\} \tag{4.21}$$

respectively. U_0 and $J_0(q)$ are intra-band Coulomb integrals, U_{ex} and $J_{ex}(q)$ are inter-band exchange integrals, U_c and $J_c(q)$ are inter-band Coulomb integrals and U_a, $J_a(q)$, U_b and $J_b(q)$ are off-diagonal matrix elements with respect to sub band indices.

From (4. 18) and (4. 21), we obtain

$$\Delta_{\lambda\mu}=\frac{1}{N}\{K_0(0)-K_{ex}(0)\}\sum_k(n_{k\mu\uparrow}-n_{k\lambda\downarrow})+K_{ex}(0)M. \tag{4.22}$$

In particular, the exchange splitting between the λ-th sub-bands with down and up spins is given by

$$\Delta_\lambda=\Delta_{\lambda\lambda}=\{K_0(0)-K_{ex}(0)\}m_\lambda+K_{ex}(0)M, \tag{4.23}$$

where $M=\Sigma_\xi m_\xi$ and m_ξ is given by (4.17). This formula, (4.23), shows that the exchange splitting in the λ-th sub-band is the sum of the term proportional to m_λ, the magnetization per atom of the λ-th sub-band, and the term proportional to $(M-m_\lambda)$, the remaining magnetization per atom except the magnetization of the λ-th sub-band, and their coefficients are the intra-band Coulomb integral and inter-band exchange integral, respectively. Moreover, it is easily seen from (4.23) that a simple molecular field approximation is valid only when $K_0(0)=K_{ex}(0)$ in the multiple band model, and that for a sub-band with a larger sub-band magnetization its exchange splitting will become larger as it is most probable that $K_0(0)-K_{ex}(0)>0$. Except at high symmetry points in the Brillouin zone, this relation between the magnetization and the exchange splitting of each sub-band seems to be consistent with the calculated results of the electronic structures for ferromagnetic metals by the self-consistent method[73,74].

Using the approximations (4.21), we can write (4.19) as,

$$\begin{aligned}&F_{\lambda\mu}(q)-Z_{\lambda\mu}(q,\omega)[\{(K_0(q)-K_{ex}(q))F_\lambda(q)\\&\quad+K_{ex}(q)\sum_\xi F_\xi(q)+K_a(q)\sum_{\xi\neq\eta}\sum F_{\xi\eta}(q)\}\delta_{\lambda\mu}\\&\quad+\{(K_c(q)-K_b(q))F_{\lambda\mu}(q)+K_a(q)\sum_\xi F_\xi(q)\\&\quad+K_b(q)\sum_{\xi\neq\eta}\sum F_{\xi\eta}(q)\}(1-\delta_{\lambda\mu})]=0,\end{aligned} \tag{4.24}$$

where $F_\xi(q)=F_{\xi\xi}(q)$ and

$$Z_{\lambda\mu}(q,\omega)=\frac{1}{N}\sum_p\frac{n_{p\mu\uparrow}-n_{p+q\lambda\downarrow}}{\tilde{\varepsilon}_\lambda(p+q)-\tilde{\varepsilon}_\mu(p)+\Delta_{\lambda\mu}-\hbar\omega}. \tag{4.25}$$

We can write (4.15) as

$$K_a(0)=0. \tag{4.26}$$

As seen from (4.24), $F_\xi(q)$ couples with $F_{\xi\eta}(q)$ through $K_a(q)$. In the case of $q=0$, two cases of (4.24), where $\lambda=\mu$ and $\lambda\neq\mu$, are considered. We consider this case of $q=0$ in the next section.

§ 4. Eigenvalues of Normal Modes with Zero Momentum

We first consider the case of $q=0$ in (4.24), because this case is mathematically simple and gives us useful insights about the spin flipping excitations in metals.

For $\lambda\neq\mu$, that is, the case of the inter-band spin flipping excitation, we get from (4.24)

$$F_{\lambda\mu}(0)-Z_{\lambda\mu}(0,\omega)[\{K_c(0)-K_b(0)\}F_{\lambda\mu}(0)+K_b(0)\sum_{\xi\neq\eta}\sum F_{\xi\eta}(0)]=0. \tag{4.27}$$

We cannot solve (4.27) without the detailed knowledge of $\tilde{\varepsilon}_\lambda(\boldsymbol{p})$ in $Z_{\lambda\mu}(0, \omega)$.

We can, however, estimate the minimum eigenvalue of the (collective) spin wave excitations due to the inter-band transitions from (4.27) in the case of two sub-bands, which are completely degenerate. Solving the second-order secular determinant which is derived from (4.27), we can get the collective excitation energies of the inter-band spin wave as,

$$\hbar\omega_0 = \frac{M}{2}\left(K_0(0) + K_{ex}(0) - K_c(0) - K_b(0)\right), \tag{4.28}$$

and

$$\hbar\omega_0 = \frac{M}{2}\left(K_0(0) + K_{ex}(0) - K_c(0) + K_b(0)\right), \tag{4.29}$$

because $\Delta_{\lambda\mu}$ is given by

$$\Delta_{\lambda\mu} = \frac{M}{2}\left(K_0(0) + K_{ex}(0)\right),$$

for all values of λ and μ in this case. From (4.27) we can find $F_{1,2}(0) = F_{2,1}(0)$ for the eigenvalue given by (4.28) and $F_{1,2}(0) = -F_{2,1}(0)$ for the one given by (4.29). Therefore, (4.28) and (4.29) are the energies of the acoustical and optical inter-band branches of spin waves, respectively.

Next, we consider the case of $\boldsymbol{q}=0$ and $\lambda=\mu$, that is, the case of the intra-band spin flipping excitations, in (4.24), and we have

$$F_\lambda(0)\left\{1 - (K_0(0) - K_{ex}(0))\frac{m_\lambda}{\Delta_\lambda - \hbar\omega}\right\} - K_{ex}(0)\frac{m_\lambda}{\Delta_\lambda - \hbar\omega}\sum_\xi F_\xi(0) = 0. \tag{4.30}$$

In the case of the two sub-bands as assumed above, solving the second-order secular determinant which is derived from (4.30), we can get the collective excitation energies of spin waves as

$$\left.\begin{aligned} &\hbar\omega = 0, \\ \text{and} \qquad & \\ &\hbar\omega = K_{ex}(0)M. \end{aligned}\right\} \tag{4.31}$$

From (4.30), we can find $F_1(0)/F_2(0) = m_1/m_2$ for $\hbar\omega=0$ and $F_1(0)/F_2(0) = -1$ for $\hbar\omega = K_{ex}(0)M$, respectively, where 1 and 2 denote sub-band indices. Two modes of spin waves obtained above are inphase and out-of-phase branches with respect to the two sub-bands and correspond to the acoustical and optical intra-band branches of spin waves, respectively.

In the case of $\hbar\omega=0$, if $f_{\lambda\lambda}(0, \boldsymbol{p})$ is constant it is seen from (4.20) that $F_1(0)/F_2(0) = m_1/m_2$. In this case, from (4.6) A_0^+ is written as

$$A_0^+ = \sum_{\boldsymbol{p}\mu} a^+_{\boldsymbol{p}\mu\downarrow}\, a_{\boldsymbol{p}\mu\uparrow},$$

and it is just a lowering spin operator S^-. The state derived by the operation of A_0^+ on the total wave function of the ground state is nothing else the state derived by the rotation of the spin quantized axis without changing the spin

arrangement of the ground state, so that the excitation energy of the state derived thus is zero. Such circumstance always occurs in the treatment of spin waves.

We can easily show that the excitation energy of the acoustical magnon is zero when $q=0$ not only for the case of two sub-bands but also for the general case of many sub-bands. Multiplying (4.30) by

$$\left\{1-(K_0(0)-K_{ex}(0))\frac{m_\lambda}{\Delta_\lambda-\hbar\omega}\right\}^{-1}$$

and taking a sum over λ, we get

$$1=\sum_\lambda \frac{K_{ex}(0)\dfrac{m_\lambda}{\Delta_\lambda-\hbar\omega}}{1-(K_0(0)-K_{ex}(0))\dfrac{m_\lambda}{\Delta_\lambda-\hbar\omega}}. \tag{4.32}$$

Using (4.23), we can obtain $\hbar\omega=0$ from (4.23) when $\hbar\omega$ is not equal to Δ_λ and $K_{ex}(0)M$. The method used to obtain (4.32) is useful to find the dispersion relation of acoustical branches of spin waves, but we cannot obtain that of optical branches by this method, because energies of the optical branches may be in the energy range of the individual excitations. We will find the dispersion relation of an acoustical branch by this method in the next section.

§ 5. General Dispersion Relations of Spin Waves in the Multiple Bands

From (4.24), we can get the following simultaneous equations for $F_\lambda(q)$ and $F_{\lambda\mu}(q)$,

$$\begin{aligned}F_\lambda(q)-Z_{\lambda\lambda}(q,\omega)[\{K_0(q)-K_{ex}(q)\}F_\lambda(q)\\ +K_{ex}(q)\sum_\xi F_\xi(q)+K_a(q)\sum_\xi\sum_{\xi\neq\eta}F_{\xi\eta}(q)]=0,\end{aligned} \tag{4.33}$$

and

$$\begin{aligned}F_{\lambda\mu}(q)-Z_{\lambda\mu}(q,\omega)[\{K_c(q)-K_b(q)\}F_{\lambda\mu}(q)\\ +K_b(q)\sum_\xi\sum_{\xi\neq\eta}F_{\xi\eta}(q)+K_a(q)\sum_\xi F_\xi(q)]=0,\quad(\lambda\neq\mu)\end{aligned} \tag{4.34}$$

where $Z_{\lambda\mu}(q,\omega)$ is given by (4.25). From (4.33) and (4.34) we can obtain the following equation, from which the dispersion relations of spin waves are determined,

$$\begin{aligned}&\left[1-\sum_\lambda\frac{Z_{\lambda\lambda}(q,\omega)K_{ex}(q)}{1-Z_{\lambda\lambda}(q,\omega)\{K_0(q)-K_{ex}(q)\}}\right]\left[1-\sum_\lambda\sum_{\lambda\neq\mu}\frac{Z_{\lambda\mu}(q,\omega)K_b(q)}{1-Z_{\lambda\mu}(q,\omega)\{K_c(q)-K_b(q)\}}\right]\\ &=K_a(q)^2\sum_\lambda\frac{Z_{\lambda\lambda}(q,\omega)}{1-Z_{\lambda\lambda}(q,\omega)\{K_0(q)-K_{ex}(q)\}}\sum_\lambda\sum_{\lambda\neq\mu}\frac{Z_{\lambda\mu}(q,\omega)}{1-Z_{\lambda\mu}(q,\omega)\{K_c(q)-K_b(q)\}},\end{aligned} \tag{4.35}$$

where

$$\sum_\lambda F_\lambda(q)\neq 0 \text{ and } \sum_\lambda\sum_{\lambda\neq\mu}F_{\lambda\mu}(q)\neq 0.$$

Eq. (4.35) shows that the acoustical intra-band and inter-band branches in the dispersion relations are coupled with each other via the right-hand side in (4.35).

First, the eigenvalue equation for the inter-band branch of spin wave is obtained from (4.35) as

$$1=\sum_{\lambda\neq\mu}\sum\frac{Z_{\lambda\mu}(\boldsymbol{q},\omega)}{1-Z_{\lambda\mu}(\boldsymbol{q},\omega)\{K_c(\boldsymbol{q})-K_b(\boldsymbol{q})\}}\times\left[K_b(\boldsymbol{q})+\frac{\sum_{\lambda}\frac{Z_{\lambda\lambda}(\boldsymbol{q},\omega)K_a(\boldsymbol{q})^2}{1-Z_{\lambda\lambda}(\boldsymbol{q},\omega)\{K_0(\boldsymbol{q})-K_{ex}(\boldsymbol{q})\}}}{1-\sum_{\lambda}\frac{Z_{\lambda\lambda}(\boldsymbol{q},\omega)K_{ex}(\boldsymbol{q})}{1-Z_{\lambda\lambda}(\boldsymbol{q},\omega)\{K_0(\boldsymbol{q})-K_{ex}(\boldsymbol{q})\}}}\right]. \tag{4.36}$$

If a crystal has an inversion symmetry, $K_a(\boldsymbol{q})$ is proportional to q^2 for small $\boldsymbol{q}$ values, because $K_a(0)$ is zero from (4.26), so that the second term in the square bracket in (4.36) is proportional to q^4. Neglecting $K_a(\boldsymbol{q})$ in (4.36), we can get the dispersion relation of the inter-band branch from (4.36) as,

$$\hbar\omega=\hbar\omega_0+aq^2. \tag{4.37}$$

Here $\hbar\omega_0$ is determined from the following equation,

$$1=\sum_{\lambda\neq\mu}\sum\frac{Z_{\lambda\mu}(0,\omega_0)K_b(0)}{1-Z_{\lambda\mu}(0,\omega_0)\{K_c(0)-K_b(0)\}}. \tag{4.38}$$

and aq^2 in (4.37) is written as,

$$aq^2=\left[\frac{K_b(0)-K_b(\boldsymbol{q})}{K_b(0)^2}+\sum_{\lambda\neq\mu}\sum\frac{\alpha_{\lambda\mu}(\boldsymbol{q})}{[1-Z_{\lambda\mu}(0,\omega_0)\{K_c(0)-K_b(0)\}]^2}+\sum_{\lambda\neq\mu}\sum\left\{\frac{Z_{\lambda\mu}(0,\omega_0)}{1-Z_{\lambda\mu}(0,\omega_0)\{K_c(0)-K_b(0)}\right\}^2\{K_c(0)-K_c(\boldsymbol{q})-K_b(0)+K_b(\boldsymbol{q})\}\right]\times\left[\sum_{\lambda\neq\mu}\sum\frac{X_{\lambda\mu}(\omega_0)}{[1-Z_{\lambda\mu}(0,\omega_0)\{K_c(0)-K_b(0)\}]^2}\right]^{-1}. \tag{4.39}$$

where

$$\alpha_{\lambda\mu}(\boldsymbol{q})=\frac{1}{N}\sum_{\boldsymbol{p}}\left[\frac{(\boldsymbol{q}\cdot\nabla)^2\tilde{\varepsilon}_{\lambda}(\boldsymbol{p})n_{\boldsymbol{p}\mu\uparrow}+(\boldsymbol{q}\cdot\nabla)^2\tilde{\varepsilon}_{\mu}(\boldsymbol{p})n_{\boldsymbol{p}\lambda\downarrow}}{2\{\tilde{\varepsilon}_{\lambda}(\boldsymbol{p})-\tilde{\varepsilon}_{\mu}(\boldsymbol{p})+\Delta_{\lambda\mu}-\hbar\omega_0\}^2}-\frac{\{(\boldsymbol{q}\cdot\nabla)\tilde{\varepsilon}_{\lambda}(\boldsymbol{p})\}^2n_{\boldsymbol{p}\mu\uparrow}-\{(\boldsymbol{q}\cdot\nabla)\tilde{\varepsilon}_{\mu}(\boldsymbol{p})\}^2n_{\boldsymbol{p}\lambda\downarrow}}{\{\tilde{\varepsilon}_{\lambda}(\boldsymbol{p})-\tilde{\varepsilon}_{\mu}(\boldsymbol{p})+\Delta_{\lambda\mu}-\hbar\omega_0\}^3}\right],$$

and

$$X_{\lambda\mu}(\omega_0)=\frac{1}{N}\sum_{\boldsymbol{p}}\frac{n_{\boldsymbol{p}\mu\uparrow}-n_{\boldsymbol{p}\lambda\downarrow}}{\{\tilde{\varepsilon}_{\lambda}(\boldsymbol{p})-\tilde{\varepsilon}_{\mu}(\boldsymbol{p})+\Delta_{\lambda\mu}-\hbar\omega_0\}^2}.$$

In the case of two sub-bands, which are completely degenerate, we can obtain $\hbar\omega_0$ as (4.28) and

$$aq^2=\frac{M}{2}\{K_c(0)-K_c(\boldsymbol{q})+K_b(0)-K_b(\boldsymbol{q})\}+\frac{1}{NM}\sum_{\boldsymbol{p}}(\boldsymbol{q}\cdot\nabla)^2\tilde{\varepsilon}(\boldsymbol{p})(n_{\boldsymbol{p}\uparrow}+n_{\boldsymbol{p}\downarrow})-\frac{4}{NM^2(K_c(0)+K_b(0))}\sum_{\boldsymbol{p}}\{(\boldsymbol{q}\cdot\nabla)\tilde{\varepsilon}(\boldsymbol{p})\}^2(n_{\boldsymbol{p}\uparrow}-n_{\boldsymbol{p}\downarrow}). \tag{4.40}$$

Secondly, the eigenvalue equation for an acoustical intra-band branch is rewritten from (4.35) as,

$$1=\sum_{\lambda}\frac{Z_{\lambda\lambda}(q,\omega)}{1-Z_{\lambda\lambda}(q,\omega)\{K_0(q)-K_{ex}(q)\}} \times\left[K_{ex}(q)+\frac{\sum\sum_{\lambda\neq\mu}\frac{Z_{\lambda\mu}(q,\omega)K_a(q)^2}{1-Z_{\lambda\mu}(q,\omega)\{K_c(q)-K_b(q)\}}}{1-\sum\sum_{\lambda\neq\mu}\frac{Z_{\lambda\mu}(q,\omega)K_b(q)}{1-Z_{\lambda\mu}(q,\omega)\{K_c(q)-K_b(q)\}}}\right]. \tag{4.41}$$

If a crystal has an inversion symmetry, the numerator of the second term in the square bracket in (4.41) is proportional to q^4. On the other hand, the solution of $\hbar\omega$, which makes the denominator of the second term in the square bracket in (4.41) zero, is just the solution of (4.36) which gives the energies of the inter-band branch, and the value of this denominator is finite for the energy of an acoustical intra-band branch of spin waves when q is sufficiently small, because the energy of the acoustical intra-band branch at $q=0$ is zero, but the corresponding energy of the acoustical inter-band branch at $q=0$ is finite (for example, $\hbar\omega_0$ given by (4.28) in the case of two degenerate sub-bands), as mentioned in § 4.

One can expand (4.41) as a power series of q for small q values. After tedious but straightfoward calculations, we can obtain the dispersion relation of the acoustical intra-band branch up to the term of q^2 as

$$\hbar\omega_{ac}=D_B q^2+D_H q^2, \tag{4.42}$$

where

$$D_B q^2=\frac{1}{2MN}\sum_{k\lambda}(q\cdot\nabla)^2\tilde{\varepsilon}_\lambda(k)(n_{k\lambda\uparrow}+n_{k\lambda\downarrow}) -\frac{1}{MN}\sum_{k\lambda}\frac{\{(q\cdot\nabla)\tilde{\varepsilon}_\lambda(k)\}^2}{\Delta_\lambda}(n_{k\lambda\uparrow}-n_{k\lambda\downarrow}), \tag{4.43}$$

$$D_H q^2=\{J_0(0)-J_0(q)-J_{ex}(0)+J_{ex}(q)\}\sum_{\lambda}m_\lambda^2/M+(J_{ex}(0)-J_{ex}(q))M. \tag{4.44}$$

The second term in the square bracket in (4.41) has a contribution to the dispersion relation of an acoustical intra-band branch as

$$-\frac{\sum\sum_{\lambda\neq\mu}\frac{Z_{\lambda\mu}(0,0)K_a(q)^2}{1-Z_{\lambda\mu}(0,0)\{K_c(0)-K_b(0)\}}}{1-\sum\sum_{\lambda\neq\mu}\frac{Z_{\lambda\mu}(0,0)K_b(0)}{1-Z_{\lambda\mu}(0,0)\{K_c(0)-K_b(0)\}}}\times M, \tag{4.45}$$

which is proportional q^4.

In the ordinary case an acoustical intra-band branch and an inter-band branch will approach with each other at the larger values of q. In such a case, the second term in the square bracket in (4.41) is large, because the denominator of this term becomes nearly equal to zero, and an acoustical intra-band branch will be shifted downward in the dispersion curve by the inter-band branch. At the same time, a similar circumstance occurs in the inter-band branch, of which eigenvalue equation is given by (4.36), and this branch will be shifted upward

by the acoustical intra-band branch. When the energy of the inter-band excitation with a reversed spin is small, the coefficient of q^4 in the dispersion relation of the acoustical intra-band branch becomes large and the leading term proportional to q^4 will be given by (4.45). The recent experimental result shows that the coefficient of q^4 in the dispersion relation of an acoustical intra-band branch is relatively large for iron and fcc cobalt metals[44)45)] and this fact means that the inter-band transitions have an important effect on the coefficient of q^4 in these metals.

Finally, we solve the integral equation (4.19) for the case of two sub-bands, instead of using the approximations (4.21), by neglecting such off-diagonal matrix elements with respect to the sub-band indices as

$$K(\boldsymbol{q}:\lambda,\xi;\xi,\mu)=U(\lambda,\xi;\xi,\mu)+J(\boldsymbol{q}:\lambda,\xi;\xi,\mu)\quad(\lambda\neq\mu),\tag{4.46}$$

because these terms have no effect on the dispersion relation of spin wave up to the term proportional to q^2. We can get a fourth-order secular equation, but this secular determinant is decomposed into two second-order determinants, by neglecting $K(\boldsymbol{q}:\lambda,\xi;\xi,\mu)$ for $\lambda\neq\mu$ given by (4.46), as follows,

$$\begin{vmatrix} 1-Z_{11}(\boldsymbol{q},\omega)K(\boldsymbol{q}:11;11) & -Z_{11}(\boldsymbol{q},\omega)K(\boldsymbol{q}:12;21) \\ -Z_{22}(\boldsymbol{q},\omega)K(\boldsymbol{q}:21;12) & 1-Z_{22}(\boldsymbol{q},\omega)K(\boldsymbol{q}:22;22) \end{vmatrix}=0,\tag{4.47}$$

and

$$\begin{vmatrix} 1-Z_{12}(\boldsymbol{q},\omega)K(\boldsymbol{q}:12;12) & -Z_{12}(\boldsymbol{q},\omega)K(\boldsymbol{q}:11;22) \\ -Z_{21}(\boldsymbol{q},\omega)K(\boldsymbol{q}:22;11) & 1-Z_{21}(\boldsymbol{q},\omega)K(\boldsymbol{q}:21;21) \end{vmatrix}=0.\tag{4.48}$$

From (4.47), we can obtain the dispersion relations,

$$\begin{aligned}\hbar\omega_{ac}=&\frac{1}{M}\sum_{\lambda\mu}\{J(0:\lambda,\mu;\mu,\lambda)-J(\boldsymbol{q}:\lambda,\mu;\mu,\lambda)\}m_\lambda m_\mu\\&+\frac{1}{2MN}\sum_{k\lambda}(\boldsymbol{q}\cdot\nabla)^2\tilde{\varepsilon}_\lambda(k)(n_{k\lambda\uparrow}+n_{k\lambda\downarrow})\\&-\frac{1}{MN}\sum_{k\lambda}\frac{1}{\Delta_\lambda}\{(\boldsymbol{q}\cdot\nabla)\tilde{\varepsilon}_\lambda(k)\}^2(n_{k\lambda\uparrow}-n_{k\lambda\downarrow})\end{aligned}\tag{4.49}$$

for the acoustical intra-band branch, and

$$\hbar\omega_{op}=K(0:1,2;2,1)M+bq^2,\tag{4.50}$$

where

$$\begin{aligned}bq^2=&\frac{1}{M}\Big[m_1m_2\{\sum_\lambda(K(0:\lambda,\lambda;\lambda,\lambda)-K(\boldsymbol{q}:\lambda,\lambda;\lambda,\lambda))\\&-2(K(0:1,2;2,1)-K(\boldsymbol{q}:1,2;2,1))\}\\&+\sum_{\lambda\neq\mu}\sum\frac{m_\lambda}{m_\mu}\frac{1}{N}\sum_p\Big\{\frac{1}{2}(\boldsymbol{q}\cdot\nabla)^2\tilde{\varepsilon}_\mu(p)(n_{p\mu\uparrow}+n_{p\mu\downarrow})\\&-\frac{\{(\boldsymbol{q}\cdot\nabla)\tilde{\varepsilon}_\mu(p)\}^2(n_{p\mu\uparrow}-n_{p\mu\downarrow})}{\{K(0:\mu,\mu;\mu,\mu)-K(0:\mu,\lambda;\lambda,\mu)\}m_\mu}\Big\}\Big]\end{aligned}\tag{4.51}$$

for an optical intra-band branch, where λ and μ are sub-band indices 1 and 2. The results similar to (4.49), (4.50) and (4.51) were obtained before by Thompson[12].

The dispersion relations of the inter-band branches of spin waves in the case of two sub-bands can be obtained from (4.48), but they are complicated formulas. If further approximations for K as (4.21) are made use of, these dispersion relations are reduced to the relations given by (4.37), (4.38) and (4.39).

§ 6. Numerical Calculations of D_B for Nickel

Now, we will estimate the coefficient of q^2 in the dispersion relation of the acoustical intra-band branch of spin waves. Recently, Shimizu[75] has roughly estimated D_B to be 0.05 eVÅ^2 for nickel and 0.08 eVÅ^2 for iron, assuming a single normal band with an effective mass and has concluded $D_B \ll D_H$ for nickel and iron.

In this section, we ascertain this conclusion from the estimation of D_B by (4.43) using a more realistic electronic structure for nickel. The approximations for the matrix elements of the Coulomb interactions which we have assumed to obtain (4.43) and (4.44), will be appropriate only for d-bands, so that we make use of these approximations for d-bands and for the sake of simplicity we neglect s-band.

As seen from the calculations by Fletcher[76] and Yamashita *et al.*[77], the Fermi surfaces of the ferromagnetic nickel, roughly speaking, are constructed from a large sphere of electrons with down spin about Γ point and a small sphere of holes with down spin about X points. Therefore, we adopt the two band model where the energy spectra are given by

$$\tilde{\varepsilon}_1(\boldsymbol{k}) = -\frac{1}{2}A\cos\left\{\frac{a}{2}\left(\frac{\pi}{3}\right)^{1/3}k\right\}, \tag{4.52}$$

and

$$\tilde{\varepsilon}_2(\boldsymbol{k}) = -\frac{\hbar^2}{2m^*}\sum_{(X)}|\boldsymbol{k}-\boldsymbol{k}(X)|^2, \tag{4.53}$$

where a is the lattice constant 3.52 Å, A is a band width of sub-band 1, $\boldsymbol{k}(X)$ denotes the value of $\boldsymbol{k}$ at the X points and 1 and 2 denote sub-band indices. These energy specra are schematically shown in Fig. 10 for the Γ-X direction. The bands with up and down spins are drawn at the left- and right-hand sides in Fig. 10, respectively. For the sub-band 1, we assume that the Brillouin zone is a sphere with the same volume as the real Brillouin zone. Further we assume a simple molecular field approximation mentioned in § 3, that is, $K_0(0)=K_{ex}(0)$, in (4.23), so that the exchange splittings of the sub-bands 1 and 2 are identical.

In order to estimate the value of D_B by (4.43), (4.52) and (4.53), we must determine the band width A in (4.52) and number of electrons per atom with down spin, n, for the sub-band 1, the exchange splitting, Δ, and the effective

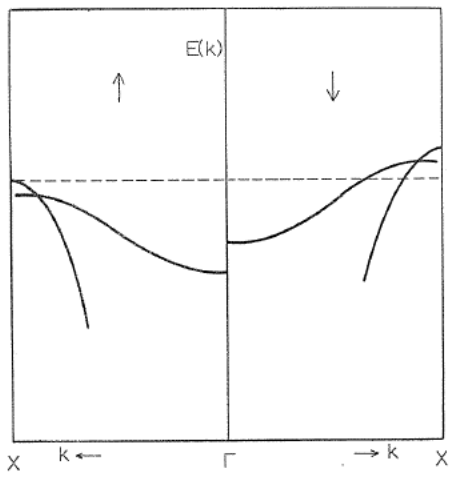

FIG. 10. Schematic electronic structure of two sub-bands for nickel. The up- and down-spin bands are drawn at the left- and right-hand sides, respectively, and the Fermi level is denoted by a broken line.

mass m^* for the sub-band 2, which contains $(n\text{-}0.4)$ holes per atom as seen from the Bohr magneton number per atom, 0.6 for nickel. Here we assume that the highest energy of the sub-bands with up spin is equal to the Fermi level of the sub-bands with down spin, as shown by the broken line in Fig. 10. In our model of two sub-bands for nickel we assume that the two sub-bands with up spin are all filled up by electrons and sub-bands 1 and 2 with down spin are occupied by $(1\text{-}n)$ and $(n\text{-}0.4)$ holes per atom, respectively. We can find a following relation among n, A and m^* from the experimental data of low temperature specific heat coefficient for nickel, $\gamma = 1.68\times10^{-4}$ cal/deg^2 mole[29],

$$\gamma = \gamma_1 + \gamma_2,$$

$$\gamma_1 = \frac{2\pi k_B^2}{A}\frac{n^{2/3}}{\sin(\pi n^{1/3})}$$

$$\gamma_2 = \frac{\pi k_B^2 a^2 m^*}{4\hbar^2}\left\{\frac{n-0.4}{\pi}\right\}^{1/3}.$$

There is another relation among m^*, $(n-0.4)$ and Δ if the highest energy of the sub-band 2 is higher than that of the sub-band 1, or among A, $(1-n)$ and Δ if the highest energy of the sub-band 1 is higher than that of the sub-band 2.

Using (4.52) and (4.53), we calculate the values of D_B by (4.43) for some values of n and A as parameters, and the numerical results are shown in Table 3 and Fig. 11. In Table 3, the numerical values of reduced effective mass of sub-band 2, m^*/m_0, low temperature specific heat coefficients for sub-bands 1 and 2, γ_1 and γ_2, exchange splitting, Δ, D_B for each sub-band, D_{B1} and D_{B2}, and $D_B(=D_{B1}+D_{B2})$ are shown for some values of n and A as parameters. In Fig. 11, the curves of D_{B1} vs n are shown for some values of A. Katsuki and Wohlfarth[78] have calculated the numerical relations between D_B and the electron numbers per atom for the case of a single band with simple cubic structure.

The exchange splitting for nickel is considered to be about 0.35 eV[17,79], so that we can guess

$$D_B \simeq 0.1 \sim 0.2 \text{ eV Å}^2, \tag{4.54}$$

from Table 3, although the value of D_B may depend sensitively on the value of the exchange splitting.

Therefore, as the observed value of $D = D_B + D_H$ for nickel obtained by Hatherly *et al.*[41] is 0.4 eVÅ^2, we can conclude that $D_B \lesssim D_H$ for nickel, although the inter-

TABLE 3. Numerical values of m^*/m_0, γ_1, γ_2, Δ, D_{B1}, D_{B2} and D_B in the two band model, as shown in Fig. 10, for nickel

n	A	m^*/m_0	γ_1	γ_2	Δ	D_{B1}	D_{B2}	D_B
atom^{-1}	eV		$\times 10^{-4}$ cal/mole deg^2		eV	eV Å^2		
0.46	0.6	0.89	16.3	0.5	0.973	0.088	0.086	0.174
	0.7	4.9	14.0	2.8	0.178	0.027	0.016	0.043
	0.8	7.8	12.2	4.6	0.111	−0.055	0.010	−0.045
	0.9	10.2	10.9	5.9	0.111	−0.088	0.014	−0.074
	1.0	12.0	9.8	7.0	0.123	−0.098	0.017	−0.081
0.48	0.7	2.9	15.0	1.8	0.367	0.080	0.036	0.116
	0.8	5.8	13.1	3.7	0.182	0.030	0.018	0.048
	0.9	8.0	11.6	5.2	0.131	−0.031	0.013	−0.018
	1.0	9.8	10.5	6.3	0.112	−0.094	0.012	−0.082
0.50	0.7	1.1	16.0	0.8	1.125	0.102	0.117	0.219
	0.8	4.0	14.0	2.8	0.307	0.076	0.032	0.108
	0.9	6.2	12.5	4.3	0.197	0.041	0.020	0.061
	1.0	8.0	11.2	5.6	0.152	−0.006	0.016	0.010
	1.1	9.5	10.2	6.6	0.128	−0.062	0.013	−0.049
0.52	0.8	2.3	15.1	1.7	0.589	0.102	0.065	0.167
	0.9	4.6	13.4	3.4	0.299	0.082	0.033	0.115
	1.0	6.4	12.1	4.7	0.214	0.054	0.024	0.078
	1.1	7.9	11.0	5.8	0.174	0.019	0.019	0.038
	1.2	9.2	10.1	6.7	0.306	0 085	0.080	0.165

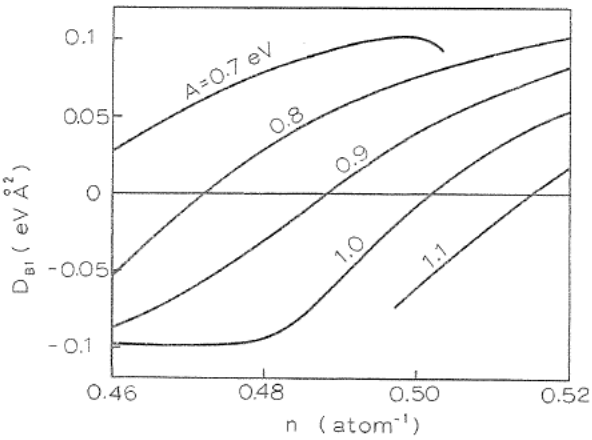

FIG. 11. Values of D_{B1} vs n. The numbers along each curve give the value of the band width, A (The experimental value of D is 0.4 eV Å^2.[41]).

atomic exchange integral will be smaller than the intra-atomic Coulomb integral.

On the other hand, we can estimate an upper limit of D_{B1} from (4.43) in the limit of strong correlation, $U=\infty$, namerly, by neglecting the second term in (4.43) since $\Delta=\infty$ when $U=\infty$, as follows,

$$D_{B1}<0.17\times A \text{ eV Å}^2, \tag{4.55}$$

for any value of n. The value of A is 0.6 eV and 1.5 eV according to the calculated results of electronic structure for nickel by Fletcher[76] and by Yamashita *et al.*[77] respectively. Both values of A give smaller values of D_{B1} than the observed value of D for nickel[41].

§ 7. General Consideration of Excitation Spectra with a Reversed Spin

We discuss the relation between the excitation energies of spin waves and individual transitions with a reversed spin (Stoner excitations). As schematically shown in Fig. 12, the spectrum of an acoustical intra-band branch of spin waves denoted by curve a is isolated from the region of the individual intra-band transitions, which is denoted by the region above curve c in Fig. 12, because the exchange splitting, which is shown by the energy gap at $q=0$, is large. In the usual case, the excitation spectra of the intra-band transitions are considered to be in the sea of the excitation spectra of the individual inter-band transitions, which are denoted by the region above curve b in Fig. 12. From the calculations in § 5, it is seen that under the sea of the individual inter-band transitions there is a lower collective spectrum due to the inter-band transitions, that is, the spectrum of the inter-band branch, denoted by curve d in Fig. 12.

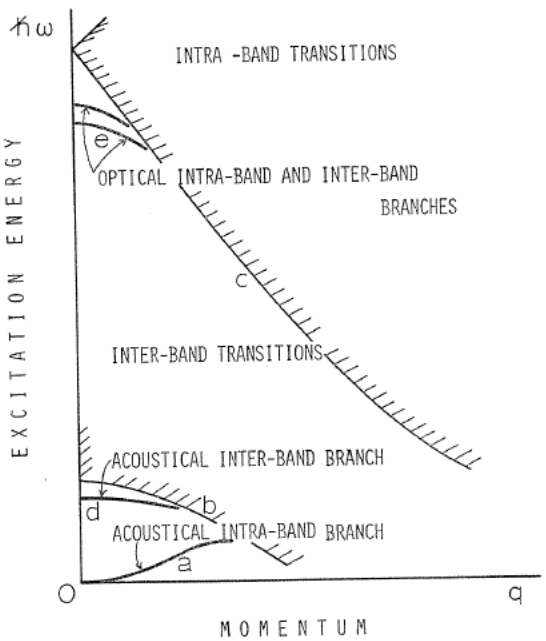

FIG. 12. Schematic curves of the excitation spectra with a reversed spin. Curves *a*, *b*, *c*, *d* and *e* are the spectrum of the acoustical intra-band branch of spin waves, the bottoms of the spectra of the inter-band transitions and the intra-band transitions, the spectrum of the inter-band branches of spin waves, and the spectrum of the optical intra- and inter-band branches of spin waves, respectively.

It will be incorrect that the only excitations, strongly in evidence in metal such as iron, will be those corresponding to the single spin wave because the bottom of the individual excitations is rised at $q=0$ by an energy equal to the exchange splitting[57]. On the other hand, according to the calculated electronic structure of iron by Wakoh and Yamashita[74], there seems to be a small region where the excitation energies of the inter-band transitions are lower than the acoustical spin wave spectrum at small finite values of q, that is, at about $q \sim 0.04$ Å^{-1}. If there are other excitations whose energies are lower than the acoustical spin wave spectrum, the spin wave should be instable and is damped into the individual excited state with

a reversed spin via the interactions such as electron correlations, although such a damping mechanism is not considered in our treatments within the random phase approximation. For iron, however, the dispersion relation of an acoustical spin wave has been observed by the inelastic neutron scattering for the value of q, 0.4 $Å^{-1}$.[44]

The higher-order terms of the momentum in the dispersion relation of spin waves have not so far been treated satisfactorily in the microscopic theory, though the macroscopic theory of spin waves in metals teaches us that the terms of q^4 in the dispersion relation of spin waves are derived from the quadratic terms of the second derivative of the magnetization density by co-ordinates, as discussed in chapter III. It should be noted that in ferromagnetic metals and alloys the fourth-power terms of momentum in the dispersion relation of spin waves are relatively important as seen from the experiments by Shirane *et al.*[44)45)].

The fact that in metals the dispersion relation of the acoustical intra-band branch may be strongly interfered by the inter-band transitions, instead of the intra-band transitions, at a relatively smaller value of q and the spin wave becomes unstable above this value of q, as discussed in § 5, can explain the question why the coefficients of q^4 in the dispersion relation for iron and fcc cobalt are fairly

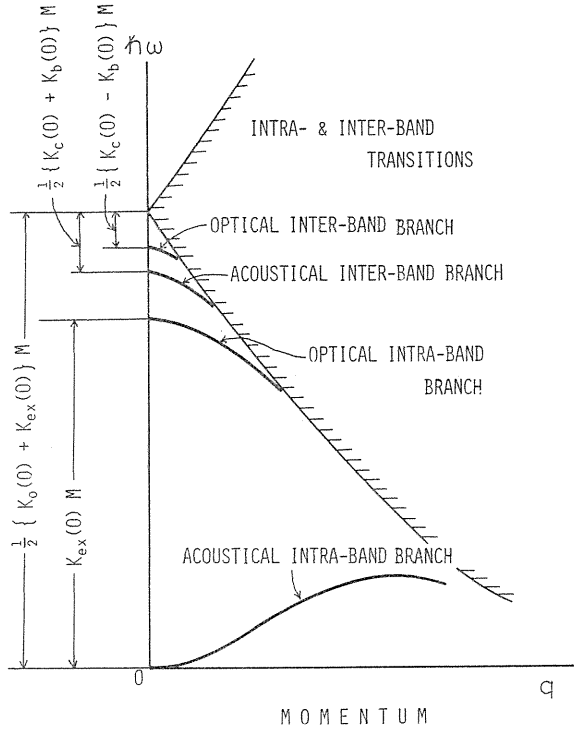

FIG. 13. Schematic curves of the energy spectra of spin waves and individual excitations in the case of two degenerate sub-bands. The energy gaps at $q=0$ are given by (4.31) for the optical intra-band branch of spin waves and by (4.28) and (4.29) for acoustical and optical inter-band branches of spin waves in the text.

large[44)45)].

On the other hand, the spectra of the optical branches will lie in the region of the individual intra- and inter-band transitions. In the two band model, however, the energy of the optical intra-band branch at $q=0$, given by $\hbar\omega=K_{ex}(0)$ M from (4.31), is expected to be smaller than any exchange splitting of each sub-band, given by (4.23), because perhaps $K_0(0)-K_{ex}(0)>0$. Therefore, the spectrum of the optical intra-band branch will lie below the bottom of the spectra of the intra-band excitations in the neighbourhood of $q=0$ as shown by curve e in Fig. 12. The detailed properties of the optical intra-band branches of spin waves, whose energy spectrum for the two band model is given by (4.50), and the inter-band branches given by (4.37) cannot be discussed further without the detailed knowledge on the electronic structure; they depend sensitively on the electronic structure of ferromagnetic metals, although we can get the energy spectra of spin waves and individual excitations at $q=0$ in the case of two degenerate sub-bands as shown in § 4 and the results are shown schematically in Fig. 13. In Fig. 13, it is assumed that $K_0(0)>K_{ex}(0)\sim K_c(0)>K_b(0)>0$, and this assumption seems to be most natural.

§ 8. Cut-Off Momentum of Spin Wave in Single Band Model

In § 7, we have qualitatively considered the excitation spectra with a reversed spin. In this section, we discuss the details of the dispersion relation of a spin wave in the single band model and evaluate the cut-off momentum of a spin wave.

In the case of the single band model, using the random phase approximation and the approximation similar to (4.13) for the Coulomb matrix elements, we get the following eigenvalue equation[68)],

$$1=\frac{1}{N}\{U+J(q)\}\sum_k \frac{n_{k\uparrow}-n_{k+q\downarrow}}{\tilde{\varepsilon}(k+q)-\tilde{\varepsilon}(k)+\Delta-\hbar\omega}, \tag{4.56}$$

where

$$\Delta=\{U+J(0)\}M,$$

by the same method as that used for deriving (4.19).

For the sake of simplicity, we assume the system to be a saturated ferromagnetic state and $\tilde{\varepsilon}(k)=\hbar^2k^2/2m$. In this simplified case, the excitation spectrum and cut-off momentum of a spin wave without $J(q)$ in (4.56) were already discussed by Thompson[80)] and Mattis[49)], but we will show that the interatomic exchange integral $J(q)$ plays an important role for the excitation spectrum and the cut-off momentum of a spin wave. The eigenvalue equation (4.56) can be written as

$$\frac{4\varepsilon_f x}{3M}\frac{1}{U+J(q)}=F(y), \tag{4.57}$$

where

$$F(y)=y+\frac{1}{2}(1-y^2)\ln\left|\frac{y+1}{y-1}\right|, \tag{4.58}$$

$$y=\{x^2+(\Delta-\hbar\omega)/\varepsilon_f\}/2x, \tag{4.59}$$

$x=q/k_f$ and ε_f and $k_f$denote the Fermi energy and Fermi momentum of up spin band, respectively.

The cut-off momentum of a spin wave q_c is obtained from

$$\begin{aligned}\hbar\omega_{q_c} &= \text{Minimum of } \{\tilde{\varepsilon}(k+q_c)-\tilde{\varepsilon}(k)+\Delta\} \\ &= \varepsilon_f\{-2x_c+x_c^2\}+\Delta,\end{aligned} \tag{4.60}$$

where $|k|<k_f$ and $x_c=q_c/k_f$. From (4.59) and (4.60) we get $y=1$, so that x_c is given by

$$x_c=\frac{3\Delta}{4\varepsilon_f}\frac{U+J(q_c)}{U+J(0)}, \tag{4.61}$$

from (4.57) and (4.58). We take an approximation for $J(q)$ as

$$J(q)=J\sum_{\rho\neq 0}\exp(iq\cdot\rho), \tag{4.62}$$

where ρ's denote lattice vectors to the nearest neighbours. For fcc structure, (4.62) is written as

$$J(q)=4J\left\{\cos\frac{1}{2}aq_x\cos\frac{1}{2}aq_y+\cos\frac{1}{2}aq_y\cos\frac{1}{2}aq_z+\cos\frac{1}{2}aq_z\cos\frac{1}{2}aq_x\right\}, \tag{4.63}$$

where a is the lattice constant. Using (4.61) and (4 63), the reduced cut-off momentum of a spin wave x_c in the (100) direction of the momentum space against J/U is calculated as shown in Fig. 14 for $\varepsilon_f/\Delta=0.6$, 0.8 and 1.0, where solid and broken curves denote $M=0.6$ and 1.0, respectively. As seen from Fig. 14, q_c/k_f decreases rapidly with increasing J/U for small values of J/U and it seems that the inter-atomic exchange integral is important for cut-off momentum.

The excitation spectrum of a spin wave can be calculated from (4.57), (4.58), (4.59) and (4.63). Calculated results are shown in Figs. 15, 16 and 17 for $M=0.6$ and $\varepsilon_f/\Delta=$ 1.0, 0.8 and 0.6, respectively. In these figures, a parabolic curve in the right-hand side denotes the minimum energy of individual excitations. In Fig. 15, the three curves for $J/U=0.1$ denote $q=(q00)$ for the upper curve, $(q/\sqrt{2}, q/\sqrt{2}, 0)$ for the middle curve and $(q/\sqrt{3}, q/\sqrt{3}, q/\sqrt{3})$ for the lower curve. This anisotropy is derived from that of $J(q)$ in (4.63). Other curves in Fig. 15 and all curves

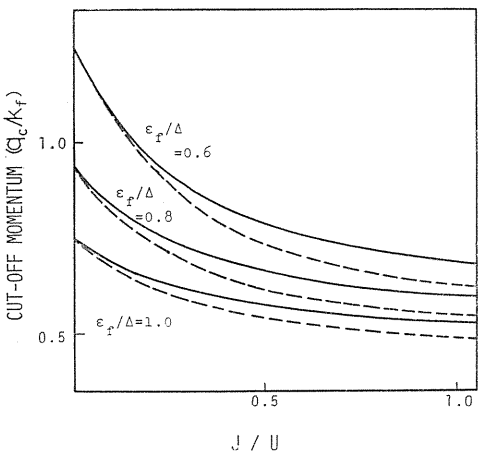

FIG. 14. Dependence of the cut-off momentum of a spin wave on the inter-atomic exchange integrals for $\varepsilon_f/\Delta=0.6$, 0.8 and 1.0. Solid and broken curves denote $M=0.6$ and 1.0, respectively.

in Fig. 16 and Fig. 17 are drawn for $q=(q00)$. In the case of $\varepsilon_f/\Delta=1$ in Fig. 15, a maximum appears in the excitation spectrum of a spin wave. But when the value of ε_f/Δ decreases, this maximum disappears.

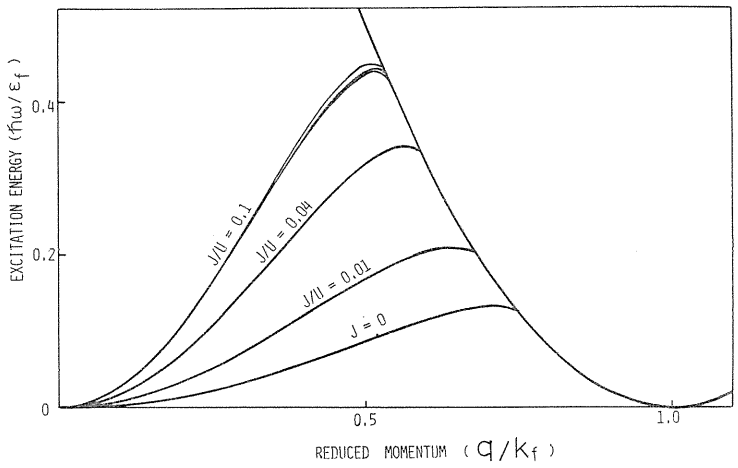

FIG. 15. Dispersion relation of a spin wave for $M=0.6$ and $\varepsilon_f/\Delta=1.0$ for some values of J/U. The parabolic curve in the right-hand side denotes the minimum energy of the individual excitations with a reversed spin.

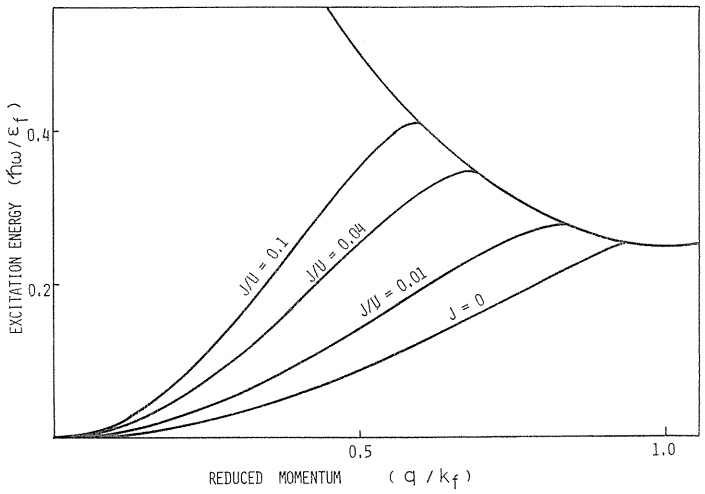

FIG. 16. Dispersion relation of a spin wave for $M=0.6$ and $\varepsilon_f/\Delta=0.8$ for some values of J/U. The parabolic curve in the right-hand side denotes the minimum energy of the individual excitations with a reversed spin.

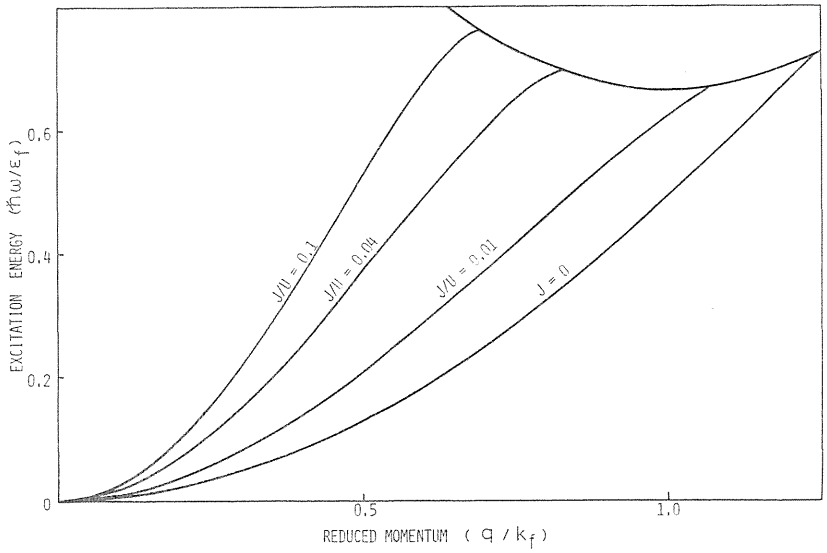

FIG. 17. Dispersion relation of a spin wave for $M=0.6$ and $\varepsilon_f/\Delta=0.6$ for some values of J/U. The parabolic curve in the right-hand side denotes the minimum energy of the individual excitations with a reversed spin.

§ 9. Dispersion Relations of Spin Waves in the Two Band Model and Stable Condition of Ferromagnetic State

In this section we calculate the dispersion relations of spin waves in the two band model with the same effective mass as shown by the one-electron energies,

$$\begin{aligned}\tilde{\varepsilon}_1(k) &= \frac{\hbar^2}{2m}k^2,\\ \tilde{\varepsilon}_2(k) &= \frac{\hbar^2}{2m}k^2+\alpha,\end{aligned} \tag{4.64}$$

where α denotes the splitting between sub-bands 1 and 2 which are schematically shown in Fig. 18, here we assume that the ground state is a saturated ferromagnetic one. In Fig. 18, the solid and broken curves denote the energy spectra of electrons with up and down spins, respectively. We assume a simple molecular field, that is, $K_0(0)=K_{ex}(0)$ in (4.23), so that the exchange splittings, Δ, of the two sub-bands are identical, as mentioned in the calculation of D_B for nickel metal. Furthermore, we assume for the sake of simplicity that

$$\begin{aligned}K_0(q) &= K_{ex}(q) = K_c(q) = K_b(q)\\ &= U+4J\left\{2\cos\frac{1}{2}aq+1\right\} = K(q),\end{aligned} \tag{4.65}$$

and

$$K_a(q) = K(0) - K(q) = 8J\left\{1-\cos\frac{1}{2}aq\right\}, \tag{4.66}$$

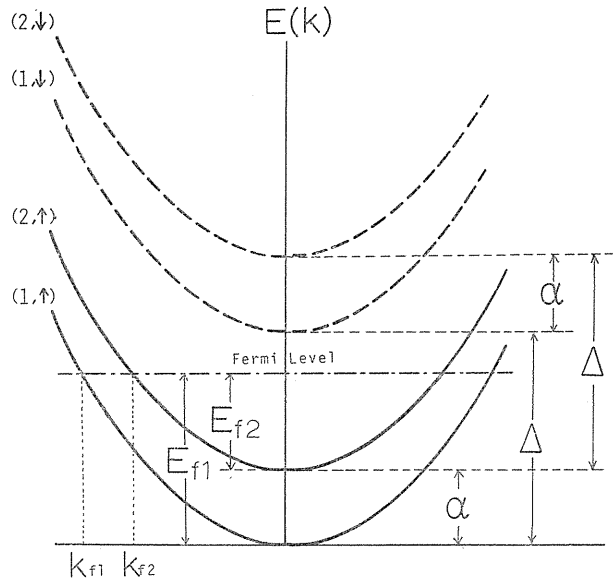

FIG. 18. Schematical curves of the energy spectra of electrons in two band model. Two sub-bands are assumed to have same effective masses. The solid curves (1, ↑) and (2, ↑) denote the sub-bands 1 and 2 with up spin, and broken curves (1, ↓) and (2, ↓) denote the sub-bands 1 and 2 with down spin.

for $q=(q00)$, where the assumption (4.66) is taken so as to satisfy (4.26).

Using assumptions (4.65) and (4.66), we get the eigen-value equation of spin waves as

$$W(q,\omega)=\{1-K(q)(Z_{11}+Z_{22})\}\{1-K(q)(Z_{12}+Z_{21})\} - K_a(q)^2(Z_{11}+Z_{22})(Z_{12}+Z_{21})=0, \tag{4.67}$$

from (4.35), where

$$Z_{ij}=\frac{3k_{fj}m_j}{4q\tilde{\varepsilon}_1(k_{fj})}F(y_{ij}),$$

$$y_{ij}=\frac{\Delta_{ij}-\hbar\omega+\tilde{\varepsilon}_1(k_{fj})q^2/k_{fj}^2}{2\tilde{\varepsilon}_1(k_{fj})q/k_{fj}},$$

and

$$\Delta_{ij}=\tilde{\varepsilon}_i(k)-\tilde{\varepsilon}_j(k)+\Delta,$$

here $F(y)$ and m_j are given by (4.58) and (4.17), respectively, and k_{fj} is the Fermi momentum of the electrons in the j-th sub-band. In calculating (4.67), we assume tentatively the following five relations for parameters,

$$\left.\begin{aligned} &k_{f1}/k_{f2} = 2, \\ &\alpha/\Delta = 3/5, \\ &J/D = 0.04, \\ &U = 1.126 \text{ eV}, \\ &\\ &M = 1. \text{ (per atom)} \end{aligned}\right\} \tag{4.68}$$

and

Using relations (4.68), we get the excitation spectra with a reversed spin from (4.67) as shown in Fig. 19. In Fig. 19, curves (*a*), (*b*) and (*c*) denote the dispersion relations of the acoustical intra-band, acoustical inter-band and optical inter-band branches of spin waves, respectively. The optical intra-band branch cannot be obtained by the assumption (4.65), because when the simple molecular field is assumed the excitation energy of the optical intra-band branch (4.31) is

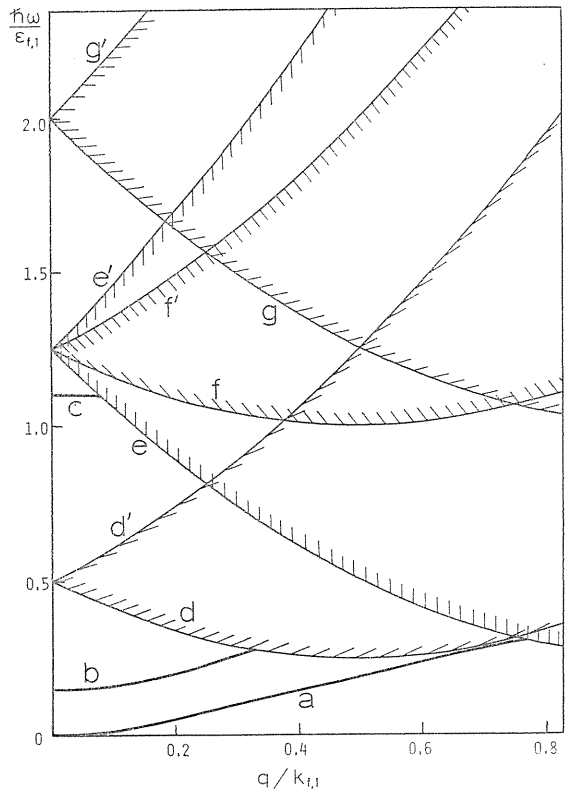

FIG. 19. Excitation spectra of electrons with a reversed spin in the two band model. Curves (*a*), (*b*) and (*c*) denote acoustical intra-band, acoustical inter-band and optical inter-band branches of spin waves, respectively. Other curves denote the maximum and minimum energies of the individual excitations of electrons with a reversed spin.

always equal to the individual excitation energies at $q=0$. The curves (d), (d'), (e), (e'), (f), (f'), (g) and (g') denote the minimum and maximum energies of the individual excitations of $(2,\uparrow)\rightarrow(1,\downarrow)$, $(1,\uparrow)\rightarrow(1,\downarrow)$, $(2,\uparrow)\rightarrow(2,\downarrow)$ and $(1,\uparrow)\rightarrow(2,\downarrow)$, respectively. In order to recognize this excitation spectra, $W(q,\omega)$ in (4.67) is drawn in Fig. 20, Fig. 21 and Fig. 22 against ω/ε_{f1} for $q/k_{f1}=0.05$, 0.1 and 0.4, respectively. In these figures the excitation energies of spin waves are obtained from the intersections of $W(q,\omega)$ with the horizontal axis $W(q,\omega)=0$, excluding the regions denoted by heavy lines on the horizontal axis, which denote the individual excitation energies with a reversed spin. In the left and upper corner of each figure, an enlarged curve of $W(q,\omega)$ for smaller values of ω is shown.

Finally, we discuss the properties of the inter-band branches of spin waves in the simplified model denoted by (4.64), (4.65) and (4.66). The energies of inter-band spin waves at $q=0$ are obtained from the eigenvalue equation (4.38) as

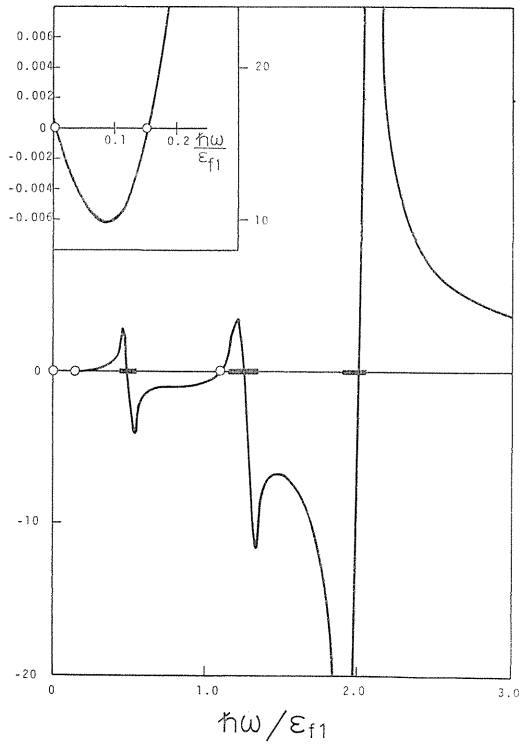

FIG. 20. Curve of $W(p,\omega)$ in (4.67) against $\hbar\omega/\varepsilon_{f1}$ for $q/k_{f1}=0.05$. Open circles denote the spin wave energies. Heavy lines on the horizontal axis denote the individual excitation energies with a reversed spin. In the left and upper corner an enlarged curve for small ω is shown.

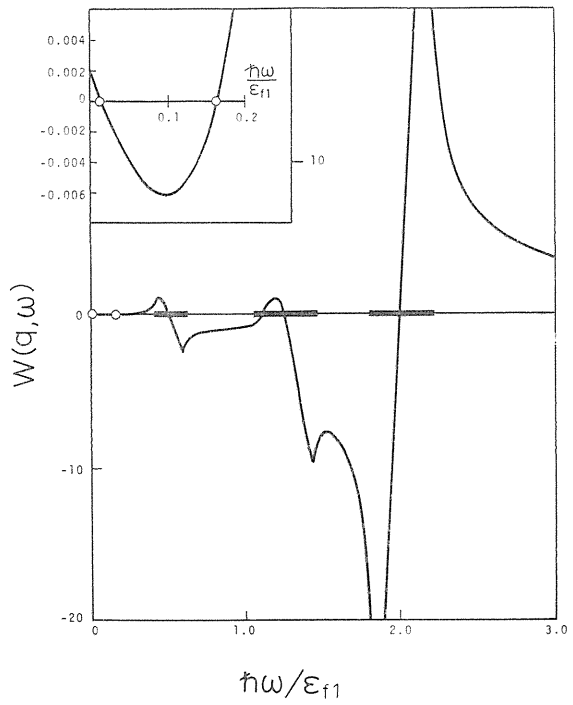

FIG. 21. Curve of $W(q, \omega)$ in (4.67) against $\hbar\omega/\varepsilon_{f1}$ for $q/k_{f1} = 0.1$. Open circles denote the spin wave energies. Heavy lines on the horizontal axis denote the individual excitation energies with a reversed spin. In the left and upper corner an enlarged curve for small ω is shown.

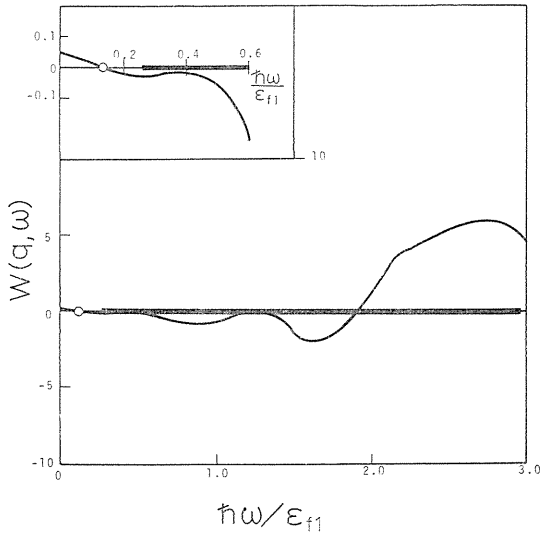

FIG. 22. Curve of $W(q, \omega)$ in (4.67) against $\hbar\omega/\varepsilon_{f1}$ for $q/k_{f1} = 0.4$. Open circle denotes the spin wave energy. Heavy line on the horizontal axis denotes the individual excitation energies with a reversed spin. In the left and upper corner an enlarged curve for small ω is shown.

$$\hbar\omega_0 = \frac{1}{2}\left[\Delta \pm \sqrt{\Delta^2+4\alpha^2-4\alpha(m_1-m_2)K(0)}\right], \tag{4.69}$$

for the saturated ferromagnetic state, where the solutions of plus and minus signs in the square bracket of (4.69) denote the optical and acoustical inter-band branches, respectively. Therefore, if

$$(m_1-m_2)K(0) < \alpha, \tag{4.70}$$

the energy of the acoustical inter-band branch is negative and the ferromagnetic state becomes unstable. Recently Katsuki and Wohlfarth[78] have obtained the stable condition of the ferromagnetic state in the single band model, by discussing the sign of the excitation energy of a spin wave. In the multiple band model, we must investigate not only the energy of the acoustical intra-band branch of spin waves but also that of the acoustical inter-band branch, in order to discuss the stable condition of the ferromagnetic state. When the excitation energy of the acoustical inter-band branch is small, the magnetic properties at low temperature are affected, for instance, the decrease of the magnetization with increasing temperature becomes larger and the Curie temperature may decrease even if the magnetization is large, as seen in the Invar alloys.

Recently Thompson and Myers[81] have calculated the dispersion relation of a spin wave (of the acoustical intra-band branch) for nickel metal. However in their calculation the inter-band transitions are not taken into account, so that the cut-off momentum does not exist. Taking account of the inter-band transitions, we must calculate the dispersion relations of spin waves for real ferromagnetic metals.

Chapter V. Plasma Osciliation in a Ferromagnetic Electron Gas[82]

§ 1. Introduction

In the last chapter, we have studied collective modes of electron excitations with a reversed spin in ferromagnetic metals. It is well-known that another collective mode of electron motions due to the density fluctuation of electrons, that is, a plasma oscillation or so-called "plasmon", exists in metals[14]. This plasmon is experimentally found by inelastic scattering of electrons not only for alkali metals but also for ferromagnetic transition metals[14]. Theoretically the plasmon in an electron gas was first studied by Bohm and Pines[83][84]. After the works of Bohm and Pines, the study of a plasmon in an electron gas has been one of the most attractive topics in the connection with the study of the correlation energy of elelctrons for many theoreticians[26][72][85].

In this chapter, we study the dispersion relation of a plasmon in a ferromagnetic electron gas (An electron gas may not show ferromagnetism, but tentatively we assume that a modified electron gas can be ferromagnetic in a certain condition, *e.g.* in the case of an electron gas with a heavy thermal mass[26].). As shown by Bohm and Pines[83][84], a plasmon can be understood by the classical considerations but it is interesting to study a plasmon in the ferromagnetic state because the ferromagnetism is explained by the quantum mechanical exchange interaction between electrons, which can not be understood by the classical theory.

In the paramagnetic state, Kanazawa *et al.*[86] have studied the effect of the exchange interaction between electrons on the dispersion relation of a plasmon. We consider this problem in the ferrcmagnetic electron gas by the method of normal modes. Although the model of an electron gas may not be appropriate to the real ferromagnetic metals, this model is the most simple one for discussing a plasmon, so that we adopt this model and see only the effect of the exchange interaction on the dispersion relation of a plasmon in the ferromagnetic state.

§ 2. Integral Equation for Normal Modes

The Hamiltonian $\mathscr{H}$ of an electron gas is given by

$$\begin{aligned}\mathscr{H} &= \mathscr{H}_0 + \mathscr{H}_1, \\ \mathscr{H}_0 &= \sum_{k,\sigma} E(k) a^+_{k,\sigma} a_{k,\sigma}, \\ \mathscr{H}_1 &= \frac{1}{2} \sum_q{}' \sum_{k,k'} \sum_{\sigma,\sigma'} v(q)\, a^+_{k+q,\sigma} a^+_{k'-q,\sigma'} a_{k',\sigma'} a_{k,\sigma},\end{aligned} \tag{5.1}$$

where

$$E(k) = \frac{\hbar^2 k^2}{2m}, \qquad v(q) = \frac{4\pi e^2}{q^2 V}, \tag{5.2}$$

$a^+_{k,\sigma}$ and $a_{k,\sigma}$ are creation and annihilation operators of an electron with momentum k and spin σ, and V denotes the volume. The prime in the summation over q denotes a sum in which $q=0$ is excluded, and this takes into account the uniform background of positive charge.

An operator which represents a normal mode of a plasmon with momentum p is defined by

$$A^+_p = \sum_{l,\sigma} f^\sigma_p(l)\, a^+_{l+p,\sigma} a_{l,\sigma}. \tag{5.3}$$

Coefficients $f^\sigma_p(l)$ in (5.3) are determined by the following equation of motion,

$$\hbar\omega A^+_p = [\mathscr{H},\ A^+_p]. \tag{5.4}$$

Using the extended random phase approximation (4.9) in the commutator between $\mathscr{H}_1$ and A^+_p[71], we can linearize this equation of motion and obtain the integral equation for $f^\sigma_p(l)$ as follows:

$$\begin{aligned}&\{E(l+p) - E(l) - \hbar\omega\} f^\sigma_p(l) \\ &\quad - v(p) \sum_{k,\sigma'} f^{\sigma'}_p(k)(n_{k+p,\sigma'} - n_{k,\sigma'}) \\ &\quad + \sum_k{}' v(k-l)\{f^\sigma_p(k) - f^\sigma_p(l)\}(n_{k+p,\sigma} - n_{k,\sigma}) = 0,\end{aligned} \tag{5.5}$$

where $n_{k,\sigma}$ denotes the occupation number with momentum k and spin σ. The prime in the summation over k in the last term denotes a sum in which $k=l$ is excluded. The reason why we use the operator of the normal modes by summing up over spin, as shown in (5.3), is explained in the following way. When we consider the equation of motion of the excitation operator, $a^+_{k+p,\sigma} a_{k,\sigma}$, this operator is found to couple with the excitation operators with the antiparallel spin,

$a^{+}_{k'+p,-\sigma}a_{k',-\sigma}$, in the same way as the operators with parallel spin, within the approximation mentioned above.

Using the approximate Hamiltonian introduced by Sawada *et al.*[72], we can obtain an equation without the last term in (5.5) and get the eigenvalue equation directly. However, because of the appearance of the last term in (5.5), it is not so easy to solve (5.5). A similar circumstance occurs in the problem of magnon in metals, but the difficulty is restored by the approximation for the matrix elements of the Coulomb interactions, as mentioned in chapter IV.

§ 3. Dispersion Relation of a Plasmon in Paramagnetic State

For small p, we can easily find the last term in the left-hand side of (5.5) to be smaller by the order of p^2 than the second term. Therefore, we can find the dispersion relation by the iteration method.

First we consider the case of the paramagnetic state. As the first approximation, if we neglect the last term in (5.5), we can obtain the same eigenvalue equation as that given by Sawada *et al.*[72],

$$2v(p)\sum_{l}\frac{n_{l+p}-n_l}{E(l+p)-E(l)-\hbar\omega_0(p)}=1, \tag{5.6}$$

and

$$f^{\circ}_{p}(l)=\frac{N_p}{E(l+p)-E(l)-\hbar\omega_0(p)}, \tag{5.7}$$

where we neglect the spin suffix and N_p is a normalization constant which depends only on p, and $f^{\circ}_{p}(l)$ and $\hbar\omega_0(p)$ denote the corresponding values at the first approximation. From (5.6), the dispersion relation of a plasmon is written as[72],

$$\hbar\omega_0(p)=\hbar\omega_0(0)+\frac{3\hbar^4k_f^2p^2}{10m^2\hbar\omega_0(0)}, \tag{5.8}$$

where

$$\hbar\omega_0(0)=\sqrt{4\pi\hbar^2ne^2/m}, \tag{5.9}$$

and n and k_f are the density of electrons and the Fermi momentum, respectively.

At the second approximation, we take account of the third term in (5.5) in which f_p is replaced by f°_{p} and in the first and second terms of (5.5), f_p and $\hbar\omega$ are replaced by $f^{\circ}_{p}+\Delta f_p$ and $\hbar\omega_0+\hbar\Delta\omega$, respectively. Multipling the following factor,

$$\frac{n_{l+p}-n_l}{E(l+p)-E(l)-\hbar\omega_0(p)},$$

to the modified equation of (5.5) and taking the sum over l, we can obtain the correction to the dispersion relation (5.8), within the linear terms of Δf_p and $\hbar\Delta\omega$ as follows,

$$\hbar\Delta\omega=\frac{\sum'_{l,k}\dfrac{(n_{l+p}-n_l)(n_{k+p}-n_k)}{E(l+p)-E(l)-\hbar\omega_0(p)}v(k-l)\{f^{\circ}_{p}(k)-f^{\circ}_{p}(l)\}}{\sum_{l}\dfrac{(n_{l+p}-n_l)f^{\circ}_{p}(l)}{E(l+p)-E(l)-\hbar\omega_0(p)}}. \tag{5.10}$$

To get (5.10), we have made use of (5.6). For small p, we can expand this exchange correction (5.10) as a power series of p and get the leading term

$$\hbar\Delta\omega = -\frac{e^2\hbar^2 k_f p^2}{10\pi m_0\hbar\omega(0)}. \tag{5.11}$$

From (5.8), (5.9) and (5.11), the dispersion relation for the paramagnetic electron gas is given by,

$$\hbar\omega_p(p) = \hbar\omega_0(0) + \frac{3\hbar^4 k_f^2}{10 m^2\hbar\omega_0(0)} p^2\left\{1 - \frac{me^2}{3\pi\hbar^2 k_f}\right\}. \tag{5.12}$$

This result agrees with that obtained by Kanazawa *et al.*[86] by using the Green's function method.

§ 4. Dispersion Relation of a Plasmon in Ferromagnetic State

In the previous section, we have considered the collective modes of an electron gas in the paramagnetic state. In this section we consider the collective modes in the ferromagnetic electron gas, that is, the numbers of electrons with up and down spins are different. It is a difficult problem to decide whether the ferromagnetic state of an electron gas is stable or not. We assume tentatively, however, that the ferromagnetic state is stable in the ground state of an electron gas by a certain circumstance.

At the first approximation, f_p^σ is independent of spin, as the second term in (5.5) is summed over spin, and the corresponding expression of f_p^σ is the same as (5.7). On the other hand, the eigenvalue equation is given by

$$v(p)\sum_{l,\sigma}\frac{n_{l+p,\sigma} - n_{l,\sigma}}{E(l+p) - E(l) - \hbar\omega_0(p)} = 1. \tag{5.13}$$

We can obtain the energy of a plasmon in the ferromagnetic state for small p as follows,

$$\hbar\omega_f^0(p) = \hbar\omega_0(0) + \frac{3\hbar^4 p^2}{10 m^2\hbar\omega_0(0)}\left(\frac{n_+ k_{f+}^2 + n_- k_{f-}^2}{n}\right), \tag{5.14}$$

where $\hbar\omega_0(0)$ is given by (5.9), and n_+ and n_- are the densities of electrons with up and down spins, and k_{f+} and k_{f-} are the Fermi momentums of electrons with up and down spins, respectively.

At the second approximation, taking account of the third term in (5.5), we get simultaneous equations with respect to up and down spins,

$$\begin{aligned}
&-\hbar\Delta\omega\sum_l\frac{n_{l+p,\sigma} - n_{l,\sigma}}{E(l+p) - E(l) - \hbar\omega_0} f_p^\sigma(l) \\
&+\sum_l\frac{v(p)(n_{l+p,-\sigma} - n_{l,-\sigma})}{E(l+p) - E(l) - \hbar\omega_0}\sum_k \Delta f_p^\sigma(k)(n_{k+p,\sigma} - n_{k,\sigma}) \\
&-\sum_l\frac{v(p)(n_{l+p,\sigma} - n_{l,\sigma})}{E(l+p) - E(l) - \hbar\omega_0}\sum_k \Delta f_p^{-\sigma}(k)(n_{k+p,-\sigma} - n_{k,-\sigma})
\end{aligned}$$

$$+\sum_{k,l}{}' \frac{(n_{l+p,\sigma}-n_{l,\sigma})(n_{k+p,\sigma}-n_{k,\sigma})}{E(l+p)-E(l)-\hbar\omega_0} v(k-l)\{f_p^\circ(k)-f_p^\circ(l)\}=0, \tag{5.15}$$

by the same method as given in § 3. We can eliminate $\Delta f_p^{\pm}$ in (5.15) by using the relation (5.13) and get the exchange correction to the dispersion relation as follows,

$$\hbar\Delta\omega=\frac{\sum_{k,l,\sigma}{}' \frac{(n_{l+p,\sigma}-n_{l,\sigma})(n_{k+p,\sigma}-n_{k,\sigma})}{E(l+p)-E(l)-\hbar\omega_0(p)} v(k-l)\{f_p^\circ(k)-f_p^\circ(l)\}}{\sum_{l,\sigma}\frac{n_{l+p,\sigma}-n_{l,\sigma}}{E(l+p)-E(l)-\hbar\omega_0(p)} f_p^\circ(l)}. \tag{5.16}$$

Expanding the correction (5.16) as a power series of p, we get a leading term,

$$\hbar\Delta\omega=-\frac{e^2\hbar^2p^3}{10\pi m\hbar\omega_0(0)}\frac{k_{f+}^4+k_{f-}^4}{k_{f+}^3+k_{f-}^3}, \tag{5.17}$$

for small p. From (5.14) and (5.17), we can get the dispersion relation for a plasmon with small momentum p in the ferromagnetic electron gas as

$$\hbar\omega_f(p)=\hbar\omega_0(0)+\frac{3\hbar^4p^2}{10m^2\hbar\omega_0(0)}\frac{n_+k_{f+}^2+n_-k_{f-}^2}{n}\left\{1-\frac{me^2}{3\pi\hbar^2}\frac{k_{f+}^4+k_{f-}^4}{k_{f+}^5+k_{f-}^5}\right\}. \tag{5.18}$$

Comparing the result (5.18) with the result in the paramagnetic case (5.12), we find that the constant parts of $\hbar\omega(p)$ in the paramagnetic and ferromagnetic states are the same, but the coefficients of p^2 in the expressions of $\hbar\omega(p)$ with respect to p, are different from each other in these two states. This difference will be roughly estimated for real ferromagnetic metals and a possibility that this difference will be observed in experiments is discussed in the next section.

§ 5. Numerical Estimations for Iron, Cobalt and Nickel

Now, we will estimate numerically the order of magnitude of the difference between plasma frequencies in the paramagnetic and ferromagnetic states for the 3 d-group ferromagnetic metals, iron, cobalt and nickel, using the results (5.12) and (5.18) obtained above. We have to consider at least six sub-bands, one s-band and five d-bands, to discuss the plasmon in these metals. The model of an electron gas is too simple to apply to these metals. We must take into account the band structures and inter-band transitions etc. to estimate quantitatively the dispersion relations in these metals. We, however, consider the model of an electron gas to be able to give an outline of the plasmon in the magnetic states of real transition metals, as the first approximation.

From (5.12) and (5.18), the coefficients of p^2, I, are written as,

$$I_p=\frac{3\hbar^4}{10\hbar\omega_0(0)m^2}(3\pi^2n)^{2/3}\left\{1-\frac{me^2}{3\pi\hbar^2}\left(\frac{1}{3\pi^2n}\right)^{1/3}\right\}, \tag{5.19}$$

in the paramagnetic state, and

$$I_f = \frac{3\hbar^4}{10\hbar\omega_0(0)m^2}(6\pi^2)^{2/3}\frac{n_+^{5/3}+n_-^{5/3}}{n} \times\left\{1-\frac{me^2}{3\pi\hbar^2}\left(\frac{1}{6\pi^2}\right)^{1/3}\frac{n_+^{4/3}+n_-^{4/3}}{n_+^{5/3}+n_-^{5/3}}\right\}. \tag{5.20}$$

in the ferromagnetic state, respectively.

Using the relation,

$$n_+ + n_- = n, \qquad n_+ - n_- = n_B,$$

where n_B denotes the density of magnetic carriers, we can expand I_f in terms of n_B/n for the weak ferromagnetic case ($n_B \ll n$) and obtain,

$$\frac{I_f - I_p}{I_p} = \frac{\frac{5}{9} - \frac{2me^2}{27\pi\hbar^2}\left(\frac{1}{3\pi^2 n}\right)^{1/3}}{1-\frac{me^2}{3\pi\hbar^2}\left(\frac{1}{3\pi^2 n}\right)^{1/3}}\left(\frac{n_B}{n}\right)^2. \tag{5.21}$$

Numerical values of $(I_f-I_p)/I_p$ in (5.21), which are given in Tables 4 and 5 for iron, cobalt and nickel metals, are obtained by the following ways. The theoretical

TABLE 4. Numbers of magnetic carriers, n_B, densities of electrons which were estimated from the observed values of $\hbar\omega_0(0)$, n_{eff}, and reduced values of the difference between coefficients of the terms proportional to p^2 in the dispersion relation of a plasmon, $(I_f-I_p)/I_p$, for Iron, cobalt and nickel metals

	Fe	Co	Ni
n_B/atom	2.2	1.7	0.6
n_{eff}/atom	3.74	3.55	4.18
$(I_f-I_p)/I_p$	0.204	0.136	0.012

TABLE 5. Numbers of magnetic carriers, n_B, densities of electrons, n, reduced effective masses which were estimated from the observed values of $\hbar\omega_0(0)$, m_{eff}/m, and reduced values of the difference between coefficients of the terms proportional to p^2 in the dispersion relation of a plasmon, $(I_f-I_p)/I_p$, for iron, cobalt and nickel metals

	Fe	Co	Ni
n_B/atom	2.2	1.7	0.6
n/atom	8	9	10
m_{eff}/m	2.13	2.53	2.39
$(I_f-I_p)/I_p$	0.0467	0.0224	0.0022

values of $\hbar\omega_0(0)$ for these metals were obtained by assuming all electrons outside the approximate closed shell are free[14]. These theoretical values of $\hbar\omega_0(0)$ for these metals were different from the experimental values[14]. In our numerical estimation we make use of the effective density of electrons, n_{eff}, or the effective mass of an electron, m_{eff}, which can give the same numerical values of $\hbar\omega_0(0)$ in (5.9) as the observed values. If we estimate n_{eff}, assuming $m_{eff}/m=1$, the values of n_{eff} are obtained as given in Table 4. Using these values of n_{eff} and the experimental data of n_B, we can get the values of $(I_f-I_p)/I_p$ in (5.21), as shown in Table 4. If we estimate m_{eff} to fit the observed values of $\hbar\omega_0(0)$ with its calculated values by (5.9), the values of m_{eff}/m are obtained as shown in Table 5 and the corresponding values of $(I_f-I_p)/I_p$ in (5.21) are obtained from the experimental data of n_B, as shown in Table 5.

Between these two numerical estimations of $(I_f-I_p)/I_p$, there are differences by one order of magnitude as seen from Tables 4 and 5, but it seems that the difference between the coefficients of p^2 in the dispersion relation of a plasmon in the ferromagnetic and paramagnetic states may be observed in the experiments of the inelastic scattering of electrons for iron and cobalt metals, because the values of $(I_f-I_p)/I_p$ are relatively large for these metals. There may be a difficulty in this sort of experiments, because the Curie temperatures of iron and cobalt are very high. However, we must notice that, as discussed above, the model of an electron gas may be too simple to discuss in detail the dispersion of a plasmon in the transition metal.

Chapter VI. High Field Susceptibility for Iron Metal and its Alloys[87]

§ 1. Introduction

Recently, susceptibilities for ferromagnetic iron and nickel metals and their alloys in high magnetic field have been measured below the Curie temperature by Stoelinga and Gersdorf[15], Freeman *et al.*[88] and Herring *et al.*[89]. It is well-known that the high field susceptibility for a ferromagnetic metal at 0°K is composed of the susceptibility due to electron spins, $\chi_s(0)$, which corresponds to the Pauli spin susceptibility in the paramagnetic state, and of the sum of the orbital-paramagnetic susceptibility and the diamagnetic one, χ_c[15)88)89)].

Wohlfarth[90] and Gersdorf[91] have shown before that in the Stoner model the values of the high field spin susceptibility, χ_s, at 0°K can be calculated by the values of the density of states at the Fermi levels of up and down spin bands and the value of a molecular field coefficient, α. Therefore, the data of the high field susceptibility are useful to obtain informations and to discuss about the values of the density of states at Fermi levels with up and down spins and the values of α and χ_c for ferromagnetic 3 d-group transition metals and their alloys.

In § 2, a more general expression of χ_s for a ferromagnetic metal at finite temperatures is derived in the band model by the method given before by Shimizu[16)17)] (hereafter, to be referred to as I and II). By using this expression of χ_s, the values of $\chi_s(0)$ for ferromagnetic metal and its alloys with bcc structure are calculated in § 2 and § 3, where the density of states curve[7] shown in Fig. 6 and the values of α[75], which were estimated from the exchange splitting in the same density of states curve, are made use of. The calculated value of $\chi_s(0)$

for iron metal is compared with the experimental datum at 4.2°K obtained by Stoelinga and Gersdorf[15] and the value of χ_c is estimated for iron metal in § 2. In § 3, the values of $\chi_s(0)$ are calculated also for iron alloys with cobalt, nickel, chromium and vanadium in the same way as that for iron metal.

In § 4, the temperature dependence of the high field susceptibility which is derived from the increase of the magnetization due to the suppression of spin wave excitations by high magnetic field, χ_{sw}, is calculated by the model of non-interacting spin waves, whose energies are determined from the experiments of the neutron scattering. It is shown that the calculated results are consistent with the observed results for iron metal and its alloys and the temperature variation of χ_{sw} is fairly larger than that of χ_s for iron metal.

In § 5, the field dependences of χ_{sw} and χ_s are calculated and it is shown that the field dependence of χ_{sw} is fairly larger than that of χ_s for iron metal. Finally, in § 6 it is pointed out that for a special density of states curve there is a possibility that the field dependence of χ_s shows a discontinuous change at a certain critical field.

§ 2. High Field Susceptibility for Iron Metal at 0°K

Following the method given in II, the difference between free energies in ferromagnetic and paramagnetic states with the external field H is written as

$$\Delta F = \int_0^n \Delta\zeta(n')dn' + E_{ex}(n) - 2\mu_B nH, \tag{6.1}$$

where

$$2n = \int_{-\infty}^{\infty} \nu(\varepsilon) f(\varepsilon - \zeta_+) d\varepsilon - \int_{-\infty}^{\infty} \nu(\varepsilon) f(\varepsilon - \zeta_-) d\varepsilon, \tag{6.2}$$

$$\Delta\zeta(n) = \zeta_+(n) - \zeta_-(n), \tag{6.3}$$

$\nu(\varepsilon)$ and $f(\varepsilon-\zeta_\pm)$ are the density of states and Fermi distribution function, respectively, ζ_+ and ζ_- are the Fermi levels of plus and minus spin bands when the magnetization is given by $M=2\mu_B n$, and E_{ex} is the exchange energy.

From (6. 1) and the extremum condition of ΔF against n, $\partial\Delta F/\partial n=0$, we have

$$\Delta\zeta(n) = 4\mu_B^2 \alpha n - 2\mu_B H, \tag{6.4}$$

where a molecular field coefficient α depends in general on n and is defined as

$$\alpha = -\frac{1}{4\mu_B^2 n}\frac{\partial E_{ex}(n)}{\partial n}.$$

If we expand (6. 4) in Taylor's series of $n-n_0=\Delta n(=\Delta M/2\mu_B)$, where n_0 is the value of n when $H=0$, we get

$$\chi_S = \frac{\partial\Delta M}{\partial H} = \left[\frac{1}{4\mu_B^2}\left(\frac{\partial\Delta\zeta(n)}{\partial n}\right)_0 - \alpha(n_0) - n_0\left(\frac{\partial\alpha}{\partial n}\right)_0\right]^{-1}, \tag{6.5}$$

where the subscript of derivatives, 0, denotes their values at $n=n_0$.

From (6. 3), (6. 5) and $\partial\zeta_\pm/\partial n=\nu(\zeta_\pm)^{-1}$ the χ_s at 0°K is given by

$$\chi_s(0)=\left[\frac{1}{4\mu_B^2}\left\{\frac{1}{\nu(\zeta_+)}+\frac{1}{\nu(\zeta_-)}\right\}-\alpha(n_0)-n_0\left(\frac{\partial\alpha}{\partial n}\right)_0\right]^{-1}. \tag{6.6}$$

The formula (6.6) is the same with that given by Wohlfarth[90] and Gersdorf[91] if α does not depend on n, that is, the last term in (6.6) is neglected. The stable condition of free energy (6.1), $\partial^2\Delta F/\partial n^2>0$, shows that (6.5) and (6.6) are positive (*cf.* eq. (8) in I and eq. (12) in II).

The dependence on n of α can be estimated from the analysis of the temperature dependence of M by the band model. For nickel and iron metals, we have already estimated the dependences on n of α, as shown in Fig. 2 and Fig. 7. In these analyses, however, we have neglected the spin wave contribution to the decrease of the magnetization, so that these dependences on n of α will not be so reliable at lower temperatures where the spin wave contribution to the decrease of M is dominant. If we use the dependence on n of α for iron metal shown in Fig. 7, the values of $n_0(\partial\alpha/\partial n)_0$ in (6.6) and α become comparable with each other and χ_s becomes negative. This curious result shows that the dependence on n of α shown in Fig. 7 is not reliable at lower temperatures and the value of $n_0(\partial\alpha/\partial n)_0$ will not be so large as the value of α. Therefore, for the sake of simplicity we assume that α does not depend on n in the following discussions of the chapter.

The values of $\alpha(n_0)$ in (6.6) for iron metal and iron alloys with cobalt, nickel, chromium and vanadium were already estimated from (6.4), using the experimental data of M and the exchange splittings $\Delta\zeta(n_0)$ which were obtained for the density of states curve shown in Fig. 6 and the results were shown in Fig. 2 a of the ref. 7 and Fig. 1 b of the ref. 75.

Other contributions to the total high field susceptibility, χ, are χ_c and χ_{sw}. The χ_{sw} is zero at 0°K, because no spin wave is excited at 0°K (This susceptibility is discussed in § 4.). Therefore, at 0°K we have

$$\chi=\chi_s(0)+\chi_c. \tag{6.7}$$

Using the density of states curve and the value of $\alpha=1.16\times10^4$ mole/emu obtained in § 3 of chapter II, we get from (6.6) $\chi_s(0)=0.99\times10^{-4}$ emu/mole for iron metal. On the other hand, the observed value of χ at 4.2°K is 2.32×10^{-4} emu/mole[15]. From (6.7) the difference between the observed value of χ and the calculated value of $\chi_s(0)$ is given by $\chi_c=1.33\times10^{-4}$ emu/mole. This value of χ_c seems to be reasonable because the values of χ_c, which were estimated from the analyses of the temperature variation of the susceptibilities for vanadium and chromium metals with the same bcc structure as that of iron metal, are 1.78×10^{-4} and 1.40×10^{-4} emu/mole, respectively[5][92].

§ 3. Concentration Dependences of High Field Susceptibility

In this section, we estimate the values of $\chi_s(0)$ for iron alloys with cobalt, nickel, chromium and vanadium, making use of the density of states curve shown in Fig. 6 and the values of $\alpha(n_0)$ shown in Fig. 1 b of the ref. 75.

For iron-cobalt alloys, the magnetization increases with increasing concentration of cobalt[93], the Fermi level of the plus spin band, ζ_+, shifts toward the right-hand side and the height of the density of states at Fermi level, $\nu(\zeta_+)$,

decreases rapidly up to about 30 at. % cobalt in iron. Therefore, the first term in the square bracket of (6. 6) increases rapidly at about this concentration of cobalt. The first term in the square bracket of (6. 6), that is, $\{\nu(\zeta_+)^{-1}+\nu(\zeta_-)^{-1}\}/4\mu_B^2$, and α against the concentration of cobalt in iron are shown by solid curves in Fig. 23, respectively. From these numerical values and (6. 6) the values of $\chi_s(0)$ for iron-cobalt alloys are obtained as shown in Fig. 24. In Fig. 24 the solid curve shows the difference $\Delta\chi_s$ between the calculated values of $\chi_s(0)$ for the alloys and pure iron metal, and open circles show the difference $\Delta\chi$ between the observed values by Stoelinga and Gersdorf[15] of χ at 4.2°K for the alloys and iron metal. A satisfactory agreement between the calculated results of $\Delta\chi_s$ and experimental data of $\Delta\chi$ is obtained for iron-cobalt alloys. From this agreement it is considered that χ_c scarcely has the concentration dependence in comparison with that of $\chi_s(0)$ and the concentration dependence of χ can be approximately explained only by that of $\chi_s(0)$.

For iron-nickel alloys, we can estimate $\Delta\chi_s$ by the same method as that for iron-cobalt alloys. The result is shown in Fig. 25 with experimental data of $\Delta\chi$[15]. The agreement between the calculated and experimental results is not so bad. (If we estimate the difference between energies in the ferromagnetic and paramagnetic states by using the density of states curve and the values of α used above for iron-nickel alloys, the energy of ferromagnetic states is higher than that of paramagnetic state at 0°K for larger concentrations of nickel in iron

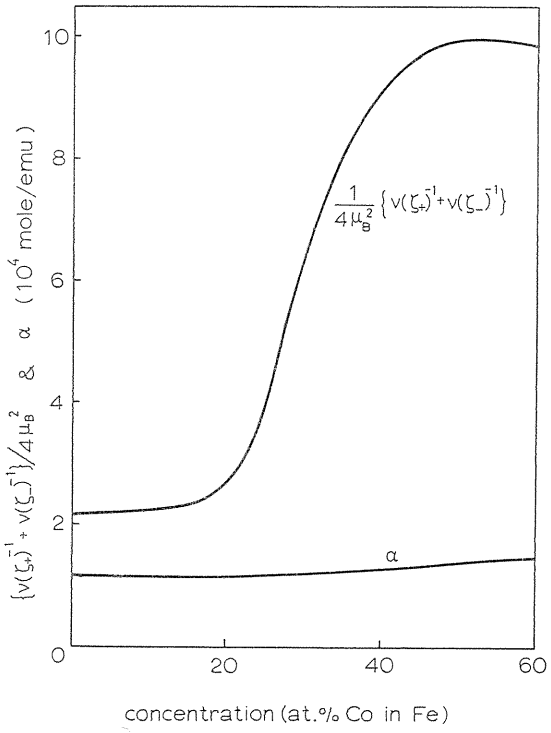

FIG. 23. Concentration dependence of $\{\nu(\zeta_+)^{-1}+\nu(\zeta_-)^{-1}\}/4\mu_B^2$ and α for iron-cobalt alloys.

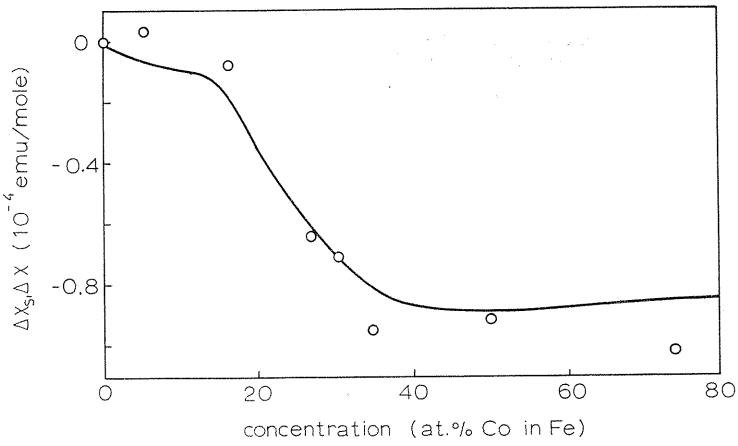

FIG. 24. Concentration dependence of $\chi_s(0)$ for iron-cobalt alloys. $\Delta\chi_s$ denotes the differences between the calculated values of $\chi_s(0)$ for the alloys and for pure iron metal. Open circles show the corresponding differences of the experimental data[15].

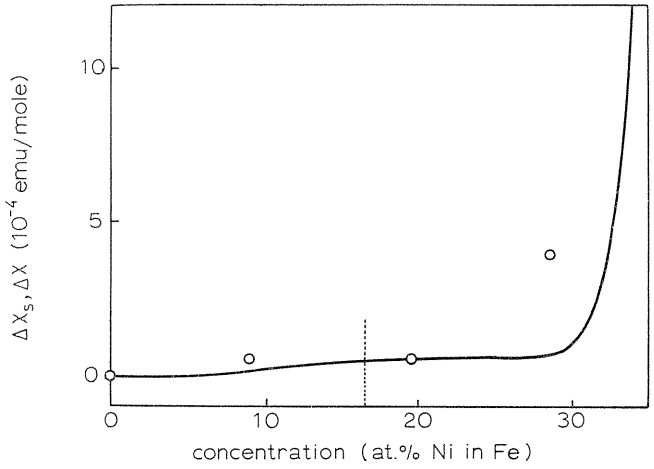

FIG. 25. Concentration dependence of $\chi_s(0)$ for iron-nickel alloys. $\Delta\chi_s$ denotes the differences between the calculated values of $\chi_s(0)$ for the alloys and pure iron metal. Open circles show the corresponding differences of the experimental data[15].

than about 17 at. % nickel shown by the vertical dotted line in Fig. 25; in experiments the ferromagnetic state is stable up to about 35 at. % nickel in iron[93]. A part of this discrepancy may be due to the uncertainties of the density of states curve and of the values of α for iron-nickel alloys, but the main part will be improved by a slight modification of the density of states curve.) For iron-chromium and iron-vanadium alloys, the calculated results of $\Delta\chi_s$ are shown in Fig. 26. Unfortunately, we have no experimental data of $\Delta\chi$ for these alloys at present and expect that the experiments are carried out for these alloys.

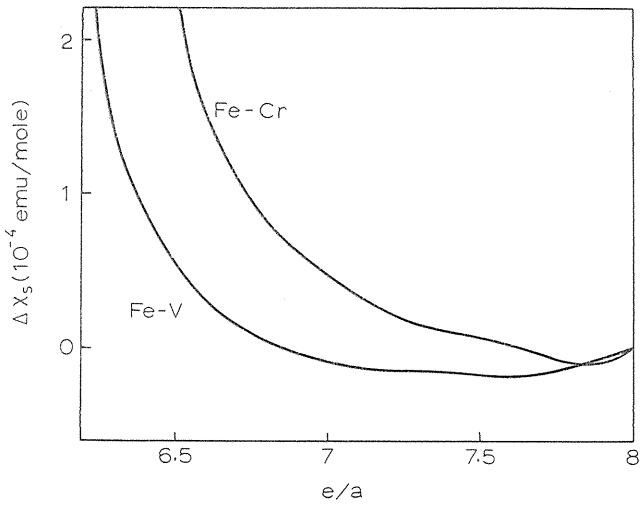

FIG. 26. Concentration dependence of $\chi_s(0)$ for iron-chromium and iron-vanadium alloys. $\Delta\chi_s$ denotes the differences between the calculated values of $\chi_s(0)$ for the alloys and pure iron metal.

§ 4. Temperature Dependence of High Field Susceptibility

As the temperature rises from 0°K, spin waves are excited in a ferromagnet and play an important role to determine the magnetic properties of the ferromagnet at low temperature. Another contribution due to the suppression of spin wave excitations by high magnetic field to the high field susceptibility appears at finite temperatures. This effect of spin waves on the high field susceptibility was first discussed by Holstein and Primakoff[94] in the Heisenberg model. In the band model, the calculation of the high field susceptibility similar to that shown by Holstein and Primakoff can be made in the following way. The difference between the magnetizations at T and 0°K in the magnetic field H is written as

$$\Delta M_{sw} = -\frac{\mu_B \Omega}{\pi^2}\int_0^{q_{\max}} \frac{q^2 dq}{\exp\{(\hbar\omega_q + 2\mu_B H)/kT\} - 1}, \tag{6.8}$$

where we take a model of non-interacting isotropic spin waves with momentum q and energy $\hbar\omega_q$, and $q_{\max}$ and Ω denote the cut-off momentum of the spin waves and the atomic volume, respectively. At low temperature, we approximately take $\hbar\omega_q = Dq^2$ and $q_{\max}$ as infinity, and we obtain

$$\chi_{sw} = \frac{d\Delta M_{sw}}{dH} = \frac{\mu_B^2 \Omega}{\pi^2}(kT)^{1/2} D^{-3/2} F(H), \tag{6.9}$$

where

$$F(H) = \int_0^\infty \frac{x^{1/2}\exp\{x + (2\mu_B H/kT)\}}{[\exp\{x + (2\mu_B H/kT)\} - 1]^2}\, dx.$$

In (6.9) we have neglected the field dependence of D. It can be calculated from the equation of motion for the normal modes of a spin flipping by the random

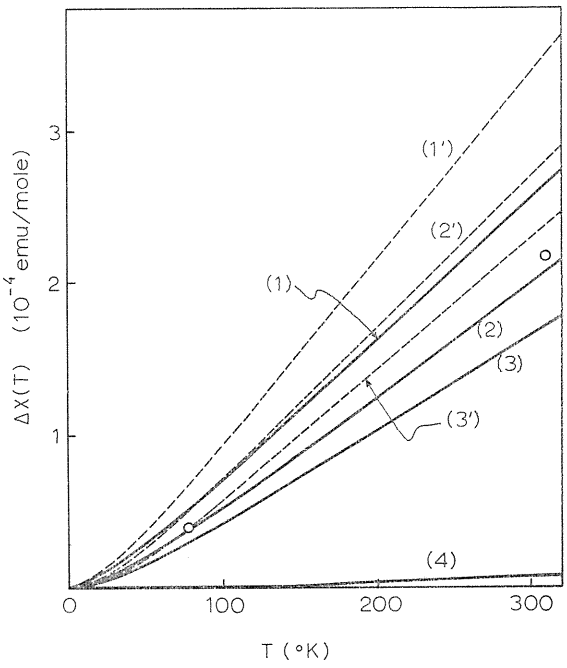

FIG. 27. Temperature dependences of χ_{sw} for iron metal. Solid curves (1), (2) and (3) are calculated for $H=100$, 150 and 200 KOe, respectively, by using the data of exchange stiffness constant measured by Lowde *et al.*[57] Broken curves (1'), (2') and (3') are calculated by using the dispersion relation of spin waves measured by Shirane *et al.*[44] Curve (4) denotes the difference between the values of χ_s at T and 0°K. Open circles denote the experimental data[15].

phase approximation and is derived from the redistribution of electrons in the plus and minus spin bands by the external magnetic field, as shown in Appendix B. The rate of this dependence is given by $\chi H/M$ from (B. 3), that is, $\sim 10^{-3}$ at $H=10^5$ Oe for iron metal, so that it is neglected in this paper.

The temperature dependence of χ_{sw} for iron metal is calculated numerically from (6. 9) for $H=100$, 150 and 200 KOe, as shown by solid curves (1), (2) and (3), respectively, in Fig. 27, where we take the value of the exchange stiffness constant D as 0.28 eVÅ^2 which was determined by the experiment of small angle inelastic neutron scattering for iron metal[57].

On the other hand, the temperature dependences of χ_s can be calculated from (6. 5) by using the numerical results of $\Delta\zeta$ obtained in § 3 of chapter II and we obtain curve (4) in Fig. 27 for iron metal. At 300°K, the temperature variation of χ_s is about five percents of that of χ_{sw} for iron metal and we can neglect the temperature variation of χ_s as compared with that of χ_{sw}. The temperature variation of χ_c will be the same order of magnitude as that of χ_s. Therefore, both temperature variations of χ_s and χ_c will be negligible as compared with that of χ_{sw} and we may assume that the temperature variation of the experimental

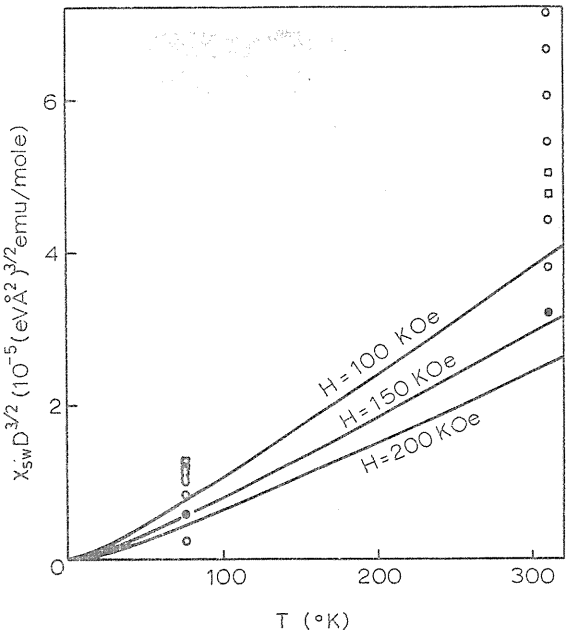

FIG. 28. Calculated temperature dependence of $\chi_{sw}D^{3/2}$ by (6.9). Experimental values, obtained from the observed values of D[57] and χ[15], are denoted by closed circles for iron metal, open circles for iron-cobalt alloys and square symboles for iron-nickel alloys.

data of the high field susceptibility is given by only that of χ_{sw}.

From (6.9), we can expect that $\chi_{sw}D^{3/2}$ will not depend on the composition of alloys, as Ω does not so sensitively depend on the composition[95], and it is a function of T and H. The temperature variation of $\chi_{sw}D^{3/2}$ calculated by (6.9) is shown by solid curves in Fig. 28 for some values of H. Using the experimental values of D determined from the neutron scattering experiments[57] and experimental values of χ measured at H between 100 and 200 KOe by Stoelinga and Gersdorf[15], we can obtain the experimental values of $\chi D^{3/2}$, as shown in Fig. 28 by closed circles, open circles and square symboles for iron metal, iron-cobalt alloys and iron-nickel alloys, respectively.

The scattering of experimental values of $\chi D^{3/2}$ at higher temperatures in Fig. 28 may be attributed to the fact that χ_{sw} shows a strong field dependence at higher temperatures and the fact that the higher order terms in the dispersion relation and the cut-off momentum of spin waves are neglected in (6.9). The former fact is discussed in the next section. We can take into account the effect of the latter fact on the temperature variation of χ_{sw} only for iron metal in the following way. Using the experimental data of the dispersion relation of spin waves for iron metal which was measured by neutron scattering experiment up to the order of q^6 where q denotes the momentum of spin waves[44], we can obtain the temperature variations of χ_{sw} from (6.8) as shown by broken curves (1′), (2′) and (3′) in Fig. 27 for some values of H. The discrepancies between the

solid curves and broken curves at lower temperatures in Fig. 27 are due to the difference between the values of D measured by Lowde *et al.*[57] and Shirane *et al.*[44] For iron alloys we have, however, no experimental data of the higher-order terms in the dispersion relation at present. If we take account of the effect of these higher-order terms on the temperature variation of χ_{sw} for these alloys, the solid curves in Fig. 28 may shift upwards. Moreover, we have no information about the cut-off momentum of spin waves for iron metal and iron alloys. When we take account of the cut-off momentum, the broken curves in Fig. 27 may, in principle, shift downwards at higher temperatures.

§ 5. Magnetic Field Dependence of High Field Susceptibility

The field dependence of χ_s can be calculated from (6. 1) as follows, we expand (6. 1) in a Taylor's series of Δn up to the terms of Δn^2 and get

$$\chi_s(H) = \frac{\partial \Delta M}{\partial H} = \chi_s - \frac{H}{8\mu_B^3}\chi_s^3\left\{\left(\frac{\partial^2 \Delta\zeta}{\partial n^2}\right)_0 - 4\mu_B^2 n_0\left(\frac{\partial^2 \alpha}{\partial n^2}\right)_0 - 8\mu_B^2\left(\frac{\partial \alpha}{\partial n}\right)_0\right\}, \quad (6.10)$$

where χ_s is given by (6. 5).

At 0°K, (6.10) is written as,

$$\chi_s(H) = \chi_s(0) + \frac{H}{8\mu_B^3}\chi_s(0)^3\left\{\frac{\nu'_+}{\nu_+^3} - \frac{\nu'_-}{\nu_-^3}\right\}, \quad (6.11)$$

where the dependence on n of α is neglected and

$$\nu'_\pm = \left(\frac{d\nu(\varepsilon)}{d\varepsilon}\right)_{\varepsilon=\zeta_\pm}.$$

It is noted that a linear term of H appears in the ferromagnetic susceptibility, given by (6. 10) or (6. 11), and its coefficient has the exchange enhancement similar to that given by the term proportional to H^2 in the paramagnetic susceptibility, as shown by Wohlfarth[96].

For iron metal, the second term in (6. 11) is estimated from the density of states curve shown in Fig. 6 and the same value of α as those used in § 2, and it becomes $-0.65\times10^{-12}\times H$ emu/mole. When H is about 10^5 Oe, the field variation of $\chi_s(0)$ is of the order of 10^{-7} emu/mole for iron metal and can be neglected. The field dependence of χ_c will be the same order of magnitude as that of $\chi_s(0)$.

From (6. 9), we can estimate the field dependence of χ_{sw}. As shown in the last section, the field dependence of D is negligibly small and we neglect this dependence. The calculated results of $\chi_{sw}(H)$ are shown in Fig. 29 for iron metal at some temperatures. At the magnetic field between 100 and 200 KOe, the field variation of χ_{sw} is negligible at lower temperatures, but large at higher temperatures, for instance, about 10^{-4} emu/mole at 300°K. Therefore, the experimental errors in the experiments of the high field susceptibility will increase with increasing temperature. The scattering of the experimental values of $\chi D^{3/2}$ at 310°K in Fig. 28 may be attributable in part to this strong field dependence of χ_{sw}.

For the magnetic field dependence of the high field susceptibility, Holstein and Primakoff[94] showed before that $\chi_{sw}(H)$ is proportional to the inverse of a

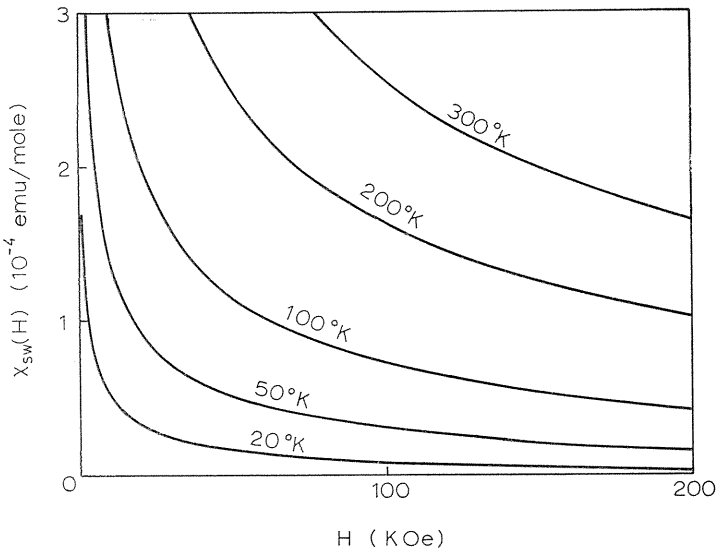

FIG. 29. Calculated field dependences of χ_{sw} for iron metal at 20, 50, 100, 200 and 300°K by (6.9). The value of D is taken as 0.28 eVÅ^2[237].

square root of H in the Heisenberg model, including the dipole-dipole interactions. The result similar to their result is obtained from (6.8) and (6.9), if we assume $\hbar\omega_q = Dq^2$ and take $q_{\max}$ as infinity and if $\mu_B H$ is far smaller than kT, as follows,

$$\chi_{sw}(H) = \frac{\mu_B Qk T}{4\pi} D^{-3/2}\left(\frac{2\mu_B}{H}\right)^{1/2}. \tag{6.12}$$

However, this result is not applicable to the comparison with experimental data used in this paper, because H is very high, about 10^5 Oe. The values of $\chi_{sw}(H)D^{3/2}$ calculated by (6.9) and (6.12) at $T=20$, 50, 100, 200 and 300°K are shown by solid curves and broken lines in Fig. 30, respectively. From Fig. 30 it is seen that χ_{sw} is not proportional to $H^{-1/2}$ at higher magnetic fields.

Finally, it is pointed out that for a special density of states curve there is a possibility of the transition from a ferromagnetic state to another ferromagnetic state which has the larger magnetization with increasing magnetic field. (In the case of the collective electron metamagnetism pointed out by Wohlfarth and Rhodes[97], the transition from a paramagnetic state to a ferromagnetic state occurs.) In the case where the difference between the energies in the ferromagnetic and paramagnetic states, ΔE, without magnetic field is schematically drawn as a function of M by the curve specified by $H=0$ in Fig. 31 (a), the energy of the state with a larger magnetization decreases with increasing magnetic field and becomes lower than the energy of the state with a smaller magnetization at the higher magnetic fields than the critical field H_c. The field dependence of the magnetization is schematically shown in Fig. 31 (b) and that of susceptibility becomes discontinuous at the critical field. There seems to be this possibility when the density of states curve has a hump at a little higher (lower) energy than the Fermi energy of plus (minus) spin band or has humps at both energy

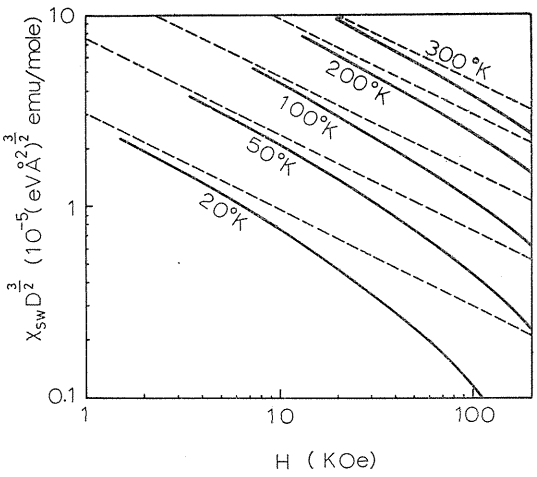

FIG. 30. Field dependences of $\chi_{sw}D^{3/2}$ at some temperatures. Solid curves and broken lines are calculated by (6.9) and (6.12), respectively.

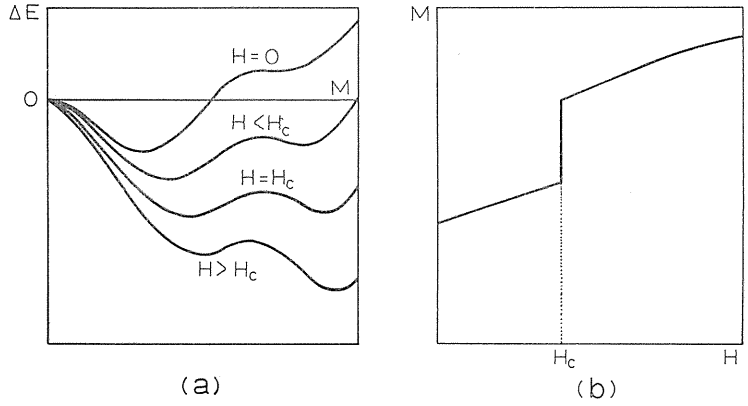

FIG. 31. (a) Schematic curves of the difference between energies in the ferromagnetic and paramagnetic states in the field H against the magnetization. H_c is the critical field when the energies of two states with smaller and larger magnetizations are equal. (b) Schematic curve of the magnetization against H. When $H>H_c$, the state with larger magnetization is stable as shown in (a), and the χ_s becomes discontinuous at H_c.

sides, because the ΔE vs M curve shows the behaviour similar to that shown in Fig. 31 (a) in these cases (*cf.* Fig. 3 of I).

Chapter VII. Conclusion and Discussion

In chapter II, we have calculated the temperature variations of the magnetization for nickel and iron metals. As shown in § 2 of chapter II, the calculated

result for nickel metal is not so strongly dependent on the details of the density of states curve, and the situation similar to this fact will occur in the case of iron metal. Therefore, the dependences of α on temperature and magnetization, which are found in chapter II, are not an apparent effect due to the method or model of our calculation but a natural result. Moreover, in chapter VI we have calculated the concentration dependence of the high field susceptibility for iron-cobalt and iron-nickel alloys, using the density of states curve shown in Fig. 6, and got a good agreement between the calculated and experimental results. From this fact it is concluded that the density of states curve for iron metal shown in Fig. 6 is also considerably reliable.

The temperature variations of the magnetization and the high field susceptibility cannot be explained in the Stoner model, as mentioned in chapters II and VI, because the fluctuation of the magnetization, that is, the spin wave motion is not taken into account in the Stoner model. In chapter III, it has been shown that spin waves can be phenomenologically derived from the energy due to the fluctuation of the magnetization and the energy of a spin wave with momentum q is written as Dq^2 at small q in a ferromagnetic medium. Further, the temperature variations of the magnetization and the high field susceptibility can be explained by assuming the non-interacting free spin waves, as shown in chapters III and VI. The numerical values of D for ferromagnetic metals which are determined from the experiments of the inelastic neutron scattering, the spin wave resonance and the temperature variation of the magnetization at low temperature are compared with each other, and it is shown that a good agreement among these values is obtained as shown in Table 2. This fact shows the validity of the theory of spin waves in metals.

From the first principle, the dispersion coefficient D has been calculated from the equation of motion for normal modes with a reversed spin within the random phase approximation for ferromagnetic metals with multiple bands in chapter IV. It has been shown that the acoustical intra-band branch of spin waves has the excitation energy of Dq^2 at small q and optical intra-band, acoustical inter-band and optical inter-band branches of spin waves have finite excitation energies at $q=0$. Therefore, the contribution to the magnetic properties from the acoustical intra-band branch is dominant at low temperature for ferromagnetic metals. Other branches of spin waves do not contribute to the magnetic properties at low temperature but will take part in at higher temperatures.

It has also been shown that the acoustical intra-band branch in the dispersion relation of spin waves is affected by the inter-band transitions at larger q. The experimental fact that the coefficient of q^4 in the dispersion relation of the acoustical intra-band branch is relatively large for iron and fcc cobalt metals[44)45)], but small for nickel metal[51)] may be explained by the effect of inter-band transitions as follows. There are only 0.6 holes per atom in nickel, so that the single band model is appropriate and the effect of the inter-band transitions may be small in nickel. On the other hand, the numbers of electrons or holes per atom are large in iron and fcc cobalt metals, so that the multiple band model is appropriate and the effect of the inter-band transitions on the dispersion relation of the acoustical intra-band branch of spin waves may appear at relatively small values of q.

In the calculations of spin wave spectrum in chapter IV, we have used some

approximations, the random phase approximation (4.9) and approximations for the Coulomb interaction (4.13) and (4.21). These approximations for the Coulomb interaction may be appropriate only for 3d-electrons and not for 4s-electrons, because the wave functions of 3d-electrons are considered to be well localized, so that it should be considered that the effects of 4s-electrons on the spin wave spectrum are neglected in our calculations. Essentially 3d-electrons take a main part in ferromagnetism, so that the results obtained in chapter IV may not be so changed by the inclusion of 4s-electrons. In future, we should take into account the role of 4s-electrons in the calculations of spin waves. Recently Thompson and Myers[81] have calculated the dispersion relation of an acoustical intra-band branch of spin waves for nickel. But in their calculation the inter-band transitions are not taken into account, so that the spectrum at larger q in their result is not so reliable, although the spectrum at smaller q will be reliable.

Next we discuss the random phase approximation (RPA). In the case of a plasmon in an electron gas, RPA is correct in the high density limit of electrons[72)85)]. On the other hand, in the case of spin waves, the (extended) RPA corresponds to the Hartree-Fock approximation, because the eigen-value equation for a spin wave similar to that obtained in the RPA can be deduced by the approximation similar to the Hartree-Fock one, that is, the first-order perturbation theory in which the Coulomb interaction is treated as the perturbing Hamiltonian[11)12)]. This fact can also be supported from the calculation in § 4 of chapter III. Therefore, the RPA will be appropriate if the Coulomb interaction is sufficiently small. Roughly speaking, when the Coulomb matrix element, which is proportional to the molecular field coefficient α given in chapters II and VI, is small, the ferromagnetism cannot expected because the unstable condition of the paramagnetic state is given by $\alpha > (2\mu_B^2 \nu_0)^{-1}$, where ν_0 is the value of the density of states at the paramagnetic Fermi level. But the value of α has an upper limit from the stable condition of the ferromagnetic state[17)]

$$\frac{1}{4\mu_B^2}\left\{\frac{1}{\nu_+}+\frac{1}{\nu_-}\right\}-\alpha>0,$$

where ν_+ and ν_- are the values of the density of states at the Fermi levels of up and down spin bands, respectively, so that the value of α must be restricted in the region

$$\frac{1}{4\mu_B^2}\left\{\frac{1}{\nu_+}+\frac{1}{\nu_-}\right\}>\alpha>\frac{1}{2\mu_B^2}\frac{1}{\nu_0},$$

for a ferromagnetic state. Even if the value of α is so small that the perturbation theory can be used, the ferromagnetism is expected only when the above condition is satisfied. Recently Kanamori[27)] has shown that the Coulomb interaction is screened by the correlation among electrons and the value of α becomes relatively small. Moreover 4s-electrons will screen the effective interaction between 3d-electrons. Therefore, we should take the values of U and J in chapter IV to be the screened values and the RPA may not be unrealistic. At any rate, the RPA is the most simple approximation to discuss spin waves in ferromagnetic metals.

The optical intra-band and the acoustical and optical inter-band branches of

spin waves, which are found in chapter IV, have not so far been observed, but there is a possibility of the observations of these branches in the experiments of inelastic neutron scattering, especially the acoustical inter-band branch may be observed because its excitation energy is lower than that of individual excitations as shown in Fig. 12 and Fig. 19.

Recently, Antonoff[98] has calculated the spectrum of spin waves in two band ferromagnetic metals, taking into account inter-band transitions. He has started from the Hamiltonian (4. 1) and calculated the equation of motion for spin-flip operators in the random phase approximation. But, as mentioned in Appendix A, the sub-band indices in (4. 1) are not suitable, so that the terms of $\langle c^{+}_{k\nu\sigma} c_{k\mu\sigma} \rangle$ for $\nu \neq \mu$ which have been neglected in Antonoff's work[98] should be taken into account to solve the equation of motion in the random phase approximation, as well as the terms of $\langle c^{+}_{k\nu\sigma} c_{k\nu\sigma} \rangle$.

The dispersion relation of a plasmon in a ferromagnetic electron gas has been found in chapter V by including the exchange correction and it has shown that there is no difference between the constant terms in the dispersion relation of a plasmon with respect to the momentum in the paramagnetic and ferromagnetic states, but the coefficients of the terms proportional to the square of momentum in these two states are different from each other. In real metals with multiple bands, we can treat the plasma oscillation also by the method of the normal modes. From the equation of motion for normal modes and by making use of the Hamiltonian (4. 4) and the random phase approximation (4. 9), we can get the same eigenvalue equation as that obtained by Pines[99] and Ehrenreich and Cohen[100]. However, further numerical calculations are not yet achieved for real ferromagnetic metals, because we must have a knowledge about the higher and lower energy spectra than the Fermi level by about 10 eV. Although it is an interesting problem to calculate the excitation spectrum of a plasmon in real metals, the magnetic properties will not be affected by plasmons at the ordinary temperatures because its excitation energy is too high.

Finally, we summarize the conclusions obtained in this paper.

(i) The magnetization dependence of the molecular field coefficient is important to fit the calculated temperature variations of the magnetization on the experimental ones for iron and nickel metals.

(ii) Spin wave-spin wave interactions are phenomenologically derived from the terms with the fourth power of the first derivative of the magnetization density with respect to space coordinates in the magnetic energy.

(iii) The spin wave spectra for ferromagnetic metals with multiple bands consist of one acoustical intra-band branch, some optical intra-band branches and new acoustical and optical inter-band branches. The acoustical intra-band branch plays an important role for magnetic properties.

(iv) Plasmons exist not only in the paramagnetic electron gas but also in ferromagnetic one and there is a difference between the terms proportional to the square of momentum of a plasmon in their respective dispersion relations.

(v) The experimental results of the high field susceptibilities for iron metal and its alloys at 4.2°K can be satisfactorily explained in the Stoner model, by making use of the density of states curve shown in Fig. 6. The temperature and magnetic field dependences of the high field susceptibilities at lower temperatures can also be explained by non-interacting free spin waves.

Acknowledgements

The author would like to express his cordial thanks to Prof. M. Shimizu for obliging guidance and valuable discussions. He also express his thanks to Dr. A. Katsuki for useful discussions and encouragements and to Mr. K. Terao for useful discussions and assistances to the calculation given in chapter II, and to Prof. H. Nakano, Dr. E. Haga and Mr. E. Hayashi who have enlightened the author by useful discussions and comments.

This thesis was submitted to the Nagoya University for the degree of Doctor of Engineering, February, 1968.

Appendix A

It is shown that the sub-band indices ν_i in (4.1) are not suitable for describing one electron states in the following way. Now, we consider a commutator of $c^+_{ps\sigma}$ with $\mathscr{H}$ in (4.1). Cubic terms with respect to c^+ and c, which are derived from the commutator of $c^+_{ps\sigma}$ with $\mathscr{H}'$, are linearized by picking up only the terms containing $n_{k\nu_1}$ $(=c^+_{k\nu_1\sigma}c_{k\nu_1\sigma})$ and treating these occupation number operators as c-numbers[71], and we find

$$\begin{aligned}[\mathscr{H}, c^+_{ps\sigma}] = {} & \in_s(p)\, c^+_{ps\sigma} \\ & + \sum_{k\nu_1\nu_2\sigma'} V(p\nu_1,\ k\nu_2\ ;\ ps,\ k\nu_2)\, n_{k\nu_2\sigma'} c^+_{p\nu_1\sigma} \\ & - \sum_{k\nu_1\nu_2} V(k\nu_2,\ p\nu_1\ ;\ ps,\ k\nu_2)\, n_{k\nu_2\sigma} c^+_{p\nu_1\sigma}. \end{aligned} \tag{A.1}$$

This shows that one electron state with momentum p, spin σ and sub-band index s is coupled with other states with the same momentnm p, the same spin σ and different sub-band indices, so that the sub-band indices in (4.1) are not suitable for describing one electron states in the further calculations of spin wave spectra.

In order to diagonalize the one electron energy with respect to sub-band indices, we add an effective potential to one electron Hamiltonian and $\mathscr{H}$ in (4.1) is rewritten as follows,

$$\left.\begin{aligned} \mathscr{H} &= \mathscr{H}^{\circ}_{eff} + \mathscr{H}'_{eff}, \\ \mathscr{H}^{\circ}_{eff} &= \sum_i h(r_i), \\ h(r_i) &= -\frac{\hbar^2\nabla_i^2}{2m} + \sum_n v(r_i - R_n) + v_{eff}(r_i), \\ \mathscr{H}'_{eff} &= -\sum_i v_{eff}(r_i) + \frac{1}{2}\sum_{i\neq j}\sum v(|r_i - r_j|), \end{aligned}\right\} \tag{A.2}$$

where the first, second and third terms in $h(r_i)$ are the kinetic energy, the interaction between electrons and ions and an effective potential which is determined later, respectively. Now, we can rewrite (A.2) by the second quantization, taking the eigen functions of $h(r_i)$ as the basis and we have

$$\begin{aligned}\mathscr{H} &= \sum_{k\lambda\sigma} E_{\lambda\sigma}(k)\, a^{+}_{k\lambda\sigma} a_{k\lambda\sigma} \\ &\quad - \sum_{kk'} \sum_{\xi\xi'\sigma} \langle k\hat{\xi} \,|\, v_{eff} \,|\, k'\hat{\xi}' \rangle\, a^{+}_{k\xi\sigma} a_{k'\xi'\sigma} \\ &\quad + \frac{1}{2} \sum_{k_1 \cdots k_4} \sum_{\xi_1 \cdots \xi_4} \sum_{\sigma\sigma'} W(k_1\hat{\xi}_1,\ k_2\hat{\xi}_2\ ;\ k_4\hat{\xi}_4,\ k_3\hat{\xi}_3) \\ &\quad \times a^{+}_{k_1\xi_1\sigma} a^{+}_{k_2\xi_2\sigma'} a_{k_3\xi_3\sigma'} a_{k_4\xi_4\sigma}, \end{aligned} \tag{A.3}$$

where

$$E_{\lambda\sigma}(k) = \int dr\, \varphi^{*}_{k\lambda}(r)\, h(r)\, \varphi_{k\lambda}(r), \tag{A.4}$$

$$\langle k\hat{\xi} \,|\, v_{eff} \,|\, k'\hat{\xi}' \rangle = \int dr\, \varphi^{*}_{k\xi}(r)\, v_{eff}(r)\, \varphi_{k'\xi'}(r), \tag{A.5}$$

and

$$\begin{aligned} &W(k_1\hat{\xi}_1,\ k_2\hat{\xi}_2\ ;\ k_4\hat{\xi}_4,\ k_3\hat{\xi}_3) \\ &= \iint dr_1 dr_2\, \varphi^{*}_{k_1\xi_1}(r_1)\, \varphi^{*}_{k_2\xi_2}(r_2)\, v(|r_1 - r_2|)\, \varphi_{k_4\xi_4}(r_1)\, \varphi_{k_3\xi_3}(r_2). \end{aligned} \tag{A.6}$$

Here, $\varphi_{k\xi}(r)$ is the eigen function of $h(r)$ in which the spin dependence is neglected. The matrix elements of $v_{eff}(r)$ are self-consistently determined such that the sum of the second term and a part of the third term in (A. 3), which can be rewritten as the second term by replacing the number operators $a^{+}a$ by c-numbers, as well as in the random phase approximation, vanishes. Thus, the matrix elements of $v_{eff}(r)$ is determined as,

$$\begin{aligned} &\langle k\hat{\xi} \,|\, v_{eff}(\boldsymbol{r}) \,|\, k'\hat{\xi}' \rangle \\ &= \delta_{kk'} \Big\{ \sum_{k_1\xi_1\sigma_1} W(k_1\hat{\xi}_1,\ k\hat{\xi}\ ;\ k_1\hat{\xi}_1,\ k\hat{\xi}')\, n_{k_1\xi_1\sigma_1} \\ &\quad - \sum_{k_1\xi_1} W(k_1\hat{\xi}_1,\ k\hat{\xi}\ ;\ k\hat{\xi}',\ k_1\hat{\xi}_1)\, n_{k_1\xi_1\sigma} \Big\}. \end{aligned} \tag{A.7}$$

Making use of (A.7), we can write $E_{\lambda\sigma}(\boldsymbol{k})$ as

$$\begin{aligned} E_{\lambda\sigma}(k) &= \int dr\, \varphi^{*}_{k\lambda}(r) \Big\{ -\frac{\hbar^2 \nabla^2}{2m} + \sum_{n} v(r - R_n) \Big\} \varphi_{k\lambda}(r) \\ &\quad + \sum_{k'\xi\sigma'} W(k'\hat{\xi},\ k\lambda\ ;\ k'\hat{\xi},\ k\lambda)\, n_{k'\xi\sigma'} \\ &\quad - \sum_{k'\xi} W(k'\hat{\xi},\ k\lambda\ ;\ k\lambda,\ k'\hat{\xi})\, n_{k'\xi\sigma}, \end{aligned} \tag{A.8}$$

and this expression is just the Hartree-Fock energy. The off-diagonal matrix element of $h(r)$ must vanish, that is,

$$\begin{aligned} &\int dr\, \varphi^{*}_{k\lambda}(r) \Big\{ -\frac{\hbar^2 \nabla^2}{2m} + \sum_{n} v(r - R_n) \Big\} \varphi_{k\mu}(r) \\ &\quad + \sum_{k'\xi\sigma'} W(k'\hat{\xi},\ k\lambda\ ;\ k'\hat{\xi},\ k\mu)\, n_{k'\xi\sigma'} \\ &\quad - \sum_{k'\xi} W(k'\hat{\xi},\ k\lambda\ ;\ k\mu,\ k'\hat{\xi})\, n_{k'\xi\sigma} = 0, \end{aligned} \tag{A.9}$$

for $\lambda \neq \mu$. From (A.3), (A.7) and (A.8), we can get the Hamiltonian, shown by (4.4) in the text.

Appendix B

We will discuss the contribution to χ due to the field dependence of the dispersion relation of spin waves. In the magnetic field H, the eigenvalue equation of a spin wave with momentum q is obtained from the equation of motion for the spin flipping normal modes as,

$$1=\frac{U+J(q)}{N}\sum_{k}\frac{n_{k,+}(H)-n_{k+q,-}(H)}{E(k+q)-E(k)+\Delta(H)+2\mu_B H-\hbar\omega(H)}, \tag{B.1}$$

where we use the single band model and the random phase approximation, U and $J(q)$ are an intra-atomic Coulomb integral and the Fourier component of inter-atomic exchange integrals, respectively, Δ is the exchange splitting, $\{U+J(0)\}M$, $E(k)$ is the energy of one electron with momentum k, $n_{k,+}(H)$ and $n_{k,-}(H)$ are occupation numbers of electrons with plus and minus spin and with momentum k in the magnetic field H and N is the number of atoms.

By the effective mass approximation, we can obtain the dispersion relation of spin waves with small q as

$$\hbar\omega(H)=2\mu_B H+D(H)q^2,$$

up to the order of q^2, where

$$\left.\begin{aligned} &D(H)=D_B(H)+D_H(H),\\ &D_B(H)=\frac{\hbar^2}{2m^*M(H)}\left\{n-\frac{4}{5}\frac{n_+(H)E_{f+}(H)-n_-(H)E_{f-}(H)}{M(H)\Delta(H)}\right\},\\ &D_H(H)=\{J(0)-J(q)\}M(H), \end{aligned}\right\} \tag{B.2}$$

and $E_{f\pm}(H)$ and $n_\pm(H)$ are the Fermi energies and number of electrons with plus and minus spins in the magnetic field H, and $n=n_+(H)+n_-(H)$ is the total number of electrons.

Expanding $n_\pm(H)$ and $E_{f\pm}(H)$ in (B.2), by the usual way in power series of H and using the relation $M(H)=M(0)+\chi H$, $D_B(H)$ and $D_H(H)$ given by (B.2) are expanded in power series of H as

$$\left.\begin{aligned} D_B(H)=D_B(0)&-\frac{\chi H}{M(0)}D_B(0)+\frac{n\hbar^2}{2m^*M(0)}\frac{\chi H}{M(0)}\\ &\times\left[\frac{4}{5n\Delta(0)}\{n_+(0)E_{f+}(0)-n_-(0)E_{f-}(0)\}\right.\\ &\left.-\frac{2M(0)}{3n\Delta(0)}\{E_{f+}(0)+E_{f-}(0)\}\right],\\ D_H(H)=D_H(0)&\left\{1-\frac{\chi H}{M(0)}\right\}, \end{aligned}\right\} \tag{B.3}$$

up to the linear term of H. Therefore, the orders of magnitude of $\{D_B(H)-D_B(0)\}/D_B(0)$ and $\{D_H(H)-D_H(0)\}/D_H(0)$ are given by $\chi H/M$, that is, 10^{-3} at $H=10^5$ Oe, and the effect of H on D can be neglected in our estimations of χ_{sw} in chapter VI. For the case of multiple bands, the order of magnitude of the difference between $D(H)$ and $D(0)$ is also $\chi H/M$, because the value of D is the simple sum of the values of D in each sub-band as shown in § 5 of chapter IV.

References

1) F. Bloch: Zeits. Phys., **57** (1929), 545.
2) J. C. Slater: Phys. Rev., **49** (1936), 537, 931.
3) E. C. Stoner: Proc. Roy. Soc. A, **165** (1938), 372, A, **169** (1939), 339.
4) N. F. Mott: Proc. Phys. Soc., **47** (1935), 571.
5) M. Shimizu, T. Takahashi and A. Katsuki: J. Phys. Soc. Japan, **17** (1962), 1740.
6) M. Shimizu, T. Takahashi and A. Katsuki: J. Phys. Soc. Japan, **18** (1963), 801.
7) M. Shimizu and A. Katsuki: *Proceedings of the International Conference on Magnetism*, Nottingham, 1964, p. 182.
8) S. Foner and E. D. Thompson: J. appl. Phys., **30** (1959), 229 S.
9) F. Bloch: Zeits. Phys., **61** (1930), 206.
10) C. Herring and C. Kittel: Phys. Rev., **81** (1951), 869.
11) C. Herring: *Magnetism*, Vol. 4 (ed. G. T. Rado and H. Suhl, Academic Press, 1966), p. 345.
12) E. D. Thompson: Adv. Phys., **14** (1965), 213.
13) D. C. Mattis: Phys. Rev., **132** (1964), 2521.
The Theory of Magnetism (Harper and Row, New York, 1965), p. 211.
14) D. Pines: *Solid State Physics*, Vol. **1** (Academic Press Inc., New York, 1955), p. 367.
15) J. H. M. Stoelinga and R. Gersdorf: Phys. Letters, **19** (1966), 640.
16) E. P. Wohlfarth: Phil. Mag., **42** (1951), 374.
17) M. Shimizu: Proc. Phys. Soc., **84** (1964), 397.
18) M. Shimizu: Proc. Phys. Soc., **86** (1965), 147.
19) M. Shimizu, A. Katsuki and H. Yamada: J. Phys. Soc. Japan, **20** (1965), 396.
20) P. Weiss and R. Forrer: Ann. Phys. (France) **5** (1926), S 153.
21) K. L. Hunt: Proc. Roy. Soc. A, **216** (1953), 103.
22) M. Shimizu, A. Katsuki, H. Yamada and K. Terao: J. Phys. Soc. Japan, **21** (1966), 1654.
23) H. H. Potter: Proc. Roy. Soc. A, **146** (1934), S 362.
24) E. M. Terry: Phys. Rev., **9** (1917), 394.
25) E. P. Wohlfarth: Rev. mod. Phys., **25** (1953), 211.
26) M. Shimizu: J. Phys. Soc. Japan, **15** (1960), 376.
27) J. Kanamori: Prog. theor. Phys., **30** (1963), 275.
28) J. Hubbard: Proc. Roy. Soc. A, **276** (1963), 238.
29) M. Dixson, F. E. Hoare, T. M. Holden and D. E. Moody: Proc. Roy. Soc. A, **285** (1965), 561.
30) N. F. Mott: Adv. Phys., **13** (1964), 325.
31) M. Shimizu and K. Terao: J. Phys. Soc. Japan, **23** (1967), 771.
32) S. Arajis and R. V. Colvin: J. appl. Phys., **35** (1964), 2424.
33) C. Domb: *Magnetism*, Vol. **2A** (ed. G. T. Rado and H. Suhl, Academic Press, 1965), p. 1.
34) F. Keffer and R. Loudon: J. appl. Phys., **32** (1961), 2 S.
35) W. Marshall: *Proceedings of the 8th International Conference on Low Temperature Physics* (ed. R. O. Davis, Butterworths, London, 1963), p. 215.
36) T. Oguchi: Phys. Rev., **117** (1960), 117.
37) T. Izuyama: Phys. Letters, **9** (1964), 293, Phys. Rev. Letters, **12** (1964), 585.
K. Kawasaki: Phys. Rev., **135** (1964), A 1371.
38) C. Herring: Phys. Rev., **87** (1952), 60.
39) M. Shimizu and H. Yamada: J. Phys. Soc. Japan, **21** (1966), 621.
40) C. Kittel: *Low Temperature Physics* (ed. C. DeWitt, D. Dreyfus and P. G. DeGennes, Gordon and Breach, New York, 1962), p. 441.
41) R. D. Lowde: J. appl. Phys., **36** (1965), 884.
M. Hatherly, K. Hirakawa, R. D. Lowde, J. F. Mallett, M. W. Stringfellow and B. H. Torrie: Proc. Phys. Soc., **84** (1964), 55.
42) L. Landau and E. Lifshitz: Phys. Z. Sowjetunion, 8 (1935), 153.
43) R. Sinclair and B. N. Brockhouse: Phys. Rev., **120** (1960), 1638.

44) G. Shirane, R. Nathans, O. Steinsvoll, H. A. Alperin and S. J. Pickart: Phys. Rev. Letters, **15** (1965), 146.
45) G. Shirane, V. J. Minkiewicz and R. Nathans: *International Conference on Magnetism*, Boston, 1967.
46) E. Frikkee and T. Riste: *Proceedings of the International Conference on Magnetism*, Nottingham, 1964. p. 299.
47) A. Furrer, T. Schneider and W. Hälg: Solid State Comm., **3** (1965), 339.
48) E. Frikkee: Physica, **32** (1966), 2149.
49) D. C. Mattis: Phys. Rev., **151** (1966), 278.
50) T. Riste, G. Shirane, H. A. Alperin and S. J. Pickart: J. appl. Phys., **36** (1965), 1076.
51) S. J. Pickart, H. A. Alperin, V. J. Minkiewicz, R. Nathans, G. Shirane and O. Steinsvoll: Phys. Rev., **156** (1967), 623.
52) C. Kittel: Phys. Rev., **110** (1958), 1295.
53) R. Weber and P. E. Tannenwald: J. Phys. Chem. Solids, **24** (1963), 1357.
54) T. G. Phillips and H. M. Rosenberg: Phys. Rev. Letters, **11** (1963), 198.
55) T. G. Phillips: Proc. Roy. Soc. A, **292** (1966), 224.
56) E. D. Thompson, E. P. Wohlfarth and A. C. Bryan: Proc. Phys. Soc., **83** (1964), 59.
57) R. D. Lowde, M. Shimizu, M. W. Stringfellow and B. H. Torrie: Phys. Rev. Letters, **14** (1965), 698.
58) G. I. Rusov: Sov. Phys. Solid State, **9** (1967), 146.
59) M. Fallot: Ann. Phys., **6** (1963), 305.
60) V. E. Rode and R. Herrmann: Sov. Phys. JETP, **19** (1964), 1081.
61) B. E. Argyle, S. H. Charap and E. W. Pugh: Phys. Rev., **132** (1963), 2051.
62) T. G. Phillips and H. M. Rosenberg: *Proceedings of the International Conference on Magnetism*, Nottingham, 1964, p. 306.
63) V. Jaccarino: Bull. Am. Phys. Soc., **23** (1959), 461.
64) H. A. Alperin, O. Steinsvoll, G. Shirane and R. Nathans: J. appl. Phys., **37** (1966), 1052.
65) E. I. Kondorskii, V. E. Rode and U. Gofman: Sov. Phys. JETP, 8 (1959), 380.
66) E. W. Pugh and B. E. Argyle: J. appl. Phys., **33** (1962), 1178.
67) T. Kasuya: Progr. theor. Phys., **16** (1956), 45.
K. Yoshida: Phys. Rev., **106** (1957), 893.
68) F. Englert and M. M. Antonoff: Physica, **30** (1964), 429.
69) T. Izuyama, D. J. Kim and R. Kubo: J. Phys. Soc. Japan, **18** (1963), 1025.
70) H. Yamada and M. Shimizu: J. Phys. Soc. Japan, **22** (1967), 1404.
71) P. A. Wolff: Phys. Rev., **120** (1960), 814.
D. Pines and P. Nozieres: *The Theory of Quantum Liquids*, Vol. **1** (W. A. Benjamin, Inc., New York, 1966), p. 270.
72) K. Sawada, K. A. Brueckner, N. Fukuda and R. Brout: Phys. Rev., **108** (1957), 507.
73) S. Wakoh: J. Phys. Soc. Japan, **20** (1965), 1894.
74) S. Wakoh and J. Yamashita: J. Phys. Soc. Japan, **21** (1966), 1712.
75) M. Shimizu: J. Phys. Soc. Japan, **23** (1967), 1187.
76) G. C. Fletcher: Proc. Phys. Soc., **65** (1951), 192.
77) J. Yamashita, M. Fukuchi and S. Wakoh: J. Phys. Soc. Japan, **18** (1963), 999.
78) A. Katsuki and E. P. Wohlfarth: Proc. Roy. Soc. A. **295** (1966), 182.
79) E. P. Wohlfarth: *Proceedings of the International Conference on Magnetism*, Nottingham, 1964. p. 51.
80) E. D. Thompson: Ann. Phys., **22** (1963), 309.
81) E. D. Thompson and J. J. Myers: Phys. Rev., **153** (1967), 574.
82) H. Yamada and M. Shimizu: J. Phys. Soc. Japan, **21** (1966), 1517.
83) D. Pines and D. Bohm: Phys. Rev., **85** (1952), 338.
84) D. Bohm and D. Pines: Phys. Rev., **92** (1953), 609.
85) M. Gell-Mann and K. A. Brueckner: Phys. Rev., **106** (1957), 364.
K. Sawada: Phys. Rev., **106** (1957), 372.

86) H. Kanazawa, S. Misawa and E. Fujita: Prog. theor. Phys., **23** (1960), 426.
87) M. Shimizu and H. Yamada: J. Phys. Soc. Japan, **24** (1968), 1236.
88) A. J. Freeman, N. A. Blum, S. Foner, R. B. Frankel and E. J. McNiff, Jr.: J. appl. Phys., **37** (1966), 1338.
89) C. Herring, R. M. Bozorth, A. E. Clark and T. R. McGuire: J. appl. Phys., **37** (1966), 1340.
90) E. P. Wohlfarth: Phys. Letters, **3** (1962), 17.
91) R. Gersdorf: J. Phys. Radium, **23** (1962), 726.
92) M. Shimizu, T. Takahashi and A. Katsuki: J. Phys. Soc. Japan, **18** (1963), 1192.
93) J. Crangle and G. C. Hallam: Proc. Roy. Soc. A, **272** (1963), 119.
94) T. Holstein and H. Primakoff: Phys. Rev., **58** (1940), 1098.
95) W. B. Pearson: *A Handbook of Lattice Spacings and Structures of Metals and Alloys* (Pergamon Press, London).
96) E. P. Wohlfarth: Phys. Letters **22** (1966), 280.
97) E. P. Wohlfarth and P. Rhodes: Phil. Mag., **7** (1962), 1817.
98) M. M. Antonoff: J. appl. Phys., **38** (1967), 1059.
99) D. Pines: *Elementary Excitations in Solids* (W. A. Benjamin, Inc., New York, 1964), p. 168.
100) H. Ehrenreich and M. H. Cohen: Phys. Rev., **115** (1959), 786.